PREDICTION OF EMBANKMENT PERFORMANCE USING IN-SITU TESTS

By

DONNA GAIL LECLAIR

B. A. Sc., The University of British Columbia, 1986

A THESIS SUBMITTED IN PARTIAL FULFILLMENT OF

THE REQUIREMENTS FOR THE DEGREE OF

MASTER OF APPLIED SCIENCE

in

THE FACULTY OF GRADUATE STUDIES

DEPARTMENT OF CIVIL ENGINEERING

We accept this thesis as conforming

to the required standard

THE UNIVERSITY OF BRITISH COLUMBIA

September, 1988

5

Department of CIVIL ENGINEERING

The University of British Columbia
Vancouver, Canada

Date 14 OCTOBER 1988

PREDICTION OF EMBANKMENT PERFORMANCE USING IN-SITU TESTS

Abstract

In-situ piezocone , flat dilatometer, and screw plate tests were carried out adjacent to the site of several large earth embankments, founded on a deep deposit of compressible soil. Settlement records since construction were available for two of the embankments. Geotechnical parameters were not back analyzed from the case record, rather, embankment performance was predicted on the basis of parameters interpreted from the in-situ tests alone.

Consolidation characteristics were interpreted from the measurement of dissipation of excess pore pressures using the piezocone and dilatometer. Both devices provided complementary results in terms of an appropriate coefficient of consolidation. The excellent stratigraphic profile furnished by the piezocone (CPTU) tests proved to be a most valuable feature. The stratigraphic detail provided by the CPTU tests performed across the site identified continuous, free draining soil layers which would generally be missed in a conventional geotechnical investigation using a drilled borehole with discrete sampling. The identification of these layers was of paramount importance in the prediction of settlement rate.

A one-dimensional analysis formed the basis for the settlement predictions, and was found to be satisfactory. Settlement magnitudes were predicted within 10% of the observed measurements, parallelling the observed rate of settlement throughout the embankment construction period in the early 1970's and to the present date.

Key words: settlement, deltaic soils, embankment, in-situ testing, piezocone, flat dilatometer, screw plate, coefficient of consolidation, compressibility, pore pressure dissipation.

Contents

List of Tables

List of Figures

Acknowledgements

I wish to express my gratitude to Dr. Peter Robertson for his assistance in selecting, as a research project, a useful exercise and practical application of geotechnical engineering, and for his continued advice through all stages of my work. I extend thanks also to Dr. Dick Campanella for his assistance in the absence of Dr. Robertson.

To all my colleagues and those in the in-situ testing group, Mark, Ian, Ross, Damika, Erick, John, and Don, I give you my thanks for your help in carrying out the field tests, and to the technical support staff, Jim, Scott, Art, and Glen, thank you.

My appreciation is extended to Transport Canada Airports Authority Group for making the area adjacent to the McConachie Way Overpass and Arthur Laing Bridge embankments accessible for this research, and to the various individuals within Transport Canada, for their cooperation in making current and historic data available.

I wish to acknowledge, and am grateful for, the financial support of the Natural Sciences and Engineering Research Council, through the UBC Civil Engineering Department's Graduate Research Assistantship, and for a Professional Fellowship from the Canadian Federation of University Women.

1. INTRODUCTION

In the construction of buildings, bridges, and earth or other structures on soil, the two key concerns are the maximum load that can be supported (bearing capacity) and the maximum amount the structure will settle. Settlement often governs foundation design. Excessive settlement of structures and bearing capacity failures have occurred in areas underlain by deep layers of compressible soil. A typical example of an area underlain by deep layers of compressible soils is the Fraser River delta region of British Columbia.

Relatively few major structures are located in the Fraser River delta, due to the presence of deep deposits of highly compressible marine silts and clays which can be subject to extensive and long-term settlement. Vancouver International Airport, however, is situated on Sea Island, shown on Fig. 1.1, which lies at the westernmost edge of the Fraser River delta.

In order to accommodate increased traffic volume from the city of Vancouver to the airport, Transport Canada planned and began constructing, in 1970, a road system including a bridge and several high approach embankments on the eastern part of Sea Island. Due to the compressible nature of the soils much attention was given to the settlements which would occur as a result of the planned embankment construction.

Predictions of settlement of the Arthur Laing Bridge south approach embankment and the McConachie Way Overpass embankments were based on conventional geotechnical analysis of laboratory tests on samples and other information obtained from drilling investigative boreholes. Realizing the uncertainty of these predictions, stemming from difficulties in field sampling and laboratory testing of the soft, sensitive Fraser delta sediments, an extensive monitoring program was conducted to supplement historical settlement data already available. At both embankment locations, settlement predictions were also made for the abutments founded in the earth embankments, and monitoring of the settlements at these locations continues today.

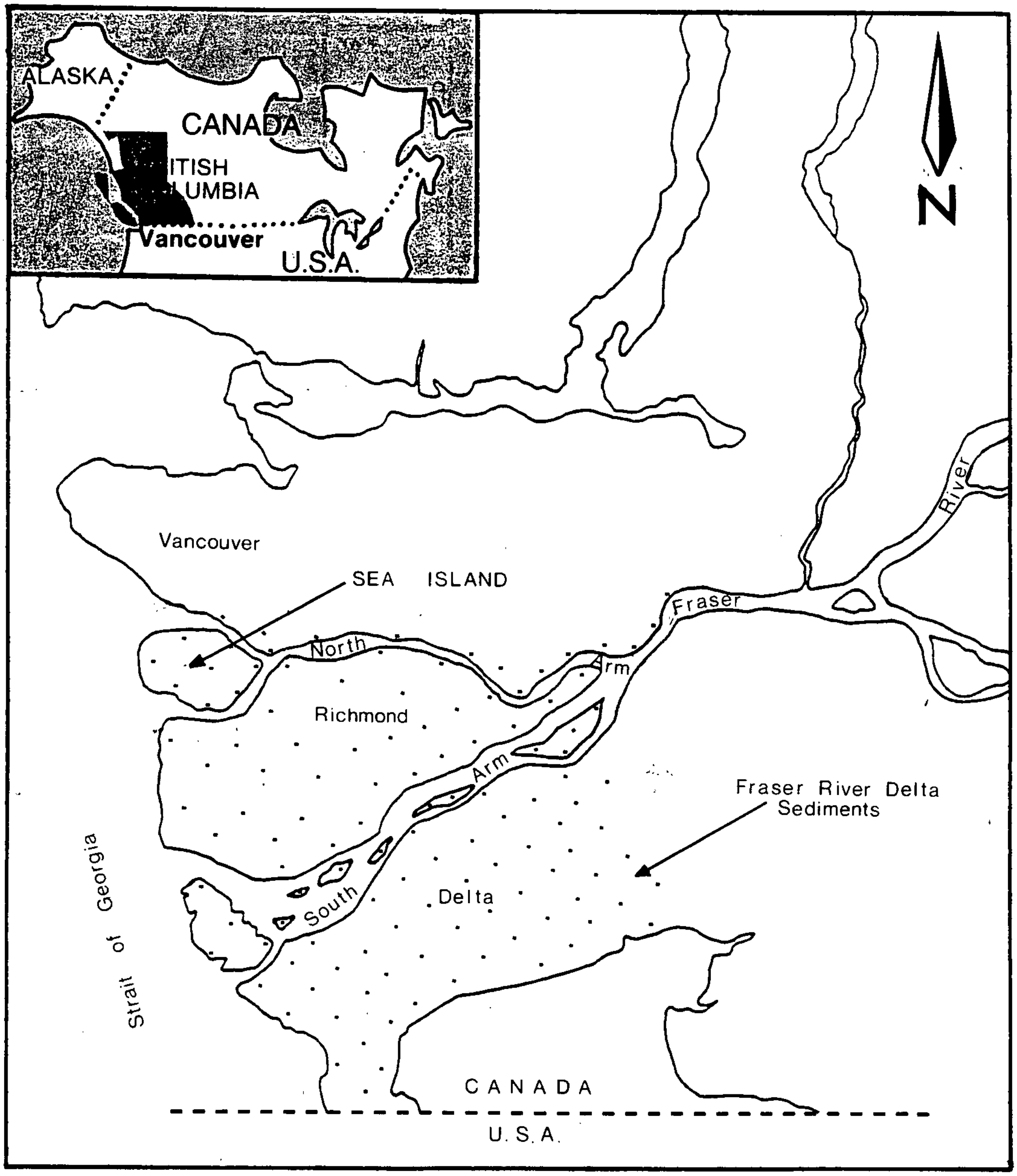

Fig. 1.1 Location of Sea Island

Without considering the rate at which settlement would occur, Transport Canada reported (Bertok, 1987) that reasonable agreement was found between the predicted and observed settlements for the Arthur Laing Bridge south approach abutment, however significant differences were found between the predicted and observed settlements of the McConachie Way Overpass abutments.

1.1 Objectives of Present Research

Current methods of arriving at the amount and rate of settlement are somewhat empirical in nature and rely heavily on sometimes simplistic assumptions about soil properties and behaviour. As exemplified in the case of the earth embankments on Sea Island, in engineering practice today, estimation of settlement is merely that, an estimate.

The measurement of soil properties using in-situ tests has gained increasing favour throughout the past decade. Mitchell *et al.* (1978) listed four main reasons for the growing interest in the use of in-situ testing techniques:

i. the ability to determine properties of soils, such as sands and offshore deposits, that cannot be easily sampled in the undisturbed state,

ii. the ability to test a larger volume of soil than can conveniently be tested in the laboratory,

iii. the ability to avoid some of the difficulties of laboratory testing, such as sample disturbance and the proper simulation of in-situ stresses, temperature, and chemical and biological environments, and

iv. the increased cost effectiveness of an exploration and testing program using in-situ methods.

With these reasons in mind, particularly the first, where field sampling in the soft, sensitive, Fraser delta sediments is known to be difficult, a program of in-situ testing was set up with the goal of obtaining the soil parameters necessary to predict the rate and magnitude of settlement caused by the embankments constructed on Sea Island. A comparison was then made between the results predicted by in-situ tests, the results predicted by the more traditional approach of borehole sampling and laboratory testing, and actual settlement measurements obtained by Transport Canada from 1971 through 1987. Such a comparison serves as a test of the viability of in-situ testing as an alternative to the traditional approach to obtaining the soil parameters required for settlement prediction.

1.2 Thesis Organization

Following a general description of the research site in chapter two, the case record of construction and monitoring of the subject embankments is summarized in chapter three of this thesis. Chapter four details the in-situ tests performed and identifies the key features of each test as they pertain to the present application. The parameters required in the prediction of rate and magnitude of settlement include, most importantly, deformation and consolidation characteristics. The interpretation of these parameters from the in-situ tests carried out, along with the interpreted soil profile, is described in chapter five. Prediction of embankment performance is made in chapter six. A one-dimensional analysis forms the basis for settlement prediction, as this is the type of analysis most routinely performed in geotechnical practice today, however, the chapter also contains some discussion on the use of more complex approaches which can also be adopted in predicting settlement of structures on soft soil. Chapter six concludes with the findings of this research, in the form of a comparison between predicted performance based on parameters interpreted from in-situ tests and observed performance to date. Finally, discussion and conclusions are presented.

2. RESEARCH SITE

The research site is situated on Sea Island, in the Fraser River delta at an elevation of about 1.5 m above sea level. Since approximately 85% of Sea Island lies below normal high tide levels, some 15 km of dykes have been constructed around the island to prevent tidal inundation and flooding by the Fraser River. The site itself is located at the eastern end of the island, as shown in Fig. 2.1, on property under the jurisdiction of Transport Canada Airports Authority Group.

2.1 Regional Geology

A description of the geology of the Fraser River delta is given in Blunden (1973). The region is founded on Pleistocene till sheets and Tertiary bedrock at depths of 225 m to 275 m below mean sea level. This base has experienced isostatic rebound which, combined with post-glacial sedimentation, has resulted in the emerging delta. The sedimentary sequence consists of 2 m to 6 m of mixed clays, silts, and organics, underlain by up to 30 m of deltaic channel fill, predominantly sand, with interbedded silts, underlain by a stratified accumulation of marine clays and silts reflecting alternating quiescent and turbulent depositional environments.

2.2 Site Description

Located adjacent to the subject embankments, the research site is level and lawn-covered, with a series of drainage ditches separating it from the surrounding roadways and embankments. The site was chosen on the basis of its proximity to the subject embankments and its accessibility. Additionally, it provided a less complicated testing area, being relatively free of the numerous, complex underground services required by Vancouver International Airport.

General site stratigraphy consists of roughly 2 m of extraneous soil, topsoil, and sandy, silty clay, below which medium dense to very dense sand extends to a depth of 20 m. Beneath

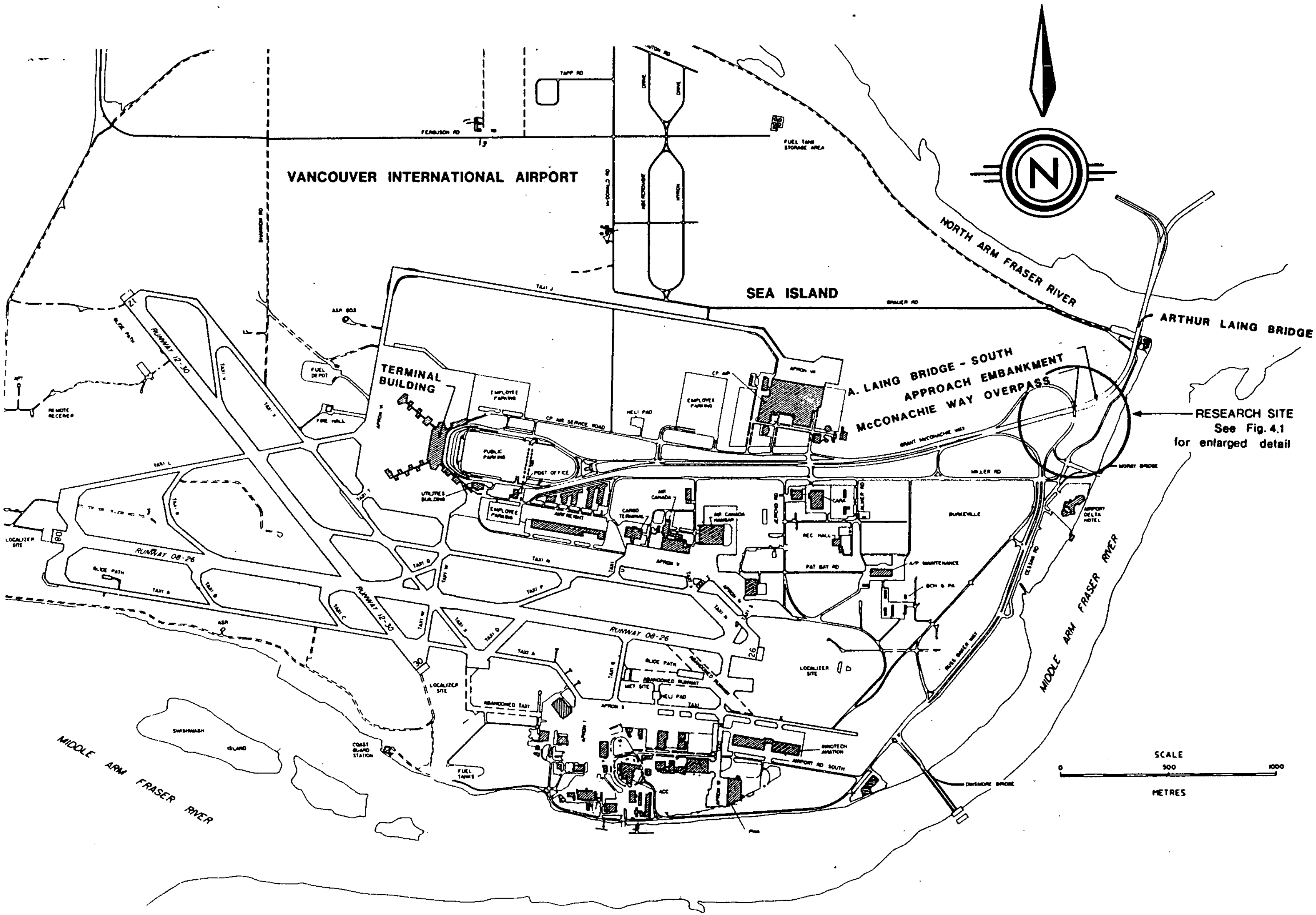

Fig. 2.1 Plan View of Sea Island Showing Vancouver International Airport Facilities and Research Site Location
(base map courtesy of Transport Canada)

this sand lies the compressible marine delta deposit. At the site, the thickness of this normally consolidated clayey silt is 40 m to 45 m. Glacial till underlies the clay silt, from a depth of approximately 61 m.

The groundwater table was generally found to lie between 1 m and 1.5 m below ground surface, with fluctuation due to tidal influence.

3. EMBANKMENTS AND FIELD OBSERVATIONS

The case record of construction and instrumentation, and a comparison between predicted and observed settlements of the McConachie Way Overpass embankments and the Arthur Laing Bridge south approach embankment is given in Bertok (1987). A brief summary of the case record is given in the following sections.

3.1 McConachie Way Overpass Embankments

Two embankments, north and south, provide the foundation for the roadway over Grant McConachie Way. Fig. 3.1 presents a perspective drawing of the completed McConachie Way Overpass south embankment and abutment.

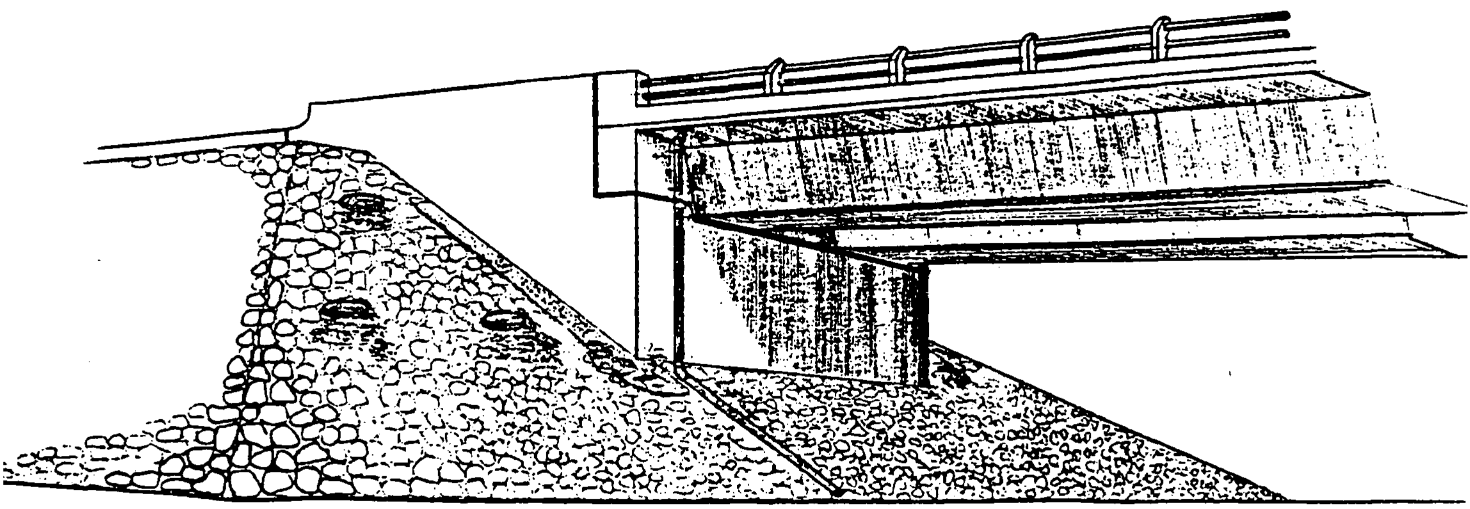

Fig. 3.1 Perspective drawing – McConachie Way Overpass south abutment
(drawing courtesy Phillips, Barratt, Hillier, Jones & Partners, 1974)

3.1.1 Construction History

Embankments for the McConachie Way Overpass are some 73 m (240 feet) in length, with a base width of 39.6 m (130 feet), and a height of 8.6 m (28 feet) at the highest point. A typical section is shown in Fig. 3.2(a). The embankments were constructed between November, 1970 and February, 1971, from compacted sand fill with a unit weight of approximately 18.2 kN/m^3. Uncompacted sand with a unit weight of approximately 16.5 kN/m^3 was placed as a surcharge 2 m thick at the high point of the embankment, decreasing in thickness to 0.9 m at the natural ground surface. The surcharge remained in place for 30 months, and was removed in August, 1973.

Abutments for the overpass were founded on 55 m^2 (600 $ft.^2$) spread footings located in the compacted sand fill approximately 1 m above the original ground surface. Abutment construction took place over the six months between October, 1974 and March, 1975.

3.1.2 Instrumentation

Field instrumentation included surface and deep settlement gauges and piezometers, as shown schematically in Fig. 3.2(b). Significant excess pore pressures were not recorded during fill construction, which was apparently indicative of piezometer malfunction.

Settlement gauges to measure surface or deep settlements consisted of wooden or steel plates attached to vertical pipes. Level surveys were taken on the tops of the pipes to record movement beneath the embankments. Field observations began in November, 1970, with embankment construction, and continued through 1973, when construction operations destroyed most of the gauges. However, observations continued through 1975 on two gauges which remained intact. Settlement of the abutments was monitored by periodic level surveys which began in November, 1974. These observations continue to the present time.

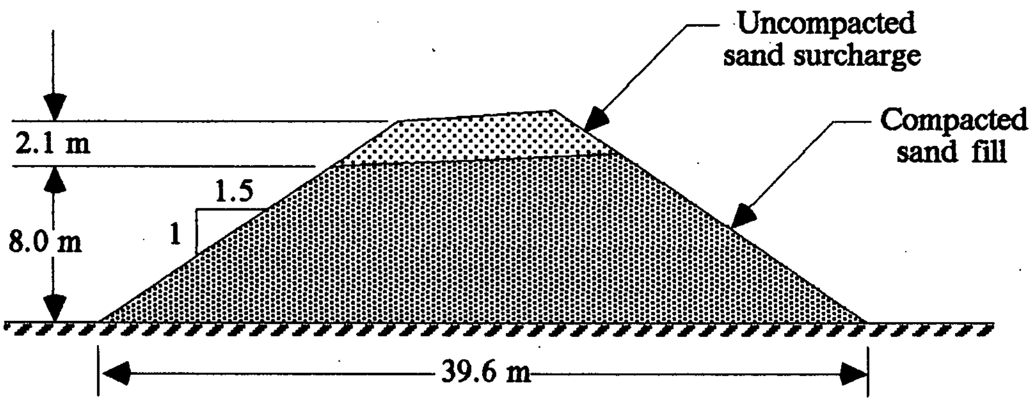

(a)

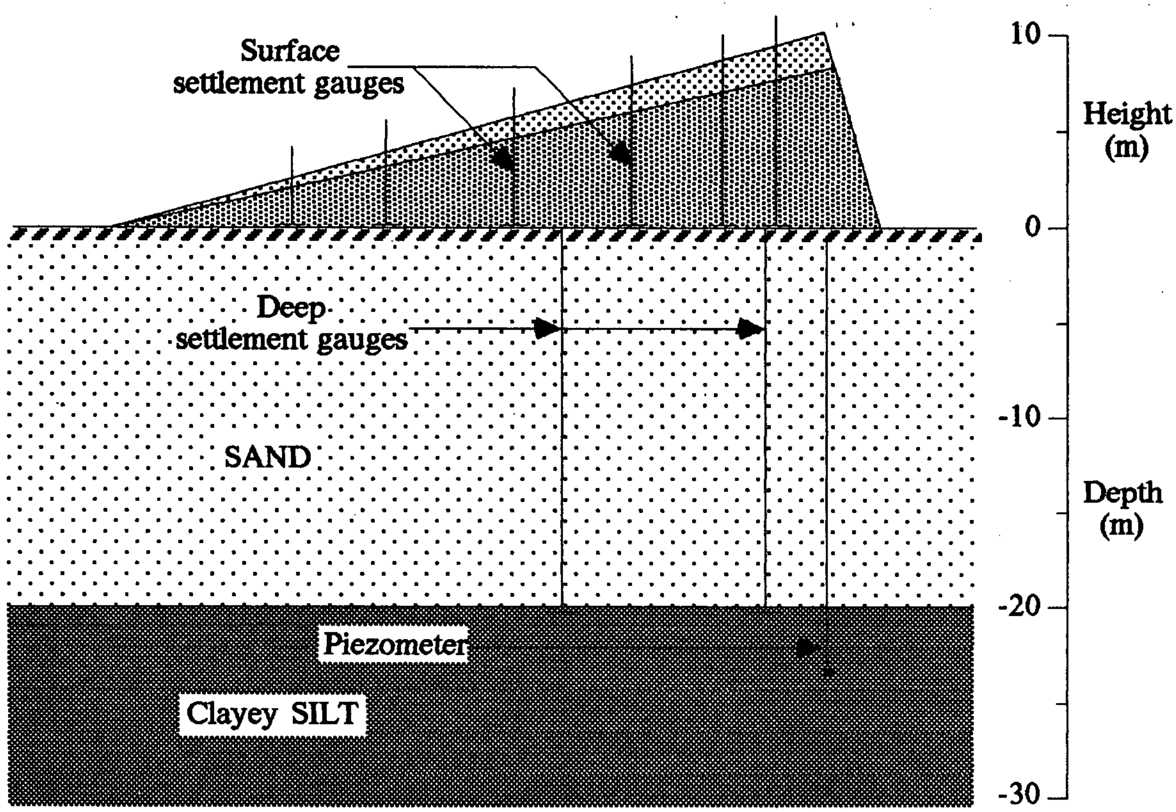

(b)

Fig. 3.2 (a) Typical section through McConachie Way Overpass embankment
(b) Instrumentation of McConachie Way Overpass north embankment

3.1.3 Observed Results

Settlement beneath the high portion of the south embankment had reached 67 cm at the commencement of abutment construction in October, 1974. Subsequent monitoring to September, 1987 indicates the north and south abutments have settled approximately 39 cm and 37 cm, respectively, for an average total settlement of 105 cm.

From data supplied by Transport Canada, the load-settlement curve for the high portion of the McConachie Way Overpass south embankment and abutment was reconstructed and is shown in Fig. 3.3. The figure reveals that final loading conditions are larger than those imposed by the embankment and surcharge, resulting in a further increase in settlement when the abutment load was applied.

3.2 Arthur Laing Bridge South Approach Embankment

The south approach to the Arthur Laing Bridge is over an embankment 67 m (220 feet) in length, with a base width of 68 m (223 feet), and a height of 9.5 m (31 feet) at its highest point.

3.2.1 Construction History

Compacted sand fill with a unit weight of approximately 18.2 kN/m^3 was used for embankment construction, which took place from May to August, 1970. Uncompacted sand with a unit weight of approximately 16.5 kN/m^3 was placed as a surcharge 3 m thick at the highest point of the embankment, decreasing in thickness to 0.9 m at the natural ground surface. The surcharge remained in place for 34 months, and was removed in July, 1973.

Abutment construction began, in February, 1973, with the surcharge still in place, and was completed in December, 1973. The abutment was founded on a 91 m^2 (980 $ft.^2$) spread footing located within the embankment, 4.8 m (16 feet) above the natural ground surface.

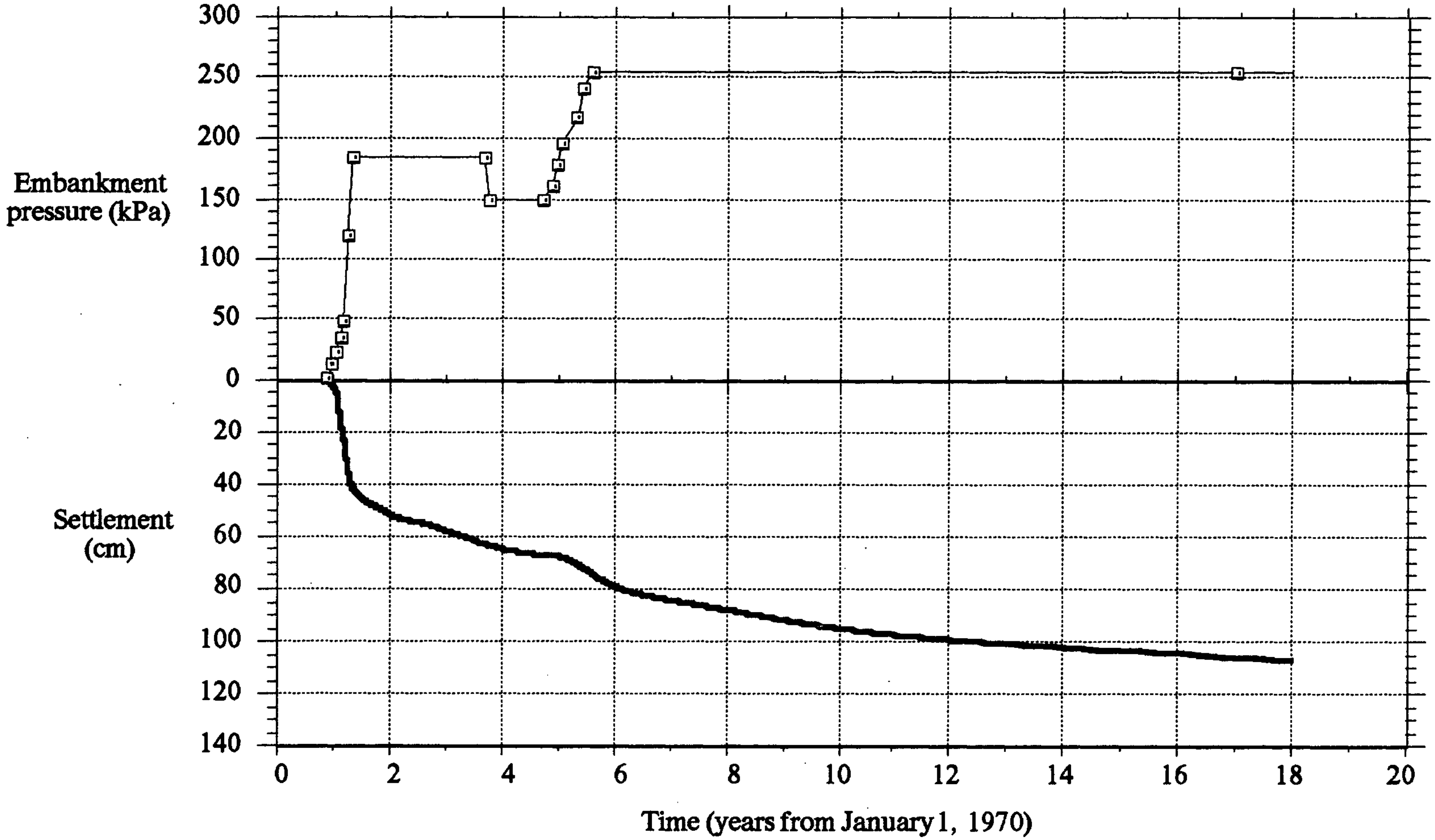

Fig. 3.3 Load-settlement record for McConachie Way Overpass south embankment and abutment

3.2.2 Instrumentation

Field observations were made on piezometers and settlement gauges distributed in a similar fashion to those in the McConachie Way Overpass embankments. The program of field observations began in May, 1970 and continued to the middle of 1973 when most settlement gauges were destroyed or damaged by abutment construction. One piezometer remained operational and was monitored through to early 1974. Monitoring of abutment settlement began in March, 1973 and is on-going to the present time.

3.2.3 Observed Results

The load-settlement curve for the high portion of the Arthur Laing Bridge south approach embankment, as reconstructed from Transport Canada data, is shown in Fig. 3.4. By mid-1973, ground surface settlement had reached 100 cm beneath the high point of the embankment, due to the embankment and surcharge, however, the rate of settlement had slowed considerably. Surcharge removal and abutment loading produced little change in the settlement process, as the surcharge appears to have been adequate to simulate final loading conditions.

Field observations showed that high pore pressures developed in the underlying clayey silt, as a result of the placement of the embankment fill, and were slow to dissipate. The record of excess pore pressures during construction, for a piezometer located within the clayey silt stratum at a depth of 35 m beneath the mid-section of the embankment, where fill height was 6 m, is shown on Fig. 3.5. Indicative of the slow rate of consolidation is an excess pore pressure head of 3 m which remained months after abutment construction had been completed.

3.3 Comparison Between Predictions and Observations

Settlement predictions made in 1968-69 were based on the results of a laboratory testing program and standard geotechnical analysis. It was recognized that reliable prediction of the

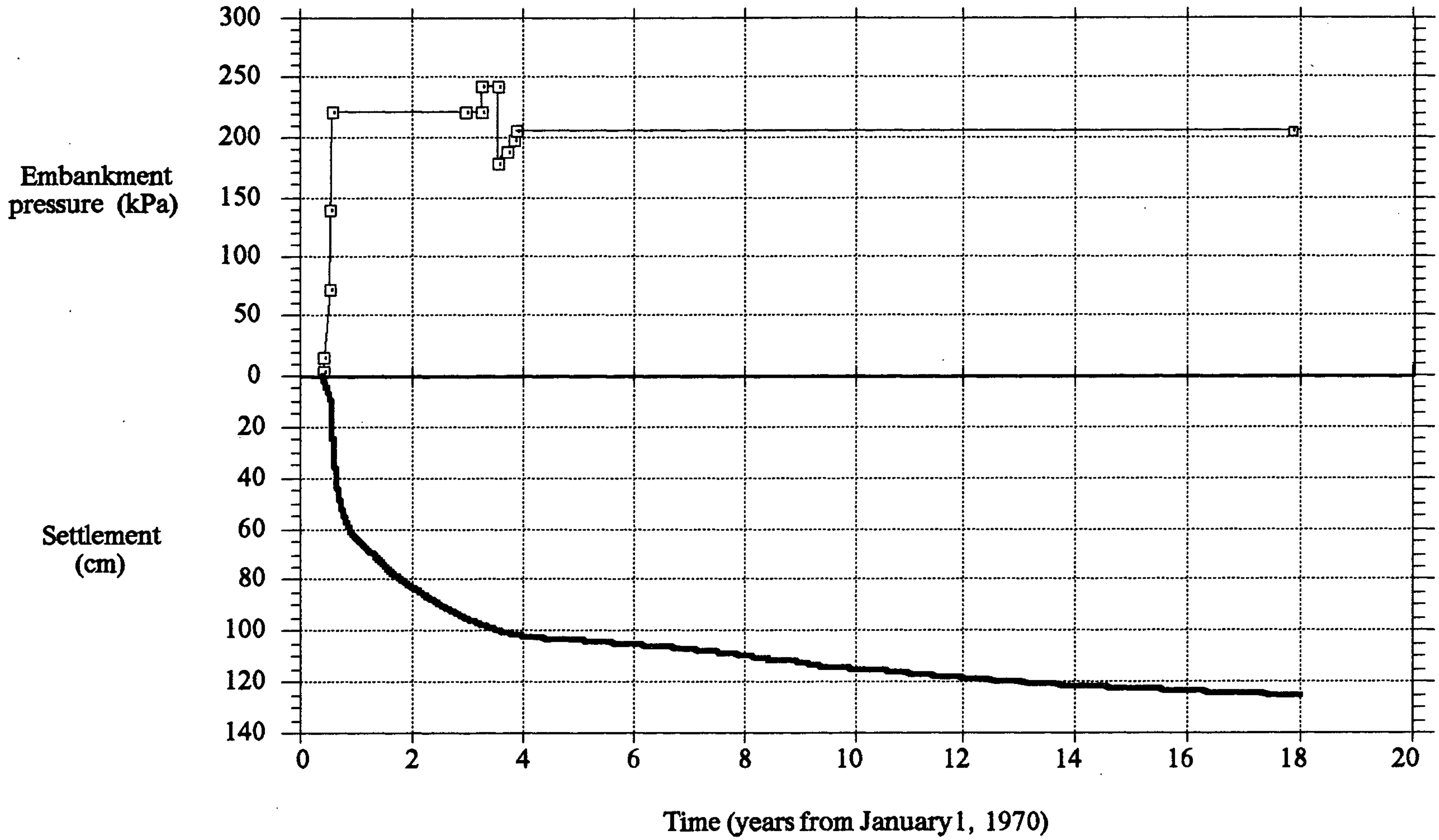

Fig. 3.4 Load-settlement record for Arthur Laing Bridge south approach embankment and abutment

magnitude and rate of settlement would be difficult due to sampling and testing problems in the soft, sensitive soil. A comprehensive picture of the subsurface stratigraphy, including the drainage effects of thin sand layers, could not be fully synthesized from the drilling and sampling program conducted in the late 1960's.

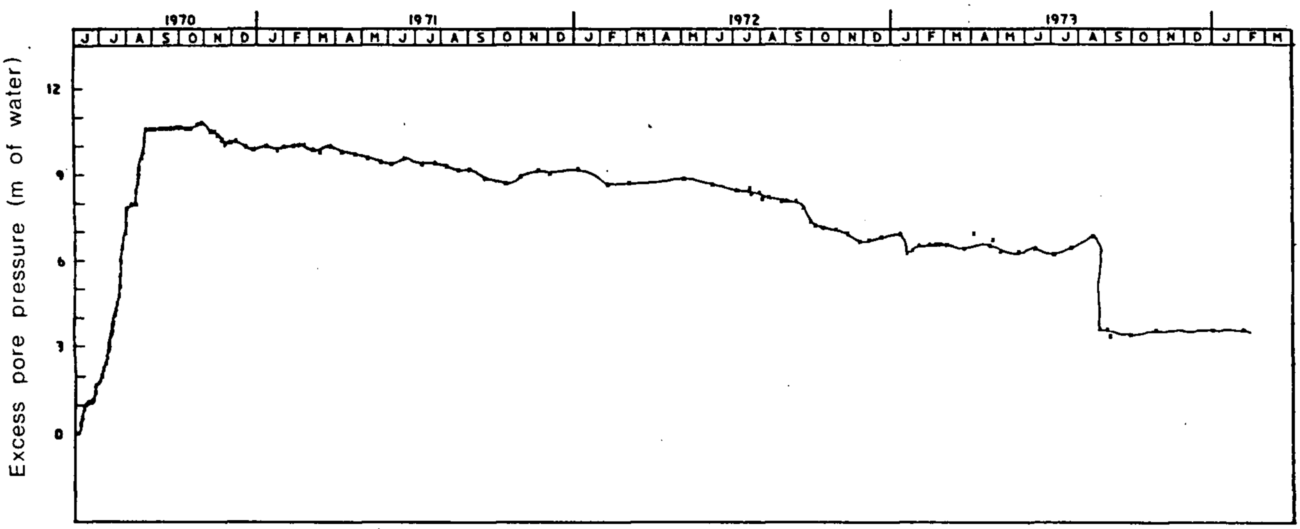

Fig. 3.5 Record of excess piezometric head beneath Arthur Laing Bridge south approach embankment
(adapted from Bertok, 1987)

Table 3.1 (modified from Bertok, 1987) compares predicted with observed settlement magnitudes to 1985. Settlement arising from the embankments was distinguished from that arising from the abutments, and, as settlement gauges were destroyed prior to the completion of abutment construction, no observed values were given in the case of the embankments. Additionally, no details were given on which to form a comparison of predicted and observed rate of settlement through the construction and post-construction period. From the Table, and as commented by Bertok (1987), reasonable agreement is shown between predicted and observed settlement in the case of the south abutment in the Arthur Laing Bridge approach embankment, however, appreciable difference is seen between predicted and observed settlement for the abutments of the McConachie Way Overpass. No explanation for the discrepancy was given.

Table 3.1 Predicted and Observed Settlements to 1985
(modified from Bertok, 1987)

Embankment or Abutment	Predicted settlement (cm): Primary consolidation and elastic settlement: With surcharge	Predicted settlement (cm): Primary consolidation and elastic settlement: Without surcharge	Predicted settlement (cm): Secondary consolidation	Observed settlement (cm)
South approach embankment of Arthur Laing Bridge*	165	119	10-12	*100†*
Approach embankments of McConachie Way Overpass**	84	67	6-8	*70†*
South abutment of Arthur Laing Bridge	23		2-3	20
Abutments of McConachie Way Overpass	20		5-6	33

* Embankment section 12.5 m high, including 3 m surcharge
** Embankment section 10.4 m high, including 2.1 m surcharge
† *These are approximate values at the commencement of abutment construction, not ultimate settlement magnitudes.*

4. FIELD TESTING

A program of field testing was undertaken in order to obtain the parameters necessary to estimate the magnitude of settlement and rate of settlement of the subject embankments on Sea Island. This chapter provides details of the tests conducted and procedures followed in carrying out the various in-situ tests. Where testing standards are in existence (such as those of the American Society for Testing and Materials; ASTM), the prescribed procedures were followed. Where no designated standard exists, procedures standard to local geotechnical practice were employed.

4.1 Testing Vehicle

All tests were conducted from the University of British Columbia (UBC) Geotechnical Research Vehicle. The truck is equipped to support testing with the mechanical cone, electronic piezometer and seismic cones, flat dilatometer, screw plate, field vane, and full displacement pressuremeter, and to obtain fixed piston samples. For specifications and a description of the testing vehicle, the reader is referred to Campanella and Robertson (1981).

4.2 In-situ Tests Performed

In-situ tests may be generally divided into two categories: logging methods and specific test methods (Robertson, 1985). Logging methods are, ideally, economical and quick to perform, and provide qualitative estimates of geotechnical parameters based on empirical correlations. Specific test methods measure specific soil parameters at a point, and are generally slower to perform. For the present study, cone penetration testing and flat dilatometer testing were the logging method tests conducted, and screw plate testing, the specific test method conducted.

Fig. 2.1 shows the general location of the research site with respect to Sea Island, while Fig. 4.1 presents a more detailed plan of the site, indicating the locations of the various in-situ

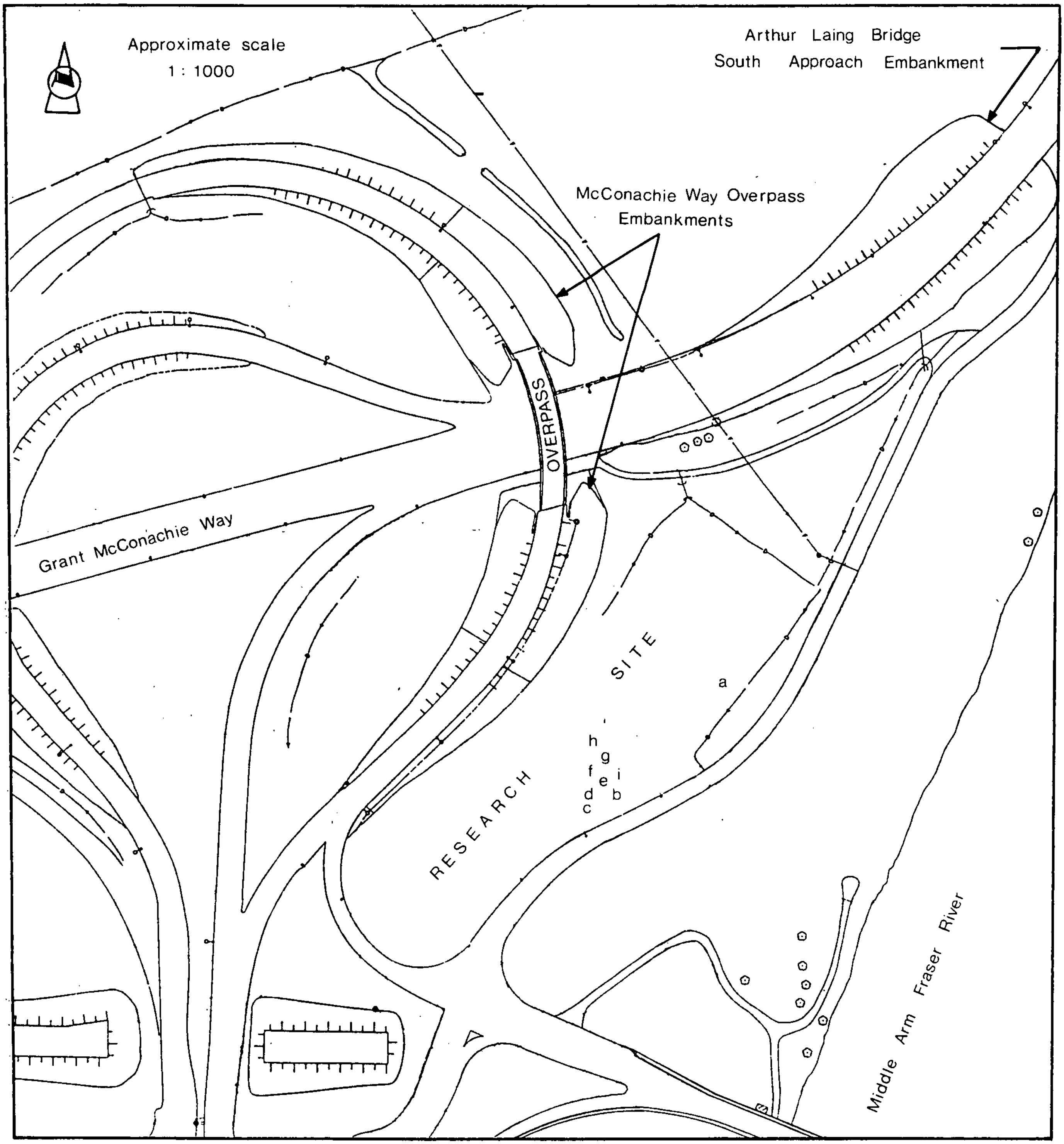

Fig. 4.1 Research Site Plan

See Table 4.1 for index of test methods

tests performed as well as the subject embankments. Table 4.1 may be used in conjunction with Fig. 4.1 for a description of the tests conducted at each location.

Table 4.1 In-Situ Testing Program

Map* Marker	Test Name	Test Type	Test Date (1987)	In-Situ Tool Used	Depth Penetrated (m)
a	CPTU-1	Piezocone penetration test	12 August	UBC Cone #8	61.08
b	CPTU-5	Piezocone penetration test	11 September	Hogentogler Super Cone	64.38
c	CPTU-2	Piezocone penetration test	24 September	Hogentogler Super Cone	29.68
d	CPTU-3	Piezocone penetration test	24 September	UBC Cone #8	29.7
e	DMT-1	Flat Dilatometer test	28 September	Blade #89	21.0
f	DMT-3	Flat Dilatometer test	1 October	Blade #89	29.8
g	DMT-2	Flat Dilatometer test	10 October	Blade #89	35.6
h	SPLT-1	Screw Plate test	29 October	250 cm^2 Plate	24.5
i	CPTU-6	Seismic Piezocone penetration test	22 October	UBC Cone #7	54.78

* refers to location on Fig. 4.1

4.2.1 Piezocone Penetration Test (CPTU)

The piezocone penetration tests performed were quasi-static penetration tests using cones with a 10 cm^2 base area and 60° apex angle. The Hogentogler electronic cone measured end resistance, q_c, and sleeve friction, f_s, continuously by means of built-in load cells, and cone inclination via an inclinometer. The UBC cones measured these same data, as well as temperature. Details on various cone designs, including the UBC and Hogentogler cones, are given in Robertson and Campanella (1986).

Pore pressure measurements were recorded at various locations along the cone both during penetration and pauses in penetration. The addition of pore pressure measurements to the standard cone penetration test is advantageous, as outlined in Campanella and Robertson (1988) for:

- distinguishing between drained, partially drained, and undrained penetration,
- correcting measured cone data to account for unbalanced water forces due to unequal end areas in cone design,
- evaluating flow and consolidation characteristics,
- assessing equilibrium groundwater conditions,
- improved soil profiling and identification, and
- improved evaluation of geotechnical parameters.

Each cone was carefully prepared and calibrated prior to each test to ensure proper functioning in the field. Polypropylene porous filter elements, 5 mm wide, were saturated with glycerine under vacuum in the laboratory prior to piezocone penetration. In the field, cone data was automatically recorded using a data acquisition system in the UBC Geotechnical Research vehicle. Data was subsequently corrected for pore pressure effects on bearing, and for temperature effects, in the case of the UBC cones. The use of equal end area friction sleeves significantly reduced the need for correction of sleeve friction measurements due to pore pressure effects. A complete discussion of these procedures and their effects on geotechnical interpretation is given in Robertson and Campanella (1986).

As there is yet no standard location for the pore pressure sensing element, much deliberation may be found in the literature over the most ideal location. Different researchers and users appear to prefer different locations. Because the measured pore pressures during piezocone testing depends on sensing element location, it is essential to state the location when discussing interpreted results. Table 4.2 provides details on element location for each CPTU performed in this study. The UBC cones were able to record pore pressures at two locations simultaneously.

Table 4.2 Details of CPTU and Pore Pressure Sensor Location

Test Name	Cone Used	Location of Pore Pressure Sensor			
		On face (1)	Behind tip (2)	Sleeve (3)	
CPTU-1	UBC Cone #8		X	X	
CPTU-2	Hogentogler Super Cone		X		
CPTU-3	UBC Cone #8	X		X	
CPTU-5	Hogentogler Super Cone		X		
CPTU-6	UBC Cone #7		X	X	

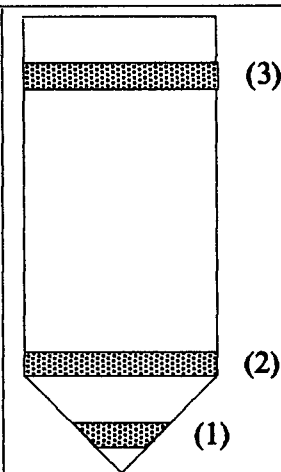

Where analysis and quantitative interpretation requires the use of CPTU pore pressure data, values recorded behind the cone tip have been used for the present study. Robertson and Campanella (1986) list the following advantages of having the pore pressure element at this location:

i. good protection of the element and less proneness to damage,

ii. generally easier saturation,

iii. gives reasonably stable pore pressure response,

iv. gives a good range of dynamic pore pressures from negative to positive, therefore good for stratigraphic logging,

v. good location for theoretical solutions to obtain consolidation characteristics from pore pressure decay,

vi. measured pore pressure dissipations are relatively unaffected by procedures,

vii. best location to apply pore pressure corrections to cone bearing and friction.

Two additional piezocone penetration tests, not detailed here, were attempted near the location of CPTU-1. In these two cases, at approximately 18 m below ground surface, the maximum pushing capacity of the Geotechnical Research vehicle (18 tons) was reached, but further penetration was refused.

4.2.2 Seismic Piezocone Penetration Test (SCPTU)

In an effort to combine the good features of logging test methods with those of specific test methods, a velocity seismometer has been incorporated into the electronic cone. Details of the UBC seismic cone penetrometer are given in Campanella *et al.* (1985). This device has provided the means to determine the small strain shear modulus, G_{max}. By elasticity theory, the shear modulus is proportional to the square of shear wave velocity, v_s, by a proportionality constant, in this case, the soil density, ρ, hence

$$G = \rho v_s^2 \qquad [4.1]$$

allows the determination of shear modulus from the shear wave velocity measured using the in-situ seismic cone penetration test. Combining downhole seismic methods with conventional piezocone penetration testing enables reliable, economic, and rapid resolution of stratigraphic, strength, and modulus information from a single sounding.

4.2.3 Flat Dilatometer Test (DMT)

The flat dilatometer was introduced in 1980 by Silvano Marchetti as a simple and cost-effective in-situ testing device. The device is a flat blade with a 60-mm diameter, flexible, stainless steel membrane located on one face of the blade. In short, testing requires insertion of the dilatometer blade into the soil, inflation of the flexible membrane using high-pressure nitrogen gas, deflation, and penetration to the next test depth. The pressure required to just lift the membrane off its seating, p_o, and that required to cause the membrane to deflect 1 mm, p_1, are recorded in the field, for each test depth. Individual tests are generally carried out at 20 cm intervals, thereby providing a discrete record of site stratigraphy. Details of the instrument and test procedures are given in the Dilatometer Users Manual (Marchetti and Crapps, 1981).

Using the values of p_o and p_1 obtained in the field (A and B readings, respectively), three intermediate index parameters are defined from which empirical correlations have been developed to determine several geotechnical parameters including overconsolidation ratio (OCR), undrained shear strength (S_u), constrained modulus (M), and friction angle (ϕ'). Correlations were developed by Marchetti (1980), based on laboratory tests on soils from ten sites, the majority of which consisted of clay deposits; only two sites involved sand deposits. Details of the sites and the original correlations may be found in Marchetti (1980); more recently-developed correlations, particularly for sands, in Schmertmann (1983).

From data collected using a sophisticated research dilatometer, Campanella *et al.* (1985) showed that, in soft clays, the basic DMT data, p_o and p_1, are dominated by large penetration pore pressures and that the pressure, when the membrane returns to the closed position, is approximately equal to the penetration pore pressure. The pressure reading when the membrane returns to the closed position is known as the C reading, or p_2. When performing DMT soundings, it is now recommended (Robertson *et al.*, 1988; Schmertmann & Crapps, Inc., 1988) that the C reading be obtained as a routine part of the procedure, since it aids in describing the character of the soil tested and helps profile the equilibrium pore water pressure in sands. During a pause in dilatometer penetration, successive C readings may be obtained to monitor the dissipation of excess pore water pressure, much the same as is done during a pause in piezocone penetration, in order to determine the consolidation characteristics of the soil.

For the present study, A, B, and C readings were obtained for all tests, and dissipation data, C readings with time, collected at selected depths. Table 4.3 presents details of the three dilatometer soundings conducted.

Table 4.3 Details of Flat Dilatometer Soundings

Test Name	Maximum Depth Penetrated (m)	Tests Conducted Between Depths (m)	Dissipation Tests Conducted at Depths (m)
DMT-1	21.0	0 - 21.0	21.0
DMT-2	35.6	21.0 - 35.6	21.0, 23.0, 32.0, 35.6
DMT-3	29.8	15.0 - 29.8	22.6, 24.0, 24.2

4.2.4 Screw Plate Test (SPLT)

The screw plate test is a modification of the plate load test whereby soil deformation properties may be obtained from observing the load-settlement behaviour of the plate. The test was first developed and reported by Kummeneje (1956), and has been improved in various applications over the past 30 years.

The screw plate used in this study consisted of a single flight of a helical auger having a cross-sectional area of 250 cm^2. A description of the instrument, installation system, and data acquisition system is given by Berzins (1983). In order to obtain soil deformation characteristics, the plate was screwed down to the desired depth, an increasing load applied from the surface, and plate settlement recorded using a linear variable differential transducer (LVDT). The plate was then advanced to the next test depth. Tests were performed at 1 m intervals to a depth of 24 m. To obtain consolidation characteristics, plate settlement was monitored with time, under constant load conditions. These static load tests were performed at 1 m intervals from 22.5 m to 24.5 m.

4.2.5 Groundwater Level Monitoring

In order to ascertain the level of the groundwater table at the research site, a 3-m length of polyvinyl chloride (PVC) pipe was placed in the open hole following piezocone penetration test CPTU-5 on September 11, 1987, and the pipe capped at ground level. On each subsequent site visit, the water level was read from the standpipe. Throughout the months of September and October, 1987, the static water level was found to vary from 1.25 m to 1.45 m below ground surface. This variation in static water level was attributed to tidal fluctuation. In the vicinity of Sea Island, the Fraser River is subject to tidal effects, and groundwater at the site is brackish.

From piezocone dissipation tests, the equilibrium pore pressure profile at the site was found to be hydrostatic.

4.3 Summary

Undoubtedly the cone penetration test is the most well known of the in-situ tests performed in this study, and proved invaluable in providing a complete and very detailed stratigraphic profile. The record of pore pressure dissipation with time during a pause in cone penetration has been recognized for some time for its usefulness in the determination of consolidation characteristics (Levadoux and Baligh, 1986; Jamiolkowski *et al.*, 1985; Torstensson, 1977). The flat dilatometer test has been used with success to determine foundation settlement (Schmertmann, 1986), and has shown promise in the determination of consolidation characteristics. The screw plate test appears to have the most rational application in settlement prediction, due to the vertical orientation of the test, however, estimation of deformation characteristics, particularly of undrained modulus in sensitive clay, is subject to considerable uncertainty. Current interpretation techniques rely on the assumptions of a homogeneous, elastic, isotropic medium and on the engineer's discretion in choosing an appropriate stress level at which to determine the modulus. Researchers (Selvadurai and Gopal, 1986; Kay and Avalle, 1982) have reported good results in obtaining consolidation characteristics by examining the settlement response of the screw plate under static load.

The testing program described above was designed to incorporate the major in-situ test methods available and most amenable to determining the parameters required to compute rate and magnitude of settlement. Logging method tests were used in conjunction with specific test methods and combined tests to provide some repetition as well as a means of developing or checking site-specific correlations.

5. GEOTECHNICAL PARAMETERS INTERPRETED FROM IN-SITU TESTS

The calculation of settlement requires knowledge of, or an estimate of, the deformation and consolidation characteristics of the soil. Additionally, a knowledge of site stratigraphy, subsurface, and groundwater conditions is essential to any project. For the Sea Island subject embankment site, these parameters have been defined using only in-situ test techniques and the most recent interpretation methods available. As consolidation of the normally consolidated clayey silt was expected to be a major factor in the settlement of the embankments, particular attention was paid to the accurate definition of parameters within this stratum.

5.1 Soil Profile

The cone penetration test has been recognized for its detail and accuracy in stratigraphic logging, and with the addition of pore pressure measurements, soil type identification has improved even more. For the five CPTU's performed at the site, consistent, repeatable results were obtained. The general stratigraphic sequence of the area interpreted from the CPTU tests was in agreement with the description given by Blunden (1973). Valuable details were also identified in the five CPTU's. Fig. 5.1 documents the results from test CPTU-6, showing corrected cone bearing, q_t, sleeve friction, f_s, friction ratio, R_f, and penetration pore pressure details.

As shown in the site plan of Fig. 4.1, sounding CPTU-1 was conducted approximately 35 m (115 ft.) north of sounding CPTU-6. Corrected cone bearing values for these two tests are shown on Fig. 5.2, within a general geologic profile of the area. Fig. 5.2 shows the site to be remarkably uniform. Little variability was exhibited among test locations, giving confidence to the definition of site stratigraphy in the vicinity of the embankments prior to their construction.

The most common method for identification of soil type from the cone penetration test makes use of cone bearing, q_c, and friction ratio, R_f, where

$$R_f = \frac{f_s}{q_c}(100\%) \qquad [5.1]$$

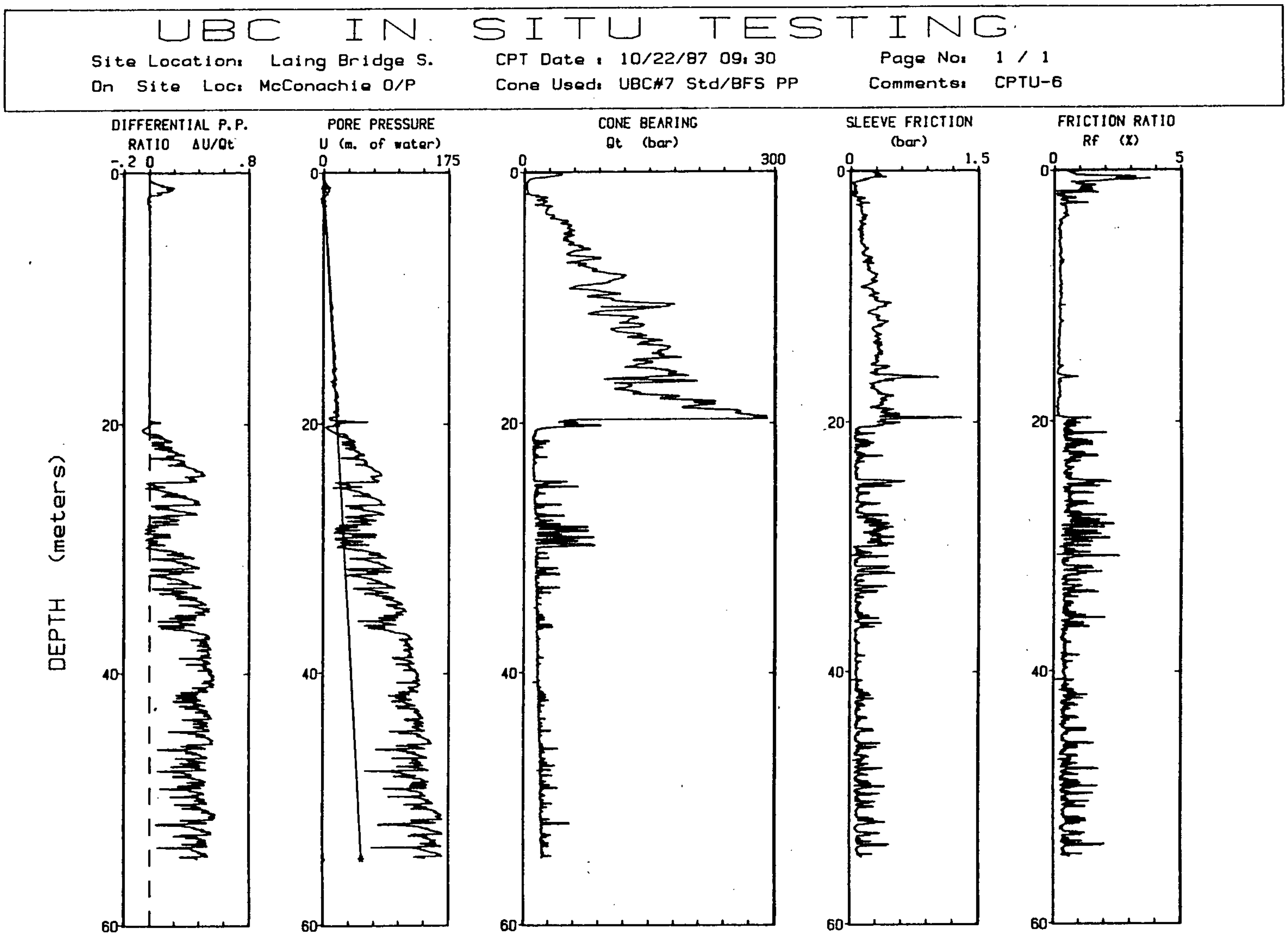

Fig. 5.1 Results from Piezocone Penetration Test CPTU-6

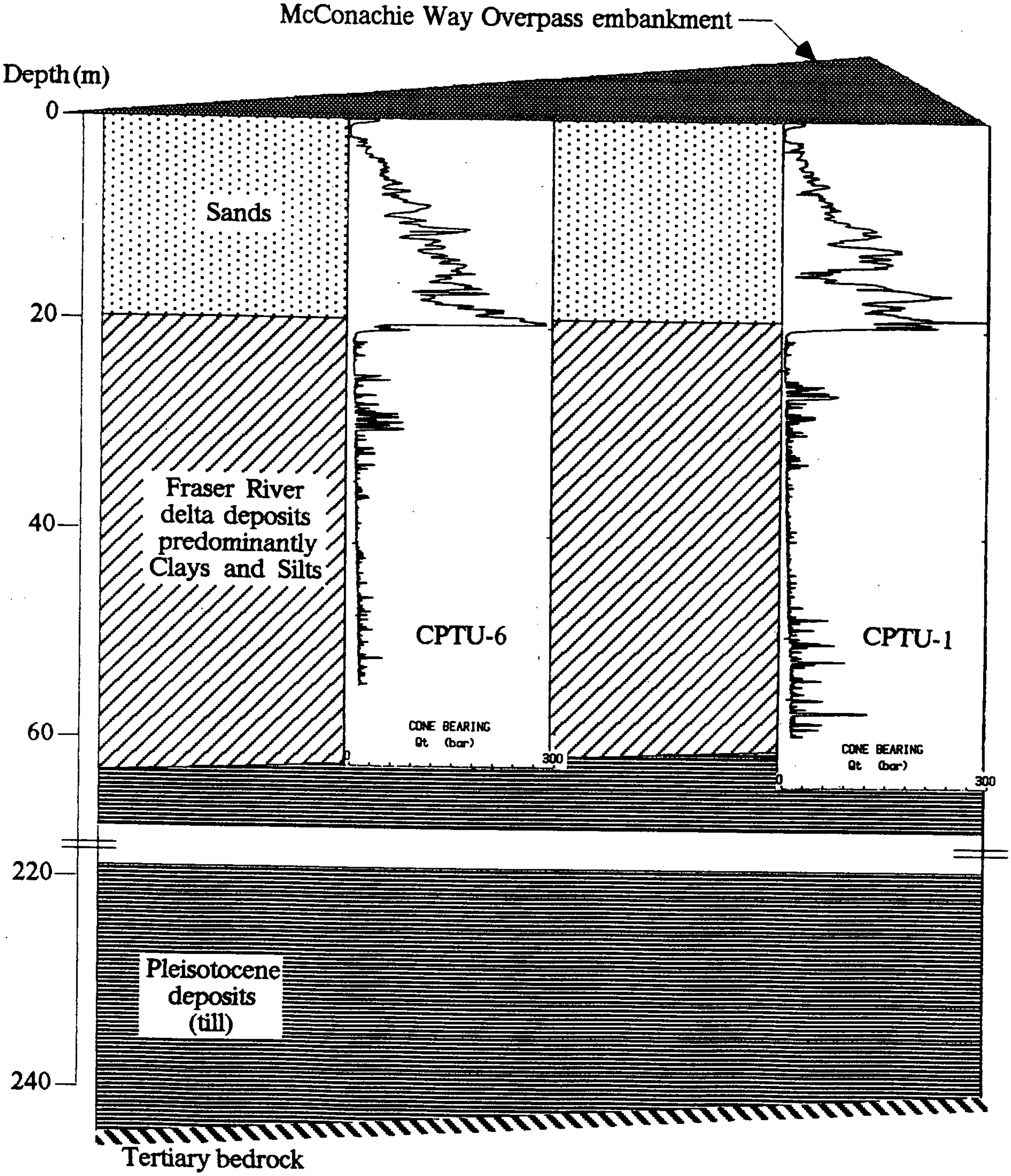

Fig. 5.2 General Site Geology and Cone Bearing Profile

Fig. 5.3 presents the soil behaviour type classification chart developed by Robertson *et al.* (1986), which incorporates UBC experience into the chart first produced by Douglas and Olsen (1981).

Using Fig. 5.3, a soil profile was interpreted for each CPTU. Fig. 5.4 compares the soil profile identified in a 1968 borehole log of R. C. Thurber and Associates Ltd. with the profile interpreted from piezocone penetration test CPTU-1. The borehole was part of the original site investigation program for the embankment construction project. The Thurber test hole was drilled approximately 50 m north of the location of test CPTU-1. Both profiles identify the same basic sequence, that is, a few metres of predominantly mixed, silty soil, underlain by clean sand increasing in density with depth, underlain by sensitive clayey silt. At the location of CPTU-1, penetration was refused below the 61 m depth, and this was assumed to be the top of the till sheet.

The interpreted profile shown on Fig. 5.4 was based only on cone bearing and sleeve friction values, using Fig. 5.3. Because the chart of Fig. 5.3 is not normalized for overburden pressure, the cone interpretation appears to incorrectly identify the soil below 51 m as silt and sand. If pore pressure information were incorporated, this stratigraphic sequence would have been identified as a cohesive deposit. Robertson (1988) has developed a modified soil behaviour type classification chart where cone resistance and friction ratio are normalized with respect to σ'_{vo}.

Aside from the very high density of the sand between the depths of 17 m and 20 m, cone penetration at this depth was impeded on two occasions by what was interpreted from the CPTU's as gravelly sand to sand. Local experience confirms the existence of shell fragments and coarse, cemented sediments near the interface of the normally consolidated clayey silt and the granular Fraser River channel deposits.

Considerably more stratigraphic detail was obtained from the piezocone sounding, as compared with the borehole. Of particular importance to this research was the identification of numerous layers, averaging 0.5 m to 0.7 m in thickness, of silty sand between the depths of approximately 26 m and 30 m.

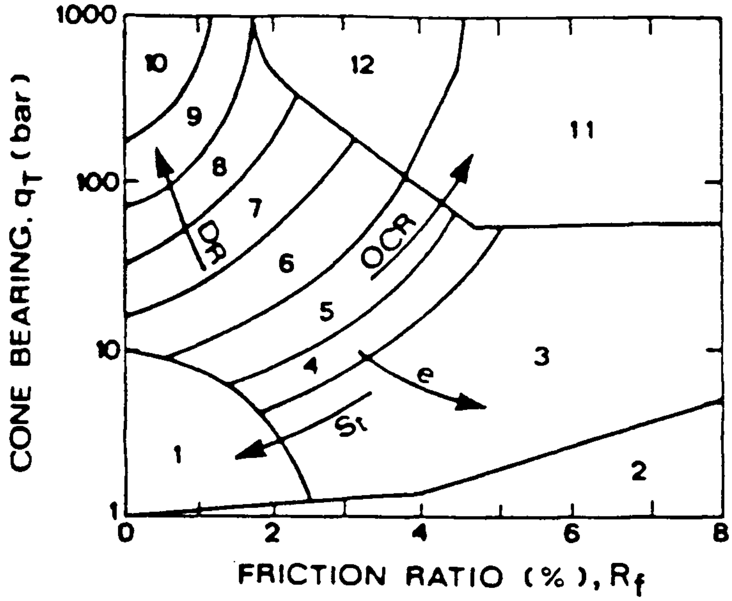

Zone	q_T/N	Soil Behaviour Type
1)	2	sensitive fine grained
2)	1	organic material
3)	1	clay
4)	1.5	silty clay to clay
5)	2	clayey silt to silty clay
6)	2.5	sandy silt to clayey silt
7)	3	silty sand to sandy silt
8)	4	sand to silty sand
9)	5	sand
10)	6	gravelly sand to sand
11)	1	very stiff fine grained (*)
12)	2	sand to clayey sand (*)

(*) overconsolidated or cemented

Fig. 5.3 Soil Behaviour Type Classification Chart
(after Robertson *et al.*, 1986)

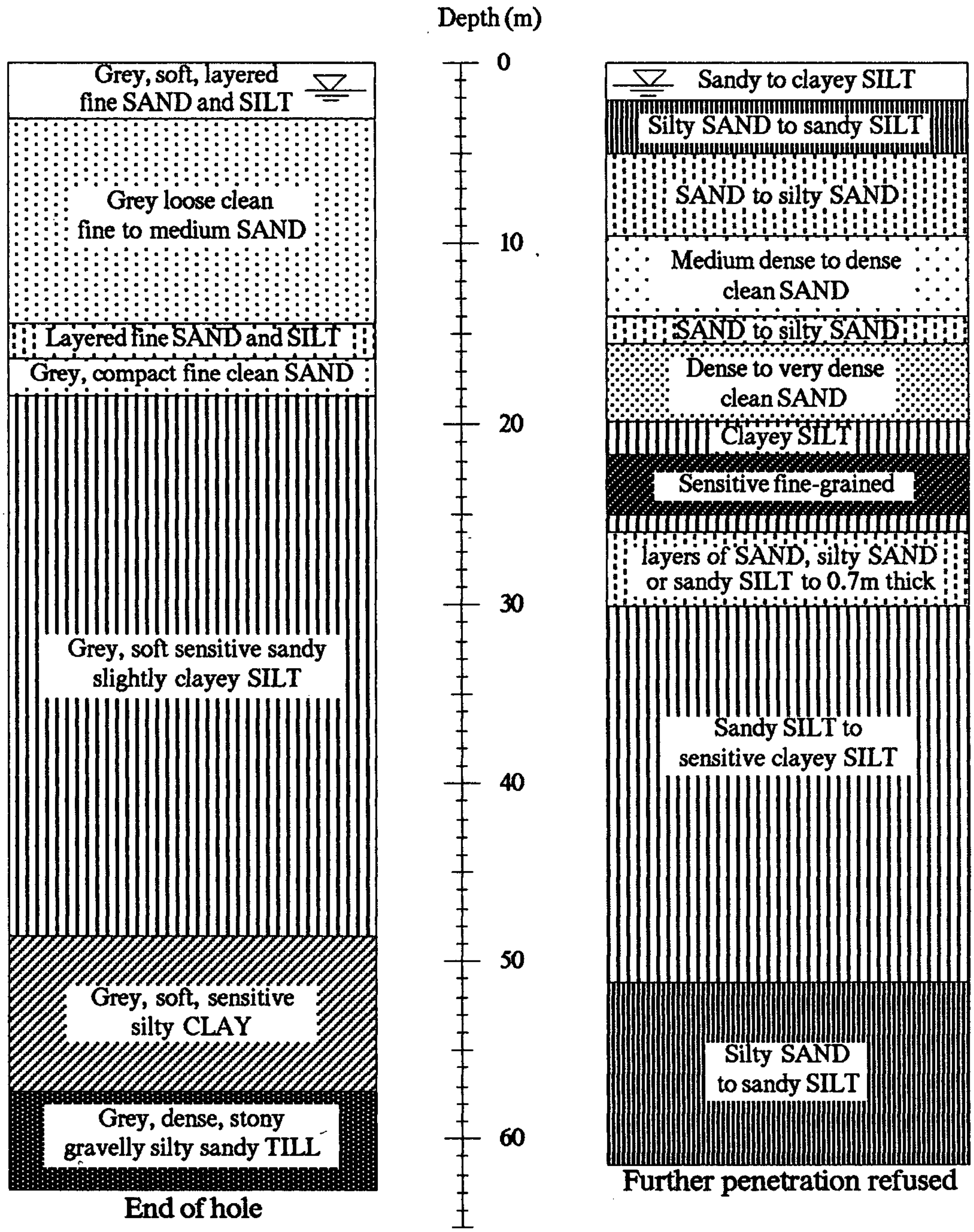

(a) Log of test hole no. 68-18
R. C. Thurber & Associates (September, 1968)

(b) Interpreted profile from cone penetration test CPTU-1 (August, 1987)

Fig. 5.4 Comparison of Soil Profiles Interpreted from Drill Hole and Piezocone Penetration Tests

5.2 Deformation Characteristics

5.2.1 Shear Modulus, G

The low-strain shear modulus, G_{max} was determined from shear wave velocities, using measurements from the seismic piezocone test CPTU-6 and equation 4.1. Previous research (Campanella *et al.*, 1985) has shown that G_{max} generally tracks well with cone bearing, inferring a relationship of the form

$$G_{max} = mq_c \qquad [5.2]$$

where m is a correlation coefficient depending on soil type. Fig. 5.5 shows shear modulus and cone bearing measurements obtained at the embankment site. While there is some scatter exhibited in the modulus values, an average ratio of G_{max} to q_c of 40 is found. That is, the m value in equation 5.2 is equal to 40 for the clay silt deposit, with G_{max} and q_c in bars.

The shear modulus determined from shear wave velocity is a low strain ($\gamma < 10^{-3}\%$) modulus. Therefore at the level of strain induced by the embankments, the shear modulus mobilized may be considerably smaller than G_{max}. However, knowledge of the shear modulus in the clay silt stratum is still pertinent to the present study since the interpretation of consolidation characteristics is dependent on rigidity index, which is the ratio of shear modulus to undrained shear strength.

Also, for seismic design, G_{max} is an important parameter and one which is easily determined from the seismic cone penetration test.

5.2.2 Young's Modulus, E

Penetration testing is generally assumed to be a drained penetration in cohesionless soils and an undrained penetration in cohesive soils. Consequently, discussion of Young's

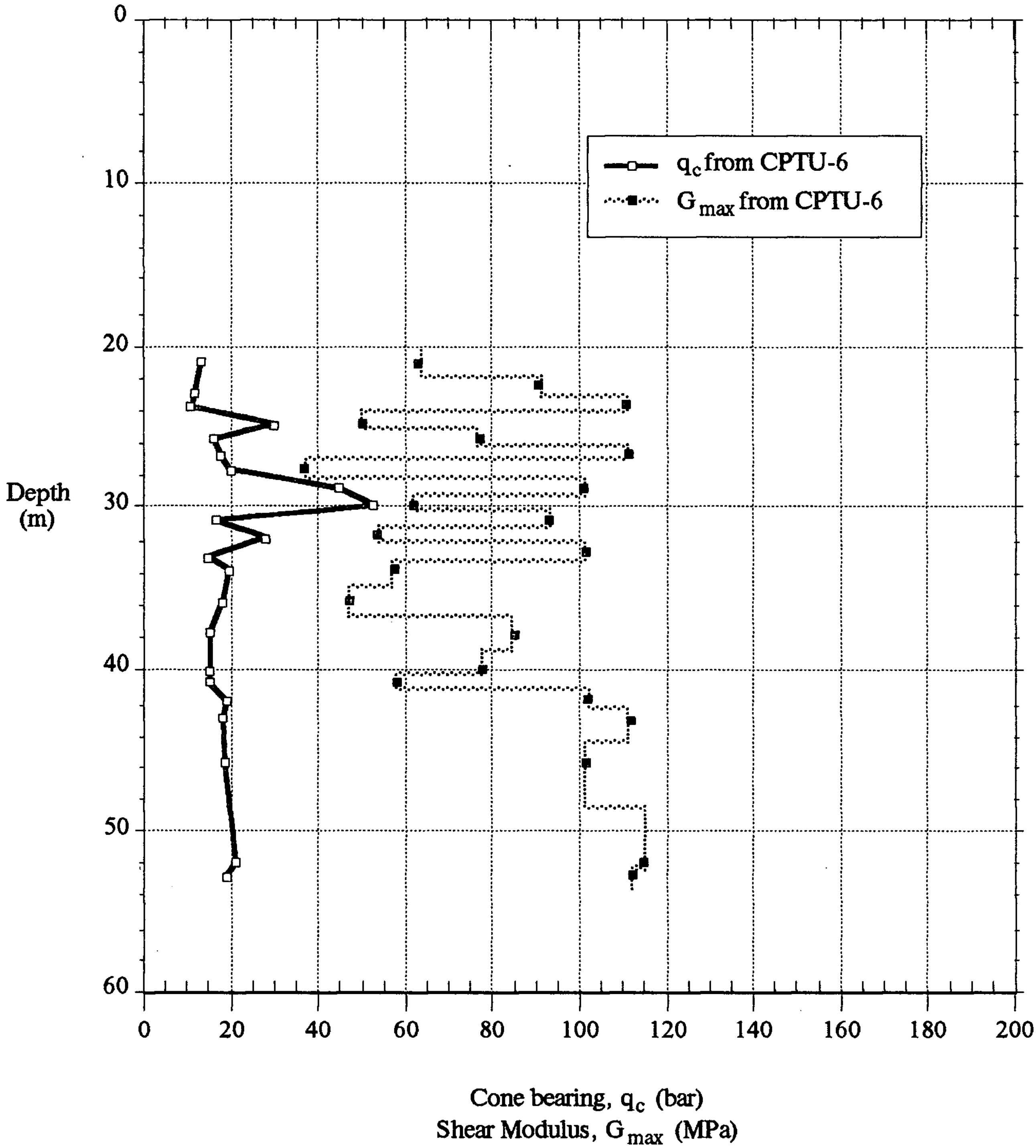

Fig. 5.5 Cone Bearing from SCPTU and Interpreted Shear Modulus

modulus will be divided into two sections, one for the drained parameter and one for the undrained.

5.2.2.1 Equivalent (Drained) Young's Modulus, E_s

An equivalent Young's modulus may be determined from the screw plate test and, using empirical correlations, from the cone penetration test.

Schmertmann (1970) presented a method for determining E_s, assuming a homogeneous, elastic half space, from the results of the screw plate test. Assuming a constant modulus within the strain area beneath the plate, Schmertmann (1970) showed that

$$E_s = 1.2C_1\frac{\Delta p}{\rho}B \qquad [5.3]$$

where: Δp = applied screw plate stress

ρ = measured plate deflection

B = screw plate diameter,

C_1 is a correction factor to incorporate the effect of strain relief due to embedment, and

$$C_1 = 1 - 0.5\frac{\sigma'_o}{\Delta p} \qquad [5.4]$$

where: σ'_o = effective vertical overburden pressure.

A complete derivation of equation 5.3 may be found in Berzins (1983). The method is basically a back calculation of modulus using elastic settlement theory, where the known load-settlement behaviour of the screw plate replaces the foundation pressure and unknown foundation settlement. The method has application over a stress range of 100 to 300 kPa, and cannot be confidently applied at low stresses, particularly at depth.

From a review of calibration chamber results (Baldi *et al.*, 1981), Robertson and Campanella (1985) provided the relationship

$$E_s = nq_c \tag{5.5}$$

between the drained secant Young's modulus and cone bearing. The Young's modulus was defined at stress levels commonly induced by shallow foundations, that is, 25% to 50% of failure stress levels. For normally consolidated, uncemented quartz sands, n was found to vary between 1.5 and 3.0, which is in agreement with the value of 2 recommended by Schmertmann (1970).

An equivalent Young's Modulus for the sand layer at the embankment site was calculated using equation 5.3. The values of Δp and ρ were obtained from the initial portion of the load-deflection curve measured in the field SPLT. Test data may be found in Appendix B.

Using the values of E_s calculated from the screw plate test and average cone bearing values from the five cone penetration tests, the value of n in equation 5.5 was found to be 1.2 ± 0.9. This value may appear to agree with recommended values given above, however, this average masks the actual results, which varied from $n = 4$ near the surface to $n = 0.4$ at a depth of 19 m. While the values of E_s from the screw plate test remained within a fairly narrow range, q_c increased markedly with depth, as the sand increased in density.

5.2.2.2 Undrained Young's Modulus, E_u, and Undrained Strength, S_u

Undrained Young's modulus is usually estimated from CPTU data using empirical correlations with undrained shear strength, S_u, of the form

$$E_u = kS_u \tag{5.6}$$

where the constant k is dependent upon stress level, stress history, sensitivity, and other factors. Therefore an estimate of undrained strength is first required.

The undrained shear strength is not a unique value for a given cohesive soil, but is a function of the type of test used. Estimates of undrained strength from cone penetration test data were made using the equation

$$S_u = \frac{q_c - \sigma_{vo}}{N_k} \qquad [5.7]$$

where: σ_{vo} is the total in-situ vertical overburden pressure

N_k is the cone factor, obtained from empirical correlations. A value of $N_k = 15$ was used for the present analysis. Lunne and Kleven (1981), using field vane strength as a reference, showed that, for normally consolidated marine clays, the cone factor generally falls between 11 and 19, with an average of 15.

Undrained shear strength may be determined from the screw plate test using a method similar to that for the cone, where

$$S_u = \frac{p_{ult} - \sigma_{vo}}{N_k} \qquad [5.8]$$

where: p_{ult} is the ultimate average plate stress

N_k depends on boundary conditions, the soil-plate interface, and plate stiffness. Selvadurai *et al.* (1980), after reviewing classic theoretical and empirical solutions, concluded that

$$N_k(\text{screw plate}) = \begin{cases} 9 \text{ for partial bonding} \\ 11.35 \text{ for full bonding} \end{cases} \qquad [5.9]$$

A value of $N_k = 10$ was assumed for the present analysis.

The data reduction program accompanying the flat dilatometer test apparatus also provides an empirical correlation for S_u. Fig. 5.6 shows the values of undrained strength predicted by each of the three in-situ test methods, CPTU, DMT, and SPLT, along with the values determined from laboratory vane tests on undisturbed field samples which were obtained

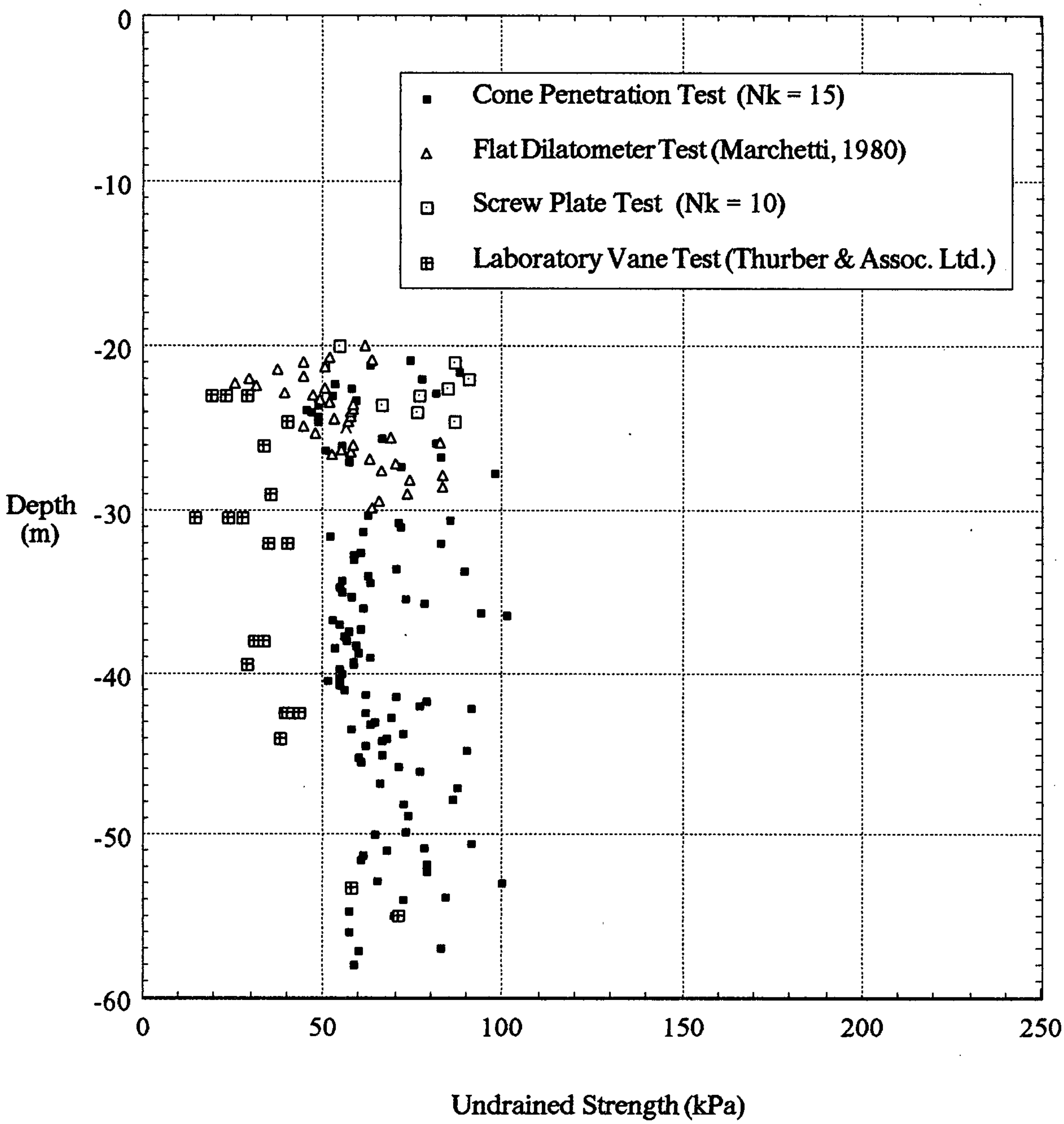

Fig. 5.6 Summary of Undrained Strength Values

in the 1968 investigation program. The three in-situ test methods show good agreement and consistently predict higher undrained strengths that the laboratory tests, which may reflect the influence of scale and sample disturbance on the lab-determined strength.

Test interpretations show a generally linear increase in S_u with depth, a trend commonly seen in normally consolidated deposits, with a departure from this trend between the depths of 26 m and 35 m, where considerable sandy silt layering is encountered. The scatter in values interpreted from the CPTU in the mixed clay and silt soil is due to internal averaging of the actual values over 0.25 m increments by a computerized interpretation program.

The undrained Young's modulus for the clayey silt at the embankment site was interpreted directly from screw plate test results, using the expression (Selvadurai and Nicholas, 1979)

$$\frac{\delta}{pa/E_u} = \lambda \qquad [5.10]$$

where: δ = plate displacement

p = average stress on screw plate

a = screw plate radius

λ = a modulus factor which falls in the range of 0.60 to 0.75. The upper limit applies when the plate is partially bonded to the soil, which may be the case in a sensitive soil, and was used for the present analysis.

The values of p and δ were obtained from the initial portion of the load-deflection curve measured in the field SPLT. Test data may be found in Appendix B.

Since the screw plate test provided estimates of both E_u and S_u, these were used to determine the constant, k, in equation 5.6. The value of k was found to range between 200 and 300 at the depths tested, between 20 m and 24.5 m.

Fig. 5.7 presents the values of Young's modulus, both drained and undrained, interpreted from the screw plate test and piezocone penetration test. The figure shows E_s and E_u as calculated directly from screw plate test results, using equations 5.3 and 5.10, respectively. From piezocone penetration tests, E_s was calculated using equation 5.5, with n = 2; E_u was calculated using equation 5.6 with k = 250 and S_u from Fig. 5.6 (N_k = 15). As Fig. 5.7 reveals, good agreement is found in the clayey silt where the two sets of data coincide; therefore, some confidence can be placed in the values correlated from the CPTU S_u values at depth. Good agreement is also manifest in the upper 10 m of sand, however from depths of 10 m to 20 m, there is significant difference in E_s. As mentioned previously, E_s correlated from cone bearing reflects the increasing density and increase in confining pressure, with depth, of the sand, whereas E_s calculated from the screw plate test remains within a narrow range. This may be due to increased friction along the rod lengths when testing within the dense sand deposit.

5.2.3 Constrained Modulus, M

The constrained modulus relates stress and strain where strain is assumed to occur only in one direction, usually vertically. Therefore the constrained modulus is often referred to as a one-dimensional modulus, and can be used to compute vertical settlements.

The data reduction program accompanying the flat dilatometer apparatus provides an empirical correlation for M, based on Marchetti (1980). As well, numerous empirical correlations have been developed between cone resistance and constrained modulus, these having the form

$$M = \alpha q_c \qquad [5.11]$$

In order to calculate the factor α for the normally consolidated clayey silt deposits of the Fraser River delta region, the M values obtained from flat dilatometer tests were compared to values of cone bearing at the same depth. The result, as shown on Fig. 5.8, is a factor of

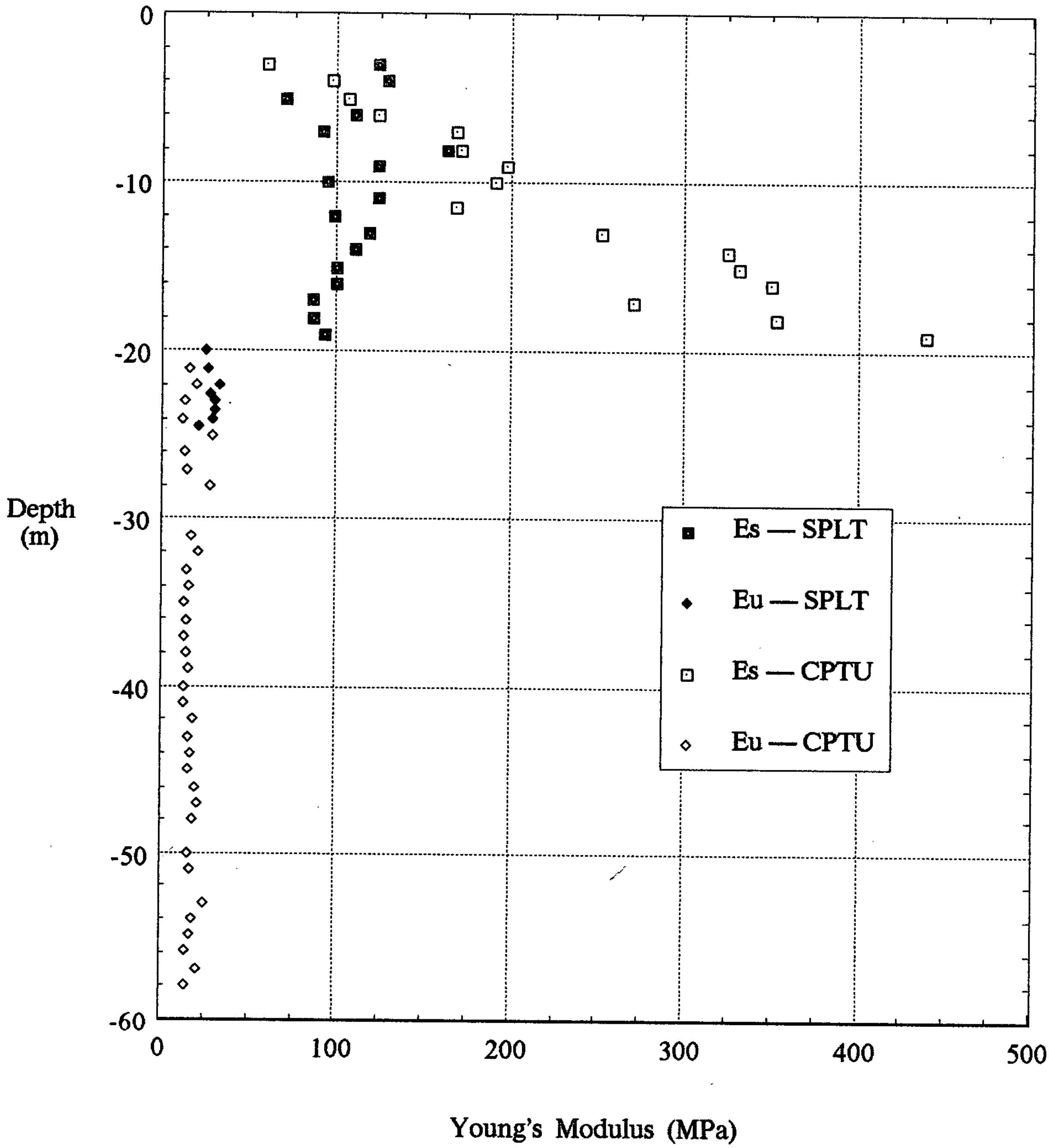

Fig. 5.7 Summary of Young's Modulus Values

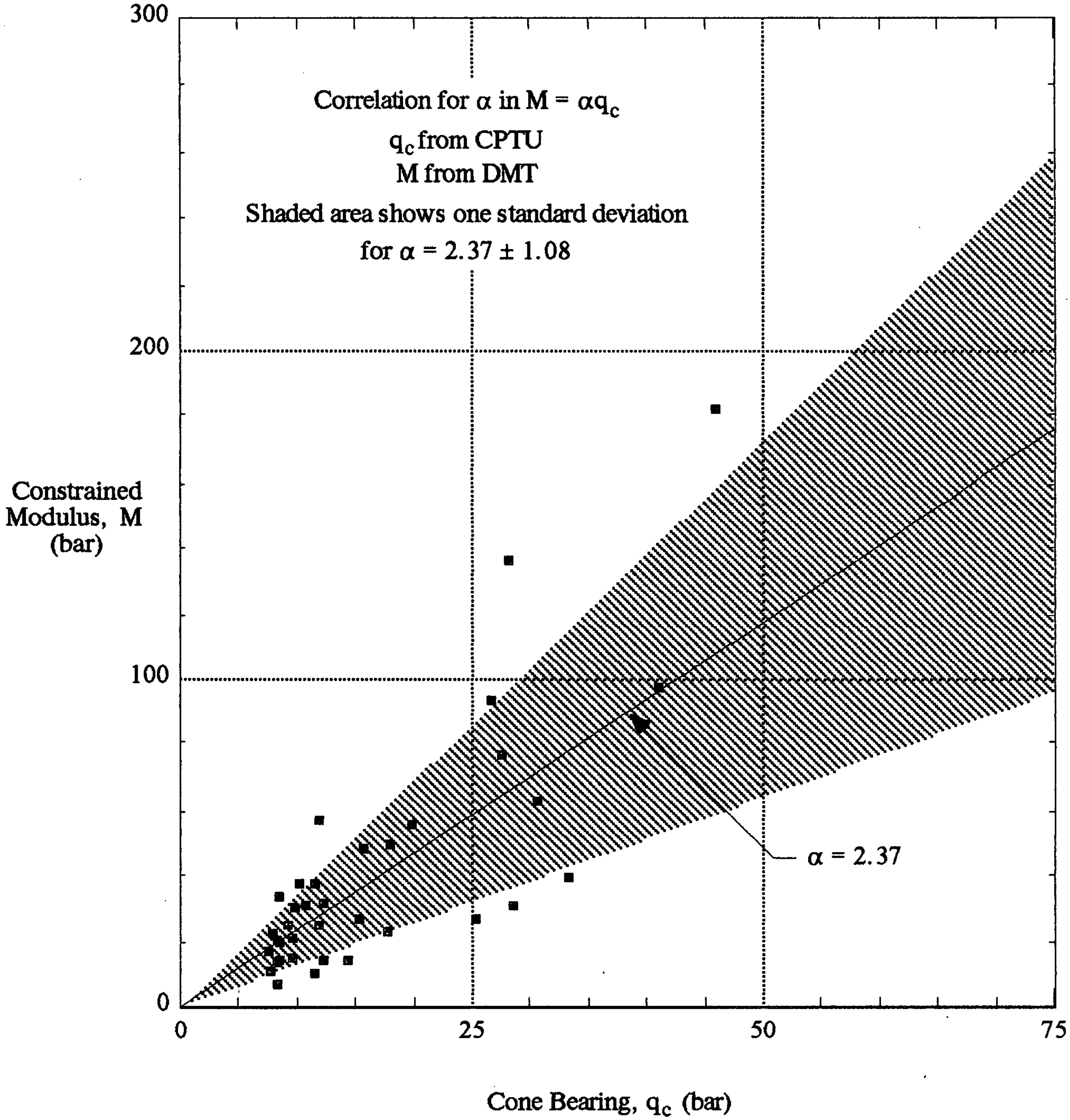

Fig. 5.8 Correlation Between One-Dimensional Constrained Modulus and Cone Bearing

$$\alpha = 2.37 \pm 1.08 \qquad [5.12]$$

which agrees very well with the range of α = 1 to 3, given by Mitchell and Gardner (1975) for silts of low plasticity where q_c is less than 20 bars. Since dilatometer testing was carried out only to a maximum depth of 35.6 m, this correlation was utilized with q_c data throughout the entire depth of clay silt to obtain a profile of M with depth. This profile is shown on Fig. 5.9, with values for the upper 20 m of sand taken directly from the dilatometer data reduction program.

Dilatometer testing was conducted sufficiently far away from the existing embankments so as to test virgin soil unaffected by the embankment load. The modulus values, as shown on Fig. 5.9, were used to calculate settlement during the embankment construction and preloading phase.

The determination of an appropriate modulus to use in settlement analysis requires considerable judgment. In-situ testing offers the advantage of testing soil at its existing level of stress, however, as modulus is stress-level dependent, decisions must be made on an appropriate level of stress at which to compute the modulus. The determination becomes even more complicated when the same soil is subject to changes in in-situ stresses, as in the case of preloading. The in-situ tests used in this analysis provided reasonably complementary results for the parameters required in settlement calculation. Where values diverged among test methods, the parameter often had minimal effect on the end result, that is, the calculated settlement was not highly sensitive to large variations in the estimated parameter value.

5.3 Consolidation Characteristics

Laboratory consolidation tests on field samples have traditionally been performed in order to measure properties for use in geotechnical settlement analyses. The ability to evaluate flow and consolidation characteristics from the time rate of pore pressure dissipation using the piezocone

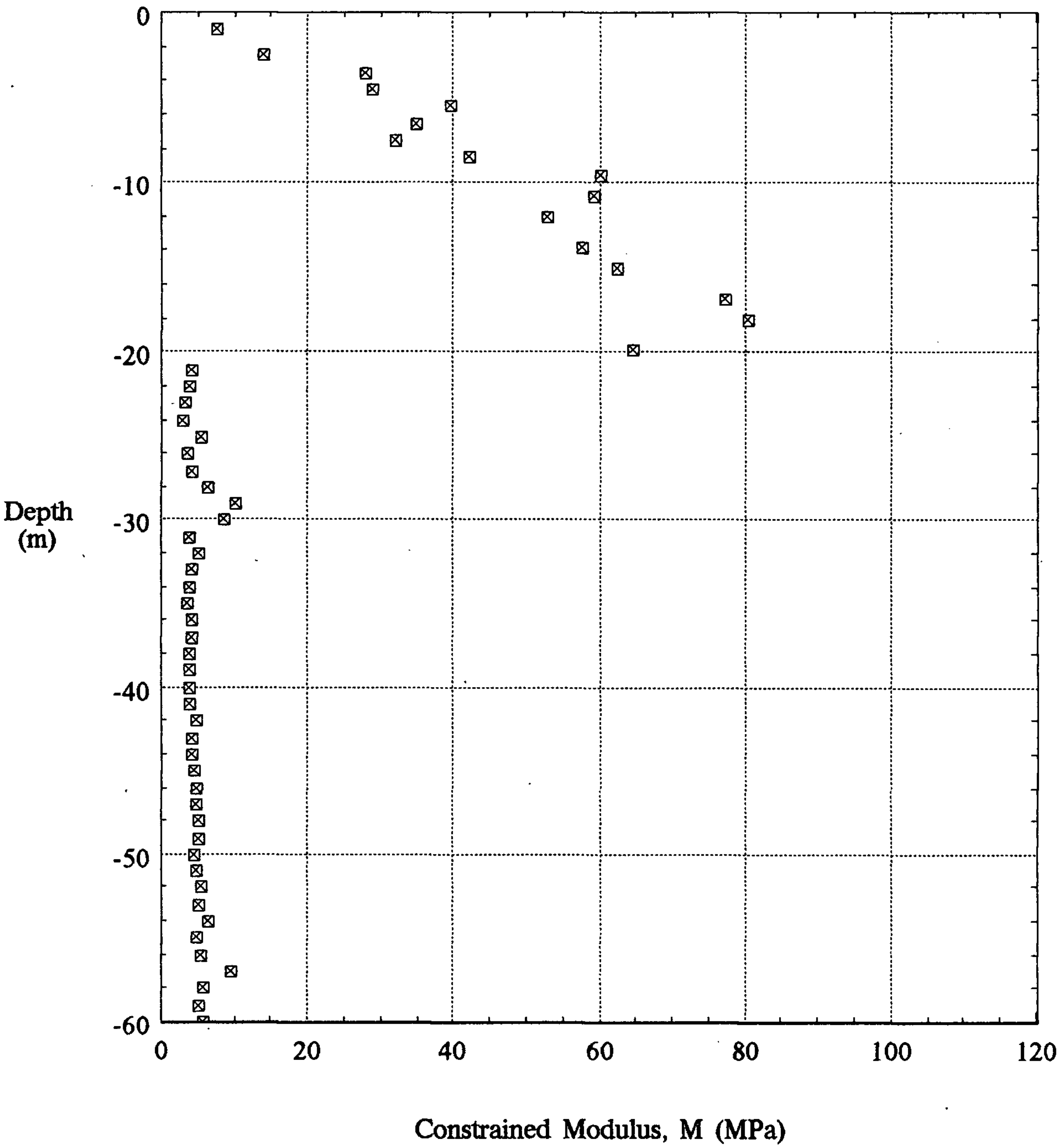

Fig. 5.9 Summary of Constrained Modulus Values

and, recently, the dilatometer, has provided an alternative approach to discerning the consolidation characteristics of a soil.

5.3.1 Pore Pressure Dissipation Tests

A piezocone dissipation test is conducted during a pause in penetration at any depth where consolidation characteristics are required. The decay of excess pore pressure is monitored with time. In the case of the present research, pore pressure measurements were taken at five-second intervals. Fig. 5.10 shows data collected at the embankment site during a dissipation test at a depth of 54.8 m, with pore pressure sensing elements at two locations on the cone, u_2 behind the cone tip, and u_3 behind the friction sleeve. The push rods were not clamped during dissipation tests since recent research (Campanella and Robertson, 1988) has shown that changes in pore pressure measurements caused by movement or creep of the rods is generally not significant when the piezometric element is located behind the cone tip. Fig. 5.10 indicates that while only three minutes are required for half of the initial excess pore pressure to dissipate, as measured at the u_2 position, times approaching one hour are required to re-establish equilibrium (hydrostatic) pore pressure.

Since the closing pressure (C reading) closely represents the pore pressure on the flat dilatometer membrane in soft clays, Robertson *et al.* (1988) imply it should be possible to record the C reading with time and obtain a dissipation curve using a standard Marchetti dilatometer. Fig. 5.11 shows DMT dissipation readings obtained by two procedures, one where membrane lift-off was achieved and C reading taken (A-C reading procedure), and another where membrane lift-off was followed by 1 mm expansion, then the C reading taken (A-B-C reading procedure). Fig. 5.11 illustrates that slightly more stable readings are obtained using the A-C reading procedure than with the A-B-C reading procedure. The difference in response is probably related to small changes in effective and total stresses around the membrane during dissipation, depending upon whether or not the soil is pushed out by expanding the membrane once more.

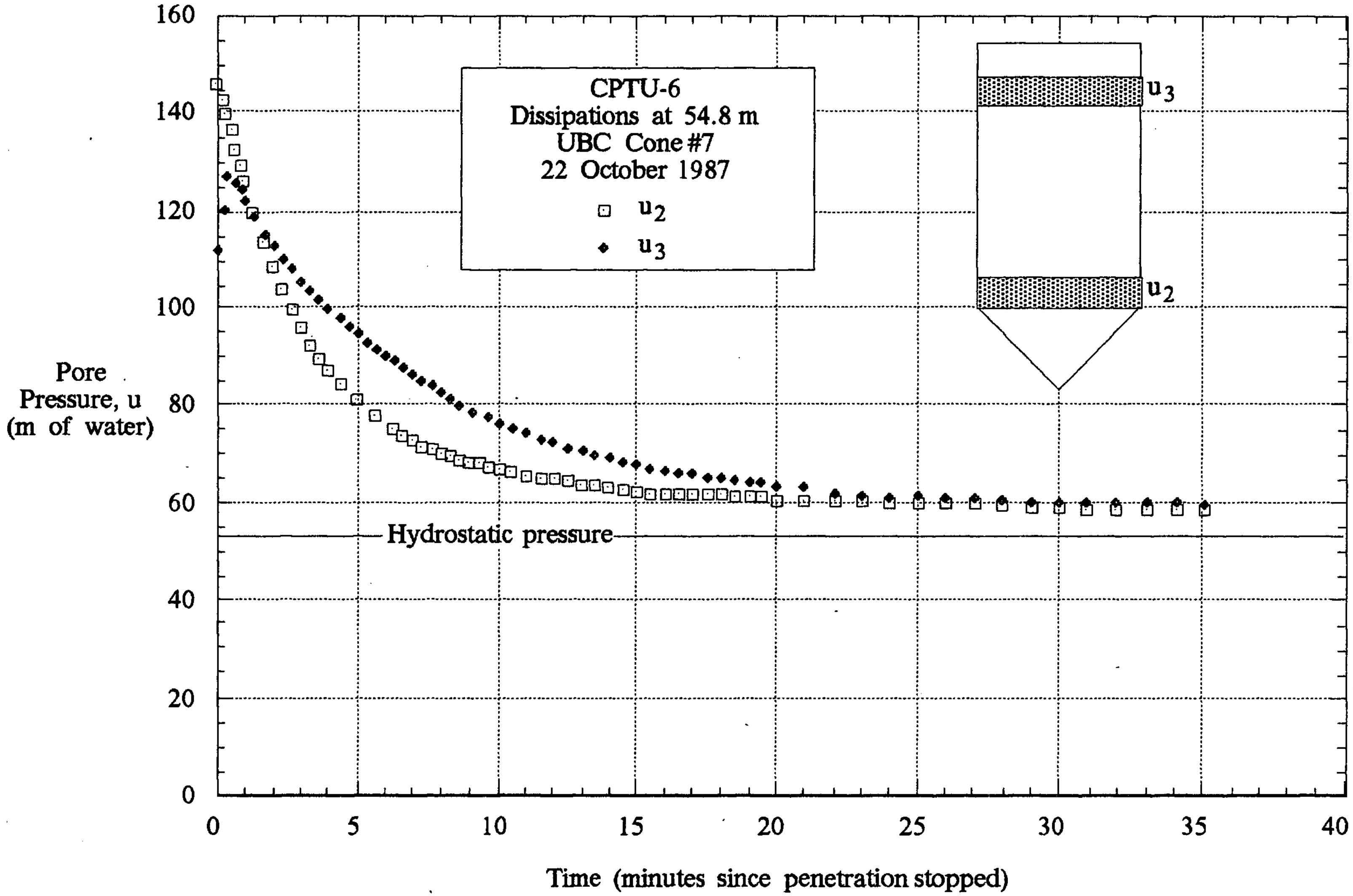

Fig. 5.10 Pore Pressure Dissipations Measured at Different Locations on Piezocone

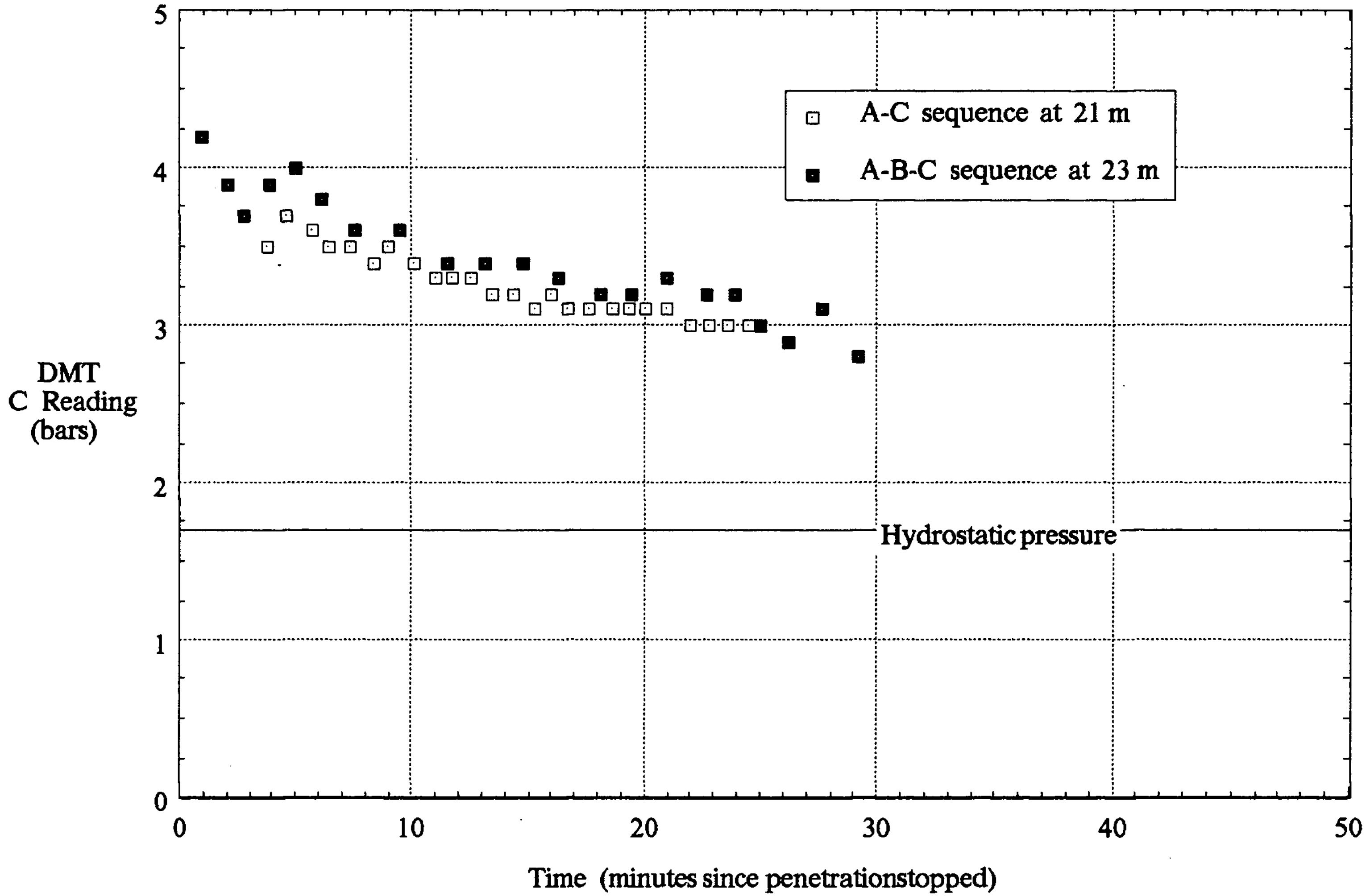

Fig. 5.11 Record of DMT Dissipations Using Two Procedures

Levadoux and Baligh (1986) suggested that normalized pore pressure, U, provides a good measure of degree of consolidation, with

$$U = \frac{\Delta u}{\Delta u_i} \qquad [5.13]$$

where $\Delta u = u_t - u_o$

$\Delta u_i = u_i - u_o$

u_t = measured pore pressure at time t

u_o = equilibrium (often assumed to be hydrostatic) pore pressure

u_i = initial pore pressure at the commencement of the dissipation test.

Extending the same idea to dilatometer C reading data, an equivalent normalized pore pressure may be obtained from:

$$U = \frac{C_t - u_o}{C_i - u_o} \qquad [5.14]$$

where C_t = C reading at time t

C_i = initial C reading at time t = 0.

While a C reading is never obtained at time = 0, this value may be obtained from a plot of C reading versus square root of time, and the initial, straight-line portion of the curve back extrapolated to zero.

When dissipation data is normalized as described above, it is possible to compare CPTU and DMT data. Fig. 5.12 shows that, at a depth of 23 m, it takes approximately eight minutes to reach 50% consolidation (t_{50} = 8 minutes) in a CPTU dissipation test using a 10 cm^2 cone, and approximately twice as long, (t_{50} = 16 minutes) in a DMT dissipation test.

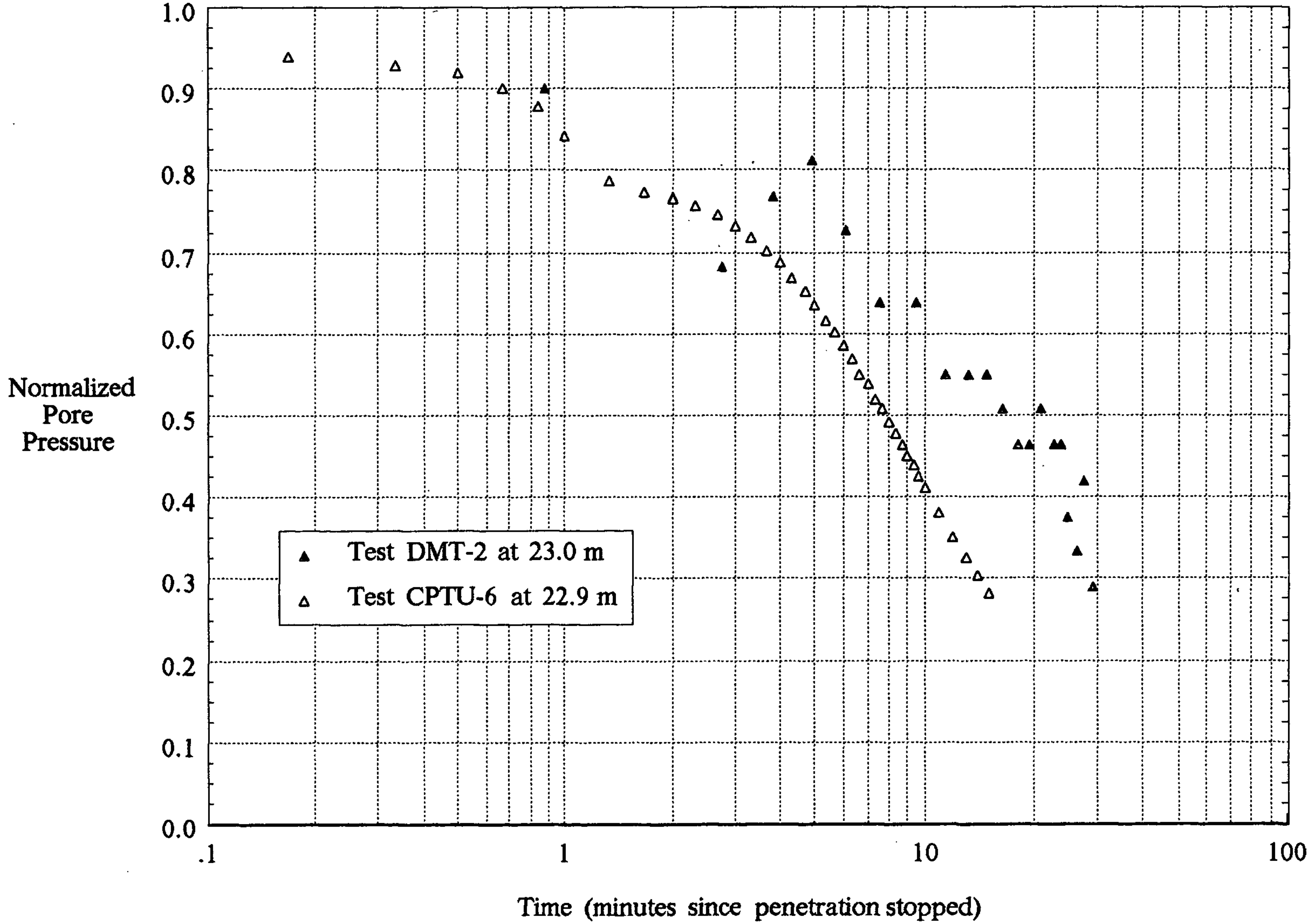

Fig. 5.12 Piezocone and Dilatometer Dissipation Record

Although a similar trend is evident in the CPTU and DMT dissipation curves shown in Fig. 5.12, Fig. 5.13 shows a different trend obtained from two dissipation tests at a depth of 35 m. At this depth, the clayey silt stratum contains numerous silty and sandy silt layers. This increased permeability is indicated by the CPTU, but not by the DMT. Therefore, it appears that piezocone measurements are more sensitive to thin drainage layers than dilatometer test measurements.

The dissipation rate of excess pore pressure is controlled by the consolidation and permeability characteristics of the soil. The coefficient of consolidation in the horizontal direction, c_h, may be calculated from a dissipation test using one of several theoretical solutions.

5.3.2 Theoretical solutions

Gillespie (1981) provides a comprehensive discussion of the theoretical solutions available for obtaining consolidation characteristics from piezocone dissipation tests. Two of these methods were utilized in the present analysis.

Torstensson (1977) theorized that pore pressures caused by steady cone penetration could be estimated by one-dimensional solutions corresponding to the expansion of spherical and cylindrical cavities. His analysis assumed an isotropic, elastic, perfectly-plastic soil with isotropic initial state of stress, and used linear, uncoupled, one-dimensional finite difference consolidation theory to estimate consolidation rates. He proposed matching theoretical predictions and measured values at 50% consolidation, U = 0.5, to find the coefficient of consolidation in the horizontal direction, c_h, using

$$c_h = \frac{T_{50}}{t_{50}} R^2 \qquad [5.15]$$

where T_{50} is the dimensionless time factor at 50% consolidation and is a function of E/S_u,

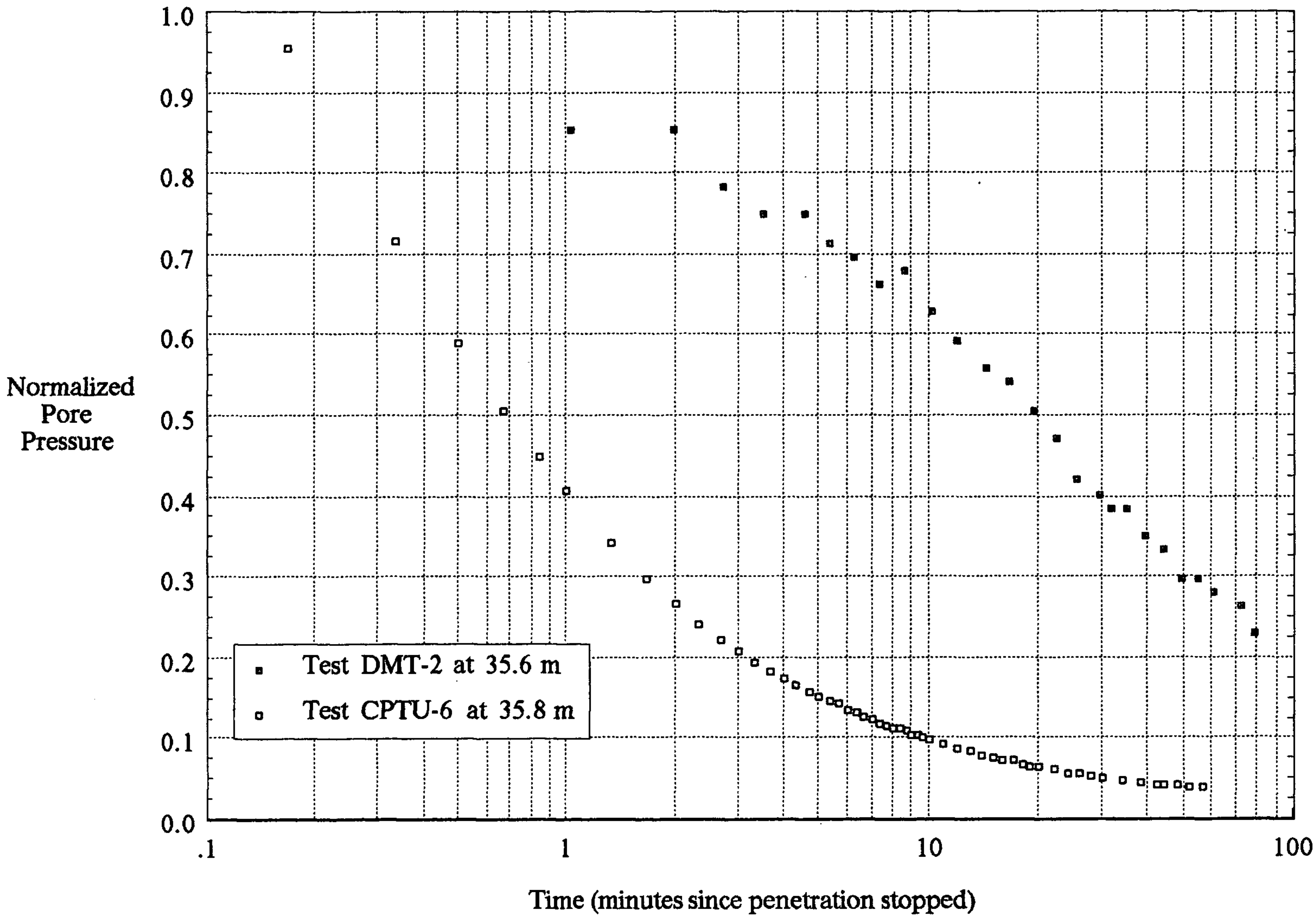

Fig. 5.13 CPTU Dissipation Exhibits Greater Sensitivity to Drainage Layers than DMT

t_{50} is the measured time to achieve 50% consolidation, and

R is an equivalent cavity radius.

Levadoux and Baligh (1986) noted that the above method for determining c_h does not account for non-linearities during consolidation, soil remoulding, or creep effects, and found no acceptable argument for curve fitting about t_{50}. Rather, Baligh and Levadoux (1986) recommend a method based on predictions obtained from linear, uncoupled consolidation analyses and initial pore pressure distributions calculated by the strain path method for undrained penetration in Boston blue clay, using the normalized excess pore pressure distribution, U, and tabulated values of the time factor, T.

5.3.3 Coefficient of Consolidation

Levadoux and Baligh (1986) report that, in clays, dissipation is principally controlled by the horizontal coefficient of consolidation, especially in the early stages of consolidation, since permeability in the horizontal direction is generally greater than in the vertical. Local research (Gillespie, 1981) has shown that consolidation in the clayey silt underlying the Fraser Delta is also controlled by horizontal drainage, therefore use of c_h in a consolidation analysis is appropriate.

For the present analysis, the horizontal coefficient of consolidation was determined by curve-fitting about t_{50}, using values of T recommended by Torstensson (1977) and by Baligh and Levadoux (1986), applying equation 5.15 to dissipation test data from both the piezocone and dilatometer. The various theoretical values of the dimensionless time factor may be found tabulated in Appendix A.

In the case of the piezocone, a value of R = 0.561 cm, the radius of a standard 10-cm^2 cone shaft, was used in equation 5.15 to estimate c_h. Fig. 5.14 provides an example of

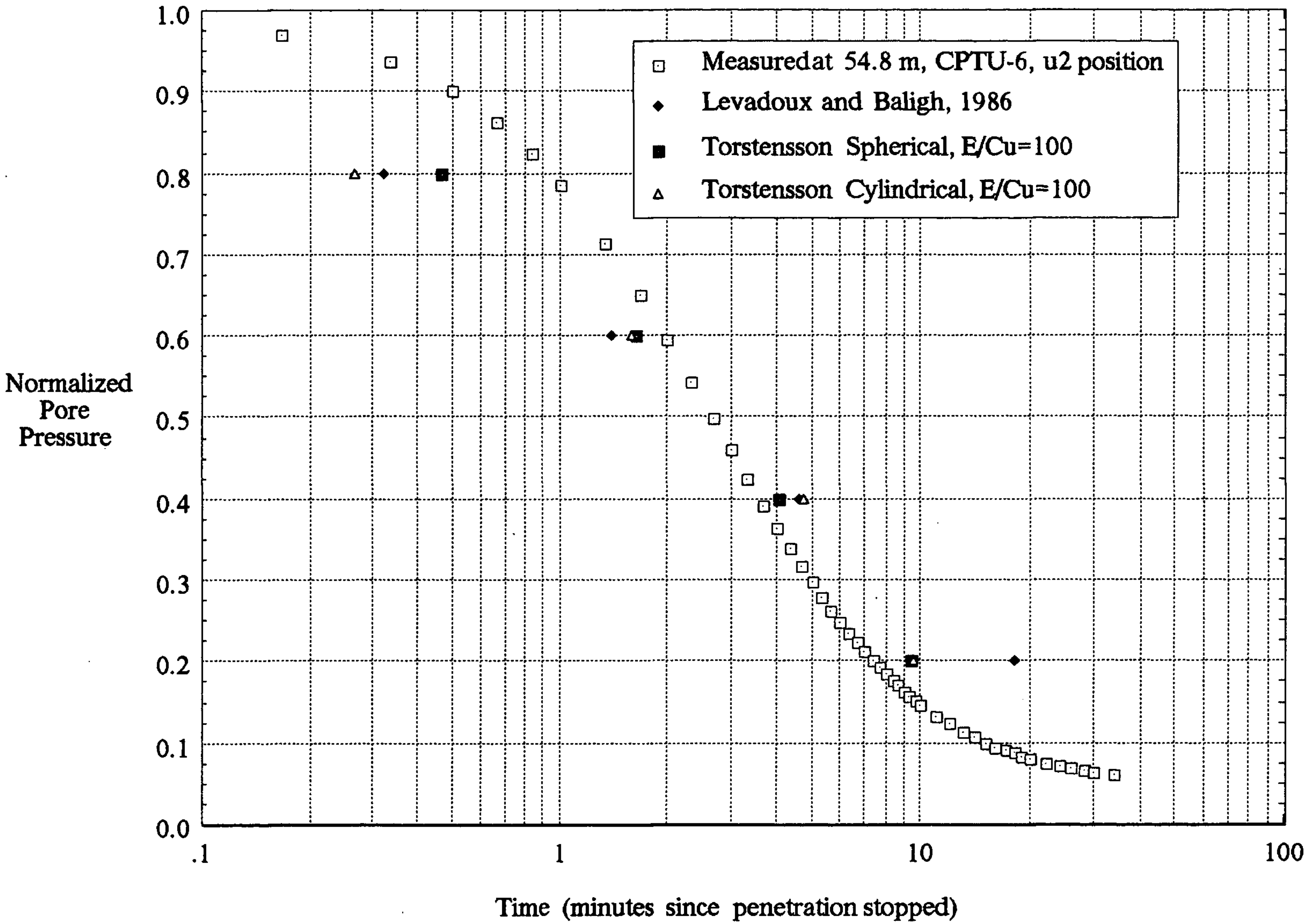

Fig. 5.14 Theoretical Curve Fitting About Time for 50% Pore Pressure Dissipation

theoretical curve fitting, presenting measured CPTU dissipation data along with data points predicted by theoretical analyses at U = 0.8, 0.6, 0.5, 0.4, and 0.2. At all stages of consolidation, the spherical solution of Torstensson (1977), with a soil rigidity index of 100, provides the best fit to the measured data. Further deviation from the measured data was observed as rigidity index was increased from 100 to 500. The interpretation of a spherical cavity is potentially the most rational, as Levadoux and Baligh (1986) indicate that contours of $\Delta u/\sigma'_{vo}$ around a 60° cone are spherical in shape.

In the case of the dilatometer, an equivalent radius of the standard Marchetti blade, of R = 2.057 cm, was used, as recommended in Robertson *et al.* (1988). To date, this procedure for the DMT has only been verified for soft, normally consolidated to lightly overconsolidated soils. As with theoretical curve fitting for CPTU data, the spherical solution of Torstensson (1977), with a soil rigidity index of 100, provided the best fit to the measured data.

A horizontal coefficient of consolidation was determined at t_{50}, using Torstensson's (1977) spherical solution, for each dissipation test conducted with the piezocone and dilatometer. Fig. 5.15 presents a summary of the c_h values determined in this manner alongside laboratory-determined values for comparison purposes. Points representing the average values obtained by R. C. Thurber & Associates Ltd. (1968), are shown. Laboratory-determined c_v values and in-situ-determined c_h values show close agreement. The majority of values fall within a narrow band averaging 4 x 10^{-3} cm^2/s. Potential drainage layers of sandy silt, where c_h is considerably greater, are clearly identified by the piezocone dissipation tests.

Levadoux and Baligh (1986) suggest that pore pressure dissipation, during early stages of consolidation of the soil in the vicinity of the piezocone, takes place in a recompression mode for both normally consolidated and overconsolidated soils, and suggest c_h in the normally consolidated (NC) range may be evaluated by:

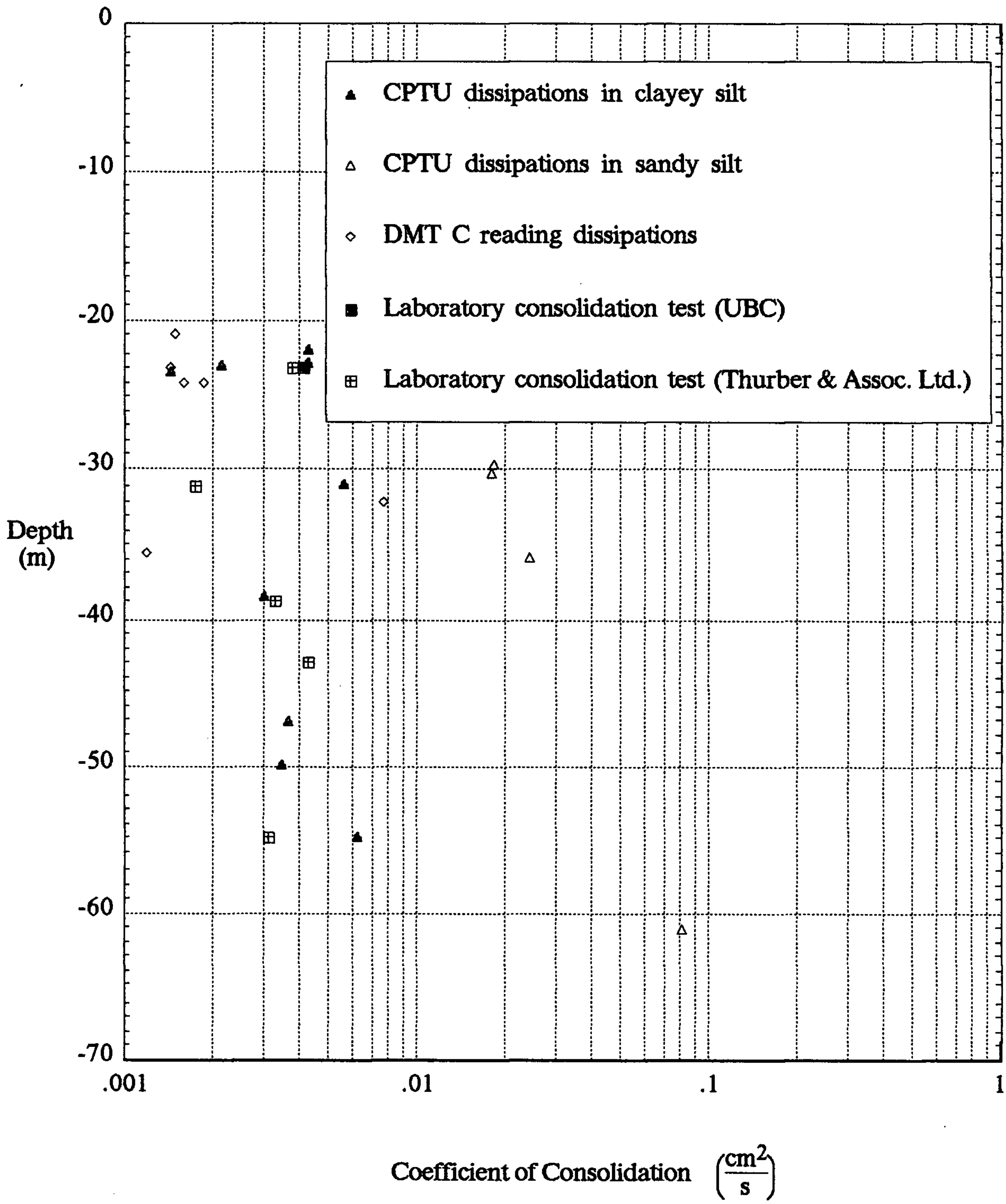

Fig. 5.15 Profile of Coefficient of Consolidation with Depth

$$c_h(NC) = \frac{RR(\text{piezocone})}{CR} c_h(\text{piezocone}) \qquad [5.16]$$

where RR (piezocone), the recompression ratio, represents the strain per log cycle of effective stress during recompression, and

CR, the compression ratio, is the average slope of the strain versus log effective stress plot in the effective stress range expected during consolidation.

The slope of the compression portion of a consolidation curve is generally five to ten times that of the recompression portion, therefore it would be expected that c_h(NC) would be approximately one-fifth to one-tenth the value determined from the early stages of a piezocone dissipation test. However, for the coefficient of consolidation determined by curve fitting about t_{50}, it is likely that consolidation is once more occurring in the compression mode, therefore the values of c_h determined in this analysis were not adjusted by the RR/CR ratio. Local experience has shown that consolidation in the Fraser River delta deposits occurs more quickly than predicted on the basis of laboratory consolidation test parameters. This is likely due, in part, to the influence of undetected drainage layers.

Judgment must be exercised when determining a coefficient of consolidation from penetration test pore pressure dissipation data. When measured pore pressures are plotted with the common logarithm of time during a pause in penetration, as in Fig. 5.14, theoretical solutions predict slower consolidation than observed for U less than 30%, that is, nearing the completion of consolidation, or a degree of consolidation greater than 70%. Conversely, theoretical solutions predict faster than observed consolidation early in the dissipation process. Therefore, different coefficients of consolidation are predicted at different degrees of consolidation, that is c_h determined at t_{50} may not be the same as that determined independently at t_{80} or t_{20}. However, for a parameter where order of magnitude estimates are frequently made, the variations in c_h found in this analysis were relatively small.

As noted by Baligh and Levadoux (1986), laboratory measurements of coefficient of consolidation or permeability in fine-grained soils can underpredict in-situ values by several orders of magnitude. Profiles determined from tests conducted on samples obtained from discrete depths typically show significant scatter and can easily miss drainage layers essential in a field scale consolidation analysis. In-situ tests offer strong advantages in identifying these important layers for subsequent specific tests.

6. PREDICTION OF PERFORMANCE

Embankment performance, in terms of rate and magnitude of settlement, was predicted using the results of piezocone, flat dilatometer, and screw plate tests. For the predictions, no new methodology was introduced. Analyses were performed using current, accepted practice.

6.1 Simplified Approach: One-Dimensional Analysis

With, perhaps, the exception of high risk structures, most settlement calculations are based on one-dimensional analyses involving the estimation of vertical displacements induced by a design load. The total settlement, S, is calculated as the sum of three components

$$S = S_d + S_c + S_s \qquad [6.1]$$

where S_d is the distortion settlement,

S_c is the consolidation settlement, and

S_s is the secondary compression settlement.

In order to evaluate each of these components, it is necessary to quantify the load applied, the resulting increase in stress, the distribution, with depth, of this stress increase, as well as the relevant soil properties.

6.1.1 Stress Increase

To evaluate the distribution of stresses within a soil mass, the theory of elasticity is invariably used. Although soil is a non-linear material, and inherently anisotropic, the assumption is often made that the soil is isotropic elastic. Rigorous solutions for more complex non-linear constitutive relationships are only possible in very few cases, and for most applications, the use of elastic theory results in an acceptable degree of accuracy for the evaluation of stress distribution.

The values of vertical stress increase at the ground surface, from each component of loading, are identified in Table 6.1. These values formed the basis for computing the distribution of stress increase with depth.

Table 6.1 Stress Increase Induced by Placement of Embankments, Surcharge, and Abutments

Location	Stress Increase (kPa) due to:		
	Embankment	Surcharge	Abutment
Arthur Laing Bridge south approach	173	50	44
McConachie Way Overpass	151	35	106

The solution for the distribution of stresses within a semi-infinite, homogeneous, isotropic mass, with a linear stress-strain relationship, due to a point load on the surface, is first credited to Boussinesq (1885). Because the solution is a linear function of applied load, the principle of superposition may be applied to account for variations in loading conditions, from point to line loads and from strip to circular areas. In an elastic analysis, an embankment is considered to be an infinite strip area carrying a combination of uniform pressure and linearly increasing pressure. Fig. 6.1 illustrates how the increase in vertical stress, $\Delta\sigma_z$, due to an embankment, may be computed by means of elastic theory.

The equations of Fig. 6.1 are commonly expressed in the form

$$\Delta\sigma_z = Iq \qquad [6.2]$$

where I is an influence factor which takes into account the geometry of the loaded area. Numerous charts have been compiled (Harr, 1966; Scott, 1963; Foster and Ahlvin, 1954; Fadum, 1948) from which values of I may be obtained for various geometric loading configurations.

In an analysis using elastic theory, the value of q, the uniform pressure, is evaluated by the "normal loading approximation"

$$q = \gamma H \qquad [6.3]$$

where γ is the unit weight of the embankment fill, and

H is the embankment height.

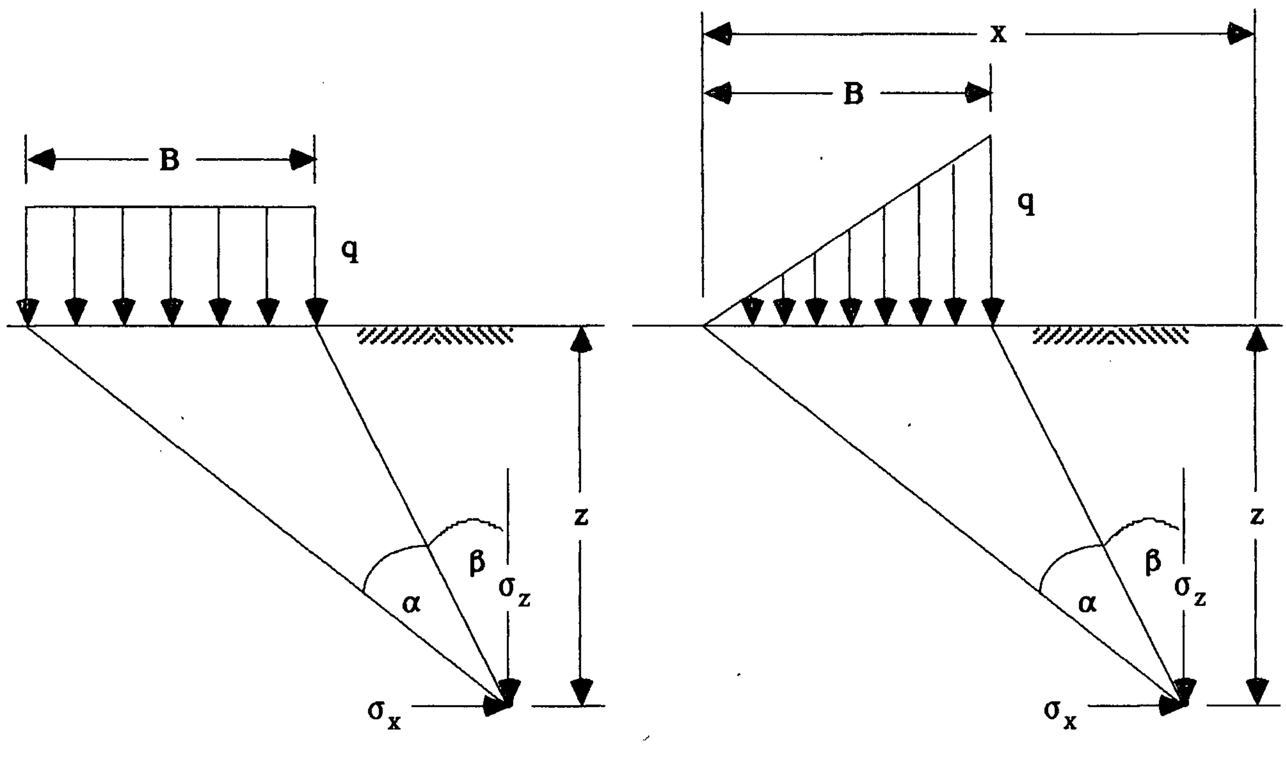

(a) Stress increase due to uniform load, q

$$\sigma_z = \frac{q}{\pi}\{\alpha + \sin(\alpha)\cos(\alpha+2\beta)\}$$

(b) Stress increase due to linearly increasing load

$$\sigma_z = \frac{q}{\pi}\left\{\frac{X}{B}\,\alpha - \frac{1}{2}\sin(2\beta)\right\}$$

Fig. 6.1 Determination of Vertical Stress Increase by Elastic Theory

Perloff (1975) comments that the above approach neglects the shear stresses which develop between an embankment and its foundation, and proposes an alternate approach (Perloff *et al.*, 1967), which considers the embankment and foundation as a single body loaded only by self weight. This is called the "elastic embankment" approach and may be more realistic because it considers the effect of the material itself on the distribution of stress, allows for shear distortions at the embankment-foundation interface, and produces a result found to be consistent with field measurements of pore pressures beneath an embankment (Bozozuk and Leonards, 1972).

Fig. 6.2 presents the distribution of vertical stress increase, with depth, for the normal loading approximation and elastic embankment methods, for the combined embankment and abutment loads of the McConachie Way Overpass. At a depth of 20 m, where the clayey silt stratum is first encountered, the elastic embankment method predicts a vertical stress increase 20% less than the normal loading approximation.

The presence of 20 m of sand may reduce the stresses distributed to the underlying compressible clay silt layer. When the stiffness of a load-bearing stratum is larger than that of an underlying soft soil, the load distributing effect can be approximately accounted for by calculating stresses in the lower layer assuming the upper stiff layer to be increased in thickness. Perloff (1975) suggests an increase of 15% in the thickness of the upper layer has been used successfully. Therefore, in calculating the stress increase in the clayey silt, for both the normal loading approximation and elastic embankment methods, an additional 3 m of sand was assumed to exist, or $\Delta\sigma_Z = \Delta\sigma_{Z+3}$ in the clay silt. For example, 21 m became 24 m for determination of the stress increase at that depth. This is evident as the break in the curves occurring at the 20 m depth in Fig. 6.3, which illustrates the distribution of stress increase due to embankment and preload but, unlike Fig. 6.2, does not include the abutment load.

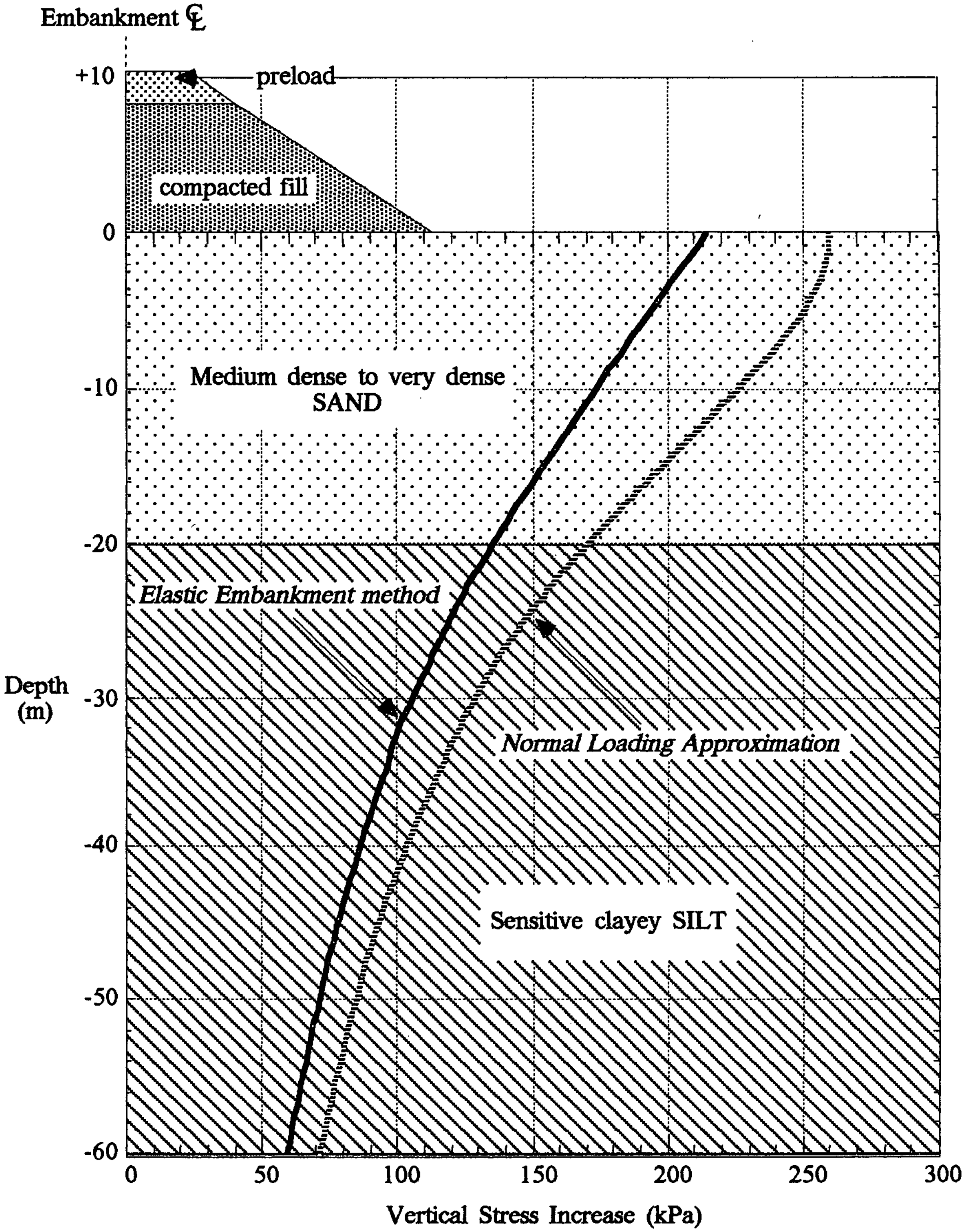

Fig. 6.2 Profile of Vertical Stress Increase Predicted by Normal Loading Approximation and Elastic Embankment Methods — McConachie Way Overpass

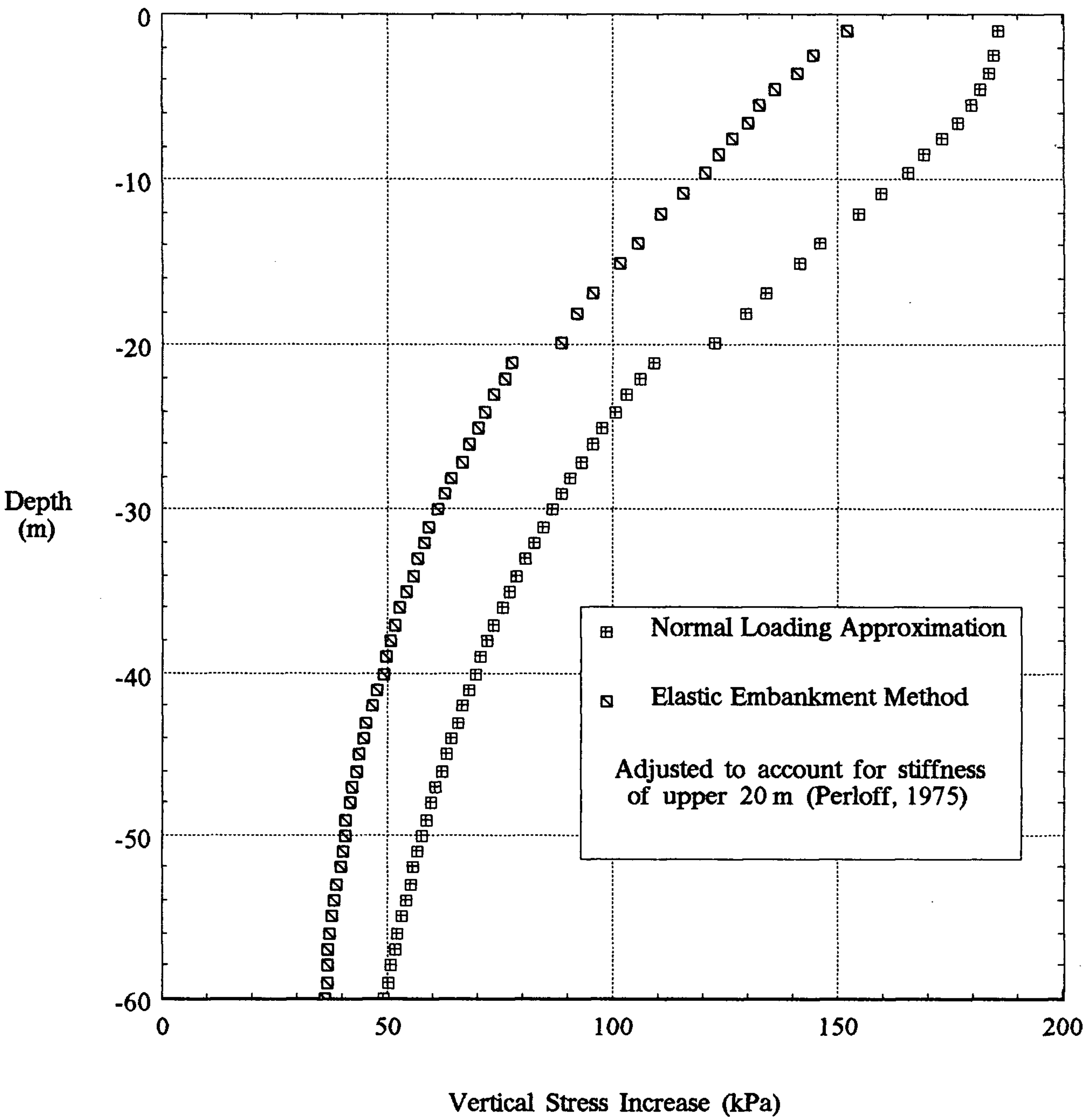

Fig. 6.3 Profile of Vertical Stress Increase Due to Embankment and Preload — McConachie Way Overpass Embankments

6.1.2 Undrained Deformation

Initial distortion settlement is an immediate deformation which takes place, in cohesive deposits, under undrained conditions. The following equation for vertical distortion settlement, S_d, due to a distributed load acting on a rectangular area near the surface of a relatively deep stratum, was first given by Schleicher (1926)

$$S_d = C_d\, p\, B \left(\frac{1-\mu^2}{E_u}\right) \qquad [6.4]$$

where C_d is a parameter to account for the shape of the loaded area and the depth of the layer for which the settlement is being calculated,

p is the magnitude of the uniformly distributed load,

B is a characteristic dimension of the loaded area,

μ is Poisson's ratio, and

E_u is the undrained Young's modulus.

When a soft, compressible stratum is underlain by rock or very hard or dense soils, as in the case of Sea Island, where the compressible clayey silt is underlain by dense glacial till, the effect of layering may have an appreciable influence on the magnitude of calculated immediate settlement. The factor C_d of equation 6.4 was replaced, in the present analysis, with the factor C_d' to account for the presence of the rigid base. Harr (1966) cites values for C_d' which depend upon the shape of the loaded area and thickness of the compressible stratum relative to the width of the loaded area.

To account for the load distributing effect of the overlying sand, it was assumed that the entire 61 m of soil beneath the embankment consisted of compressible clayey silt, and the distortion settlement, S_{d61}, was calculated using equation 6.4 and C_d'. The distortion settlement in the upper 20 m of sand, S_{d20}, was then calculated by the same method, and this value subtracted from S_{d61}. The distortion settlement in the clayey silt stratum alone, arising from the combined embankment and preload pressure of the McConachie Way Overpass embankment, was thus found to be 18.4 cm. A similar calculation performed for the south approach embankment of the Arthur Laing Bridge yielded a distortion settlement in the clayey silt stratum of 25.1 cm.

It is evident when considering equation 6.4, that calculated distortion settlements depend directly on the assumed values of Young's modulus and Poisson's ratio. For saturated clayey soils, which are thought to deform at constant volume during the initial time in which elastic distortion settlements develop, a value of Poisson's ratio of $\mu = 0.5$ was assumed, and the undrained Young's Modulus as determined from the screw plate test, $E_u = 28$ MPa, was used.

As discussed previously, use of the screw plate to determine Young's modulus may underestimate E_u due to the influence of inhomogeneities and the small size of the plate with respect to embankment size. Comparing the initial modulus value, $E_i = 28$ MPa, with the unload-reload modulus, $E_{u\text{-}r} = 40$ MPa, indicates the Sea Island clayey silt is a strain hardening material. If the value of Young's modulus were allowed to vary between 28 MPa and 40 MPa, and the value of Poisson's ratio to vary between 0.35 and 0.5, the calculated distortion settlement in the clayey silt stratum would range, for the McConachie Way Overpass embankments, between 14.5 cm and 22 cm. The value of $S_d = 18.4$ cm used in prediction lies in the middle of this range, and the potential variation of ±4 cm is insignificant in comparison to the settlement which occurs due to consolidation of this stratum.

Because of the high permeability of sands, the distortion settlements occur at the same time as consolidation settlements. The prediction of settlements of cohesionless soils is often based on semiempirical methods, correlated for compatibility with field observations. The method proposed by Schmertmann (1970) uses the following equation

$$S_d = C_1 C_2 \Delta p \sum_{i=1}^{n} \left(\frac{I_z}{E}\right)_i \Delta z_i \qquad [6.5]$$

where Δp is the net load intensity at the foundation depth,

I_z is a strain influence factor,

E is the Young's modulus for the centre of the i^{th} layer,

Δz_i is the thickness of the i^{th} layer, and

C_1 and C_2 are correction factors.

and was used in the present analysis.

To incorporate the effect of strain relief due to embedment, the correction factor C_1 is defined as follows, with a limiting lower bound of 0.5:

$$C_1 = 1 - 0.5\left(\frac{\sigma'_o}{\Delta p}\right) \geq 0.5 \qquad [6.6]$$

where σ'_o is the effective vertical overburden pressure at the depth of interest.

The correction factor C_2 accounts for the time-dependent increase in settlement due to creep which is observed to occur.

$$C_2 = 1 + 0.2 \log\left(\frac{t}{0.1}\right) \qquad [6.7]$$

where t is time, in years.

To use equation 6.5, the upper 20 m of sand at the site was divided into layers, the first layer being 3 m thick and encompassing the mixed sandy, silty, clayey soil, and the remaining layers of primarily clean sand each being 1 m thick. An influence factor was calculated using both the normal loading approximation and elastic embankment method, and Young's modulus as determined from the screw plate test, for each layer, was used in equation 6.5. As a result, S_d calculated for the upper 20 m of cohesionless soil was found to be 2.4 cm and 1.7 cm by the normal loading approximation and the elastic embankment method, respectively, in the case of the

McConachie Way Overpass embankments, and 2.9 cm and 2.1 cm in the case of the south approach embankment of the Arthur Laing Bridge.

As was the case for the compressible clay silt, distortion settlement of the cohesionless stratum is dependent upon Young's modulus. While correlations from in-situ tests to deformation moduli are empirical in nature and may not be considered highly reliable (Jamiolkowski *et al.*, 1985), wide variations in this parameter have a negligible effect on the overall results of the present analysis, as the magnitude of this component of settlement, approximately 2 cm, is extremely small in comparison to the total settlement.

6.1.3 Drained(Consolidation)Deformation

The effect of foundation loads applied rapidly to cohesive soils is manifest by increased pore water pressure. With time, water flows out of soil voids, and pore pressures dissipate. This process is known as primary consolidation. If boundary conditions in the field are such that volumetric strains and accompanying settlements are only vertical, for instance, when the dimensions of the loaded area are large relative to the thickness of the compressible stratum, or when the compressible material lies between two stiffer soils whose presence tends to reduce the magnitude of horizontal strains, a one-dimensional (vertical) consolidation analysis is appropriate, and may be conducted in two steps:

1. Evaluation of ultimate consolidation settlement (amount, or magnitude),
2. Estimation of time-settlement history (rate).

This comprises the simplified approach of the present analysis.

6.1.4 Amount of Settlement

One-dimensional consolidation analysis assumes zero lateral strain. In reality, the condition of zero lateral strain is not often met, especially where deep compressible strata are involved. In practice, however, except in the case of high risk structures, generally a one-dimensional settlement analysis is carried out.

To estimate the magnitude of settlement, a soil profile is divided into layers and the increment of consolidation settlement, dS_c, for that layer is computed from

$$dS_c = m_v \Delta\sigma_z dz \qquad [6.8]$$

where $\Delta\sigma_z$ is the stress increase at the centre of the layer,

dz is the thickness of the layer, and

m_v is the coefficient of volume compressibility, equal to 1/M, the reciprocal of constrained modulus at the centre of the layer. Hence, equation 6.8 can be rewritten as

$$dS_c = \frac{\Delta\sigma_z}{M} dz \qquad [6.8a]$$

The total settlement for the entire soil profile is the summation over all the layers, i. e.

$$S_c = \Sigma\ dS_c = \Sigma\ \frac{\Delta\sigma_z}{M} dz \qquad [6.9]$$

To determine the consolidation settlement due to embankment load and surcharge load for the McConachie Way Overpass embankments and Arthur Laing Bridge south approach embankment, the 61 m thick soil profile was divided into 56 layers. The majority of the layers were taken as 1 m in thickness, with the exception of the top layer, which was 2 m in thickness, and the seven sand layers from the 10 m through the 20.5 m depths, which were taken as 1.5 m in thickness. The constrained modulus values shown in Fig. 5.9 were used in equation 6.9.

A vertical stress increase was determined for the centre of each layer from the profile shown in Fig. 6.3, using both the normal loading approximation and the elastic embankment methods.

In-situ tests for this study were performed at sufficient distance from the embankments to ensure foundation soils were not influenced by the added loads. The values of constrained modulus determined from those tests are valid, therefore, for the initial loading conditions. Once the foundation soils had been preloaded, however, the soil would possess different properties, as the subsequent removal of preload would leave the soil with a stress history, that is, in a lightly overconsolidated state. The M values used to compute settlement due to embankment and surcharge, therefore, required some modification for the calculation of settlement due to abutment loading.

Schmertmann (1986) proposed a special method for computing foundation settlement, from dilatometer test results, which accounts for the variation in M with varying stress level. This method recognizes that the effective stress at the time of structure loading may not be the same as at the time the DMT was conducted, whether due to excavation, surcharge, dewatering, or other circumstances. This special method involves construction of an appropriate modulus-effective stress curve for both normally consolidated and overconsolidated soil conditions, using the values of preconsolidation pressure, p'_c, determined from the DMT, effective stress at the time of the DMT, p'_d, effective stress at the time of structure loading, σ'_o, and structure load, $\Delta\sigma'_z$.

The Schmertmann (1986) method uses the tangent modulus relation of Janbu (1967) to compute the adjusted modulus at the revised stress level, $\sigma' = \sigma'_o + \Delta\sigma_z$

$$M = k_m p_a \left(\frac{\sigma'}{p_a}\right)^{1-a} \qquad [6.10]$$

where k_m is a dimensionless modulus number,

p_m is atmospheric pressure, a reference stress,

σ' is the appropriate level of effective stress, and

a is a stress exponent, approximately equal to 0.5 for sands and silts and 0 for clays.

For the present analysis, the stress exponent was taken equal to 0.5, and values of k_m were back calculated for each soil layer from the original M values shown in Fig. 5.9. The average values of back calculated modulus numbers, 400 in the upper dense sand, 24 in the clayey silt, and 52 in the sandy silt, are within the range of typical values cited by Janbu (1967).

Equation 6.10 defines the curve for normally consolidated conditions. In order to reconstruct the overconsolidated portion of the curve, the point (M, p'_d), representing the values obtained at the time of the DMT, is plotted and connected to the point (M, p'_c) on the normally consolidated portion of the curve corresponding to the revised preconsolidation pressure. Fig. 6.4 illustrates this methodology for the clay silt at a depth of 23.6 m. Entering a curve of the type shown in Fig. 6.4 at a revised stress level including the abutment load, an appropriate constrained modulus was obtained for use in equation 6.9 to compute the settlement due to abutment construction.

Table 6.2 presents the results of the first step of this one-dimensional settlement analysis, showing the magnitude of distortion and ultimate consolidation settlement, beneath the embankment centreline, predicted due to embankment, surcharge, and abutment construction. Observed and predicted settlements given in Bertok (1987) are provided for comparison. Settlements predicted from in-situ tests appear somewhat closer to the observed settlements than those predicted from laboratory test results.

6.1.5 Rate of Settlement

Settlements calculated in the preceding section and shown in Table 6.2 reflect the ultimate consolidation settlement that could be expected when all excess pore pressures have dissipated. The expulsion of water from soil pore spaces (consolidation) takes time, and at any time between the application of a load, and the time when the excess pore pressures have dissipated, the amount of settlement can be determined from the average degree of consolidation, U(t), with

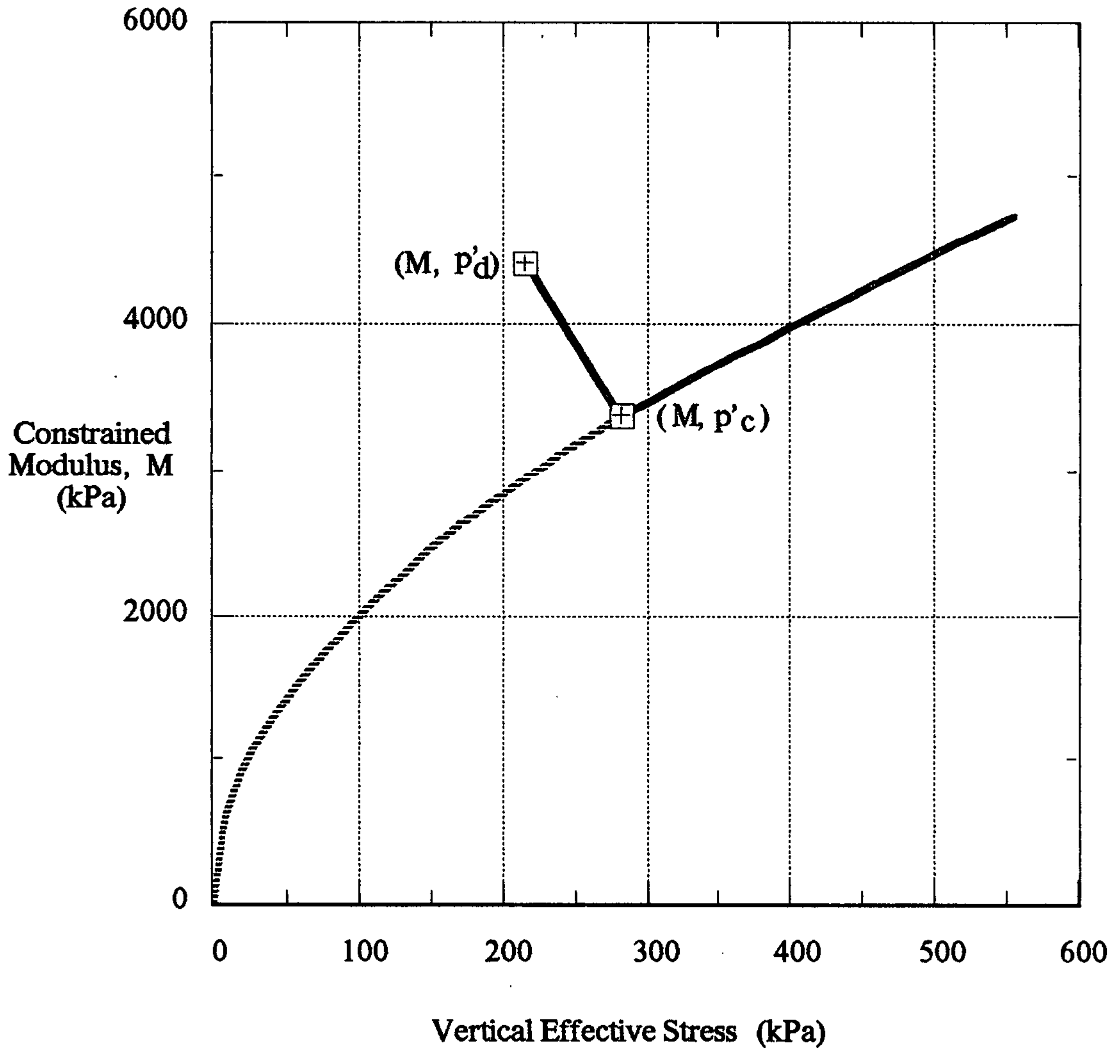

Fig. 6.4 Variation of Constrained Modulus with Effective Stress by the Special Method of Schmertmann (1986)

Table 6.2 Comparison of Predicted and Observed Settlements

Embankment or Abutment	Predicted primary consolidation and distortion settlement (cm): Reported by Bertok (1987)	Methods Using In-situ Test Parameters: Normal Loading	Methods Using In-situ Test Parameters: Elastic Embankment	Observed settlement (cm)
South approach embankment of Arthur Laing Bridge*	165	124	128	*100†*
Approach embankments of McConachie Way Overpass**	84	101	78	*70†*
South abutment of Arthur Laing Bridge	23	17	20	20
Abutments of McConachie Way Overpass	20	35	28	33

* Embankment section 12.5 m high, including 3 m surcharge
** Embankment section 10.4 m high, including 2.1 m surcharge

† These are approximate values at the commencement of abutment construction, not ultimate settlement magnitudes.

$$U(t) = \frac{S_c(t)}{S_c} \tag{6.11}$$

where S_c is the ultimate magnitude of consolidation settlement and

$S_c(t)$ is the magnitude of consolidation settlement at time t.

One-dimensional consolidation theory relates the quantities excess pore water pressure, u, depth, z, and time, t, through the partial differential equation

$$\frac{\partial u}{\partial t} = c\frac{\partial^2 u}{\partial z^2} \tag{6.12}$$

where c is the coefficient of consolidation, c_v in the vertical direction or c_h in the horizontal direction.

The initial distribution of excess pore water pressure, however, depends on in-situ stress conditions, which may vary from a simple linear distribution with depth to very complicated distributions. While the solution to equation 6.12 involves integration, analytical solutions to the integrals have been developed for several distributions of excess pore water pressure. These solutions relate U(t) and the dimensionless factor, T, where

$$T = \frac{ct}{d^2} \tag{6.13}$$

and d is the length of the longest path by which pore water may escape. The drainage path, d, is equal to the full thickness of the compressible stratum if drainage can occur at only one boundary, or half the thickness of the stratum if drainage can occur at both top and bottom.

One of the greatest sources of error in predicting time rate of settlement is the definition of drainage boundary conditions. For predicting rate of settlement at the embankment site, the compressible clayey silt was divided into two strata, separated by a more freely draining sandy silt layer at a depth of about 28 m. Fig. 6.5 presents a schematic diagram of the boundary conditions assumed for calculating the rate of settlement. Each of the two clayey silt strata was

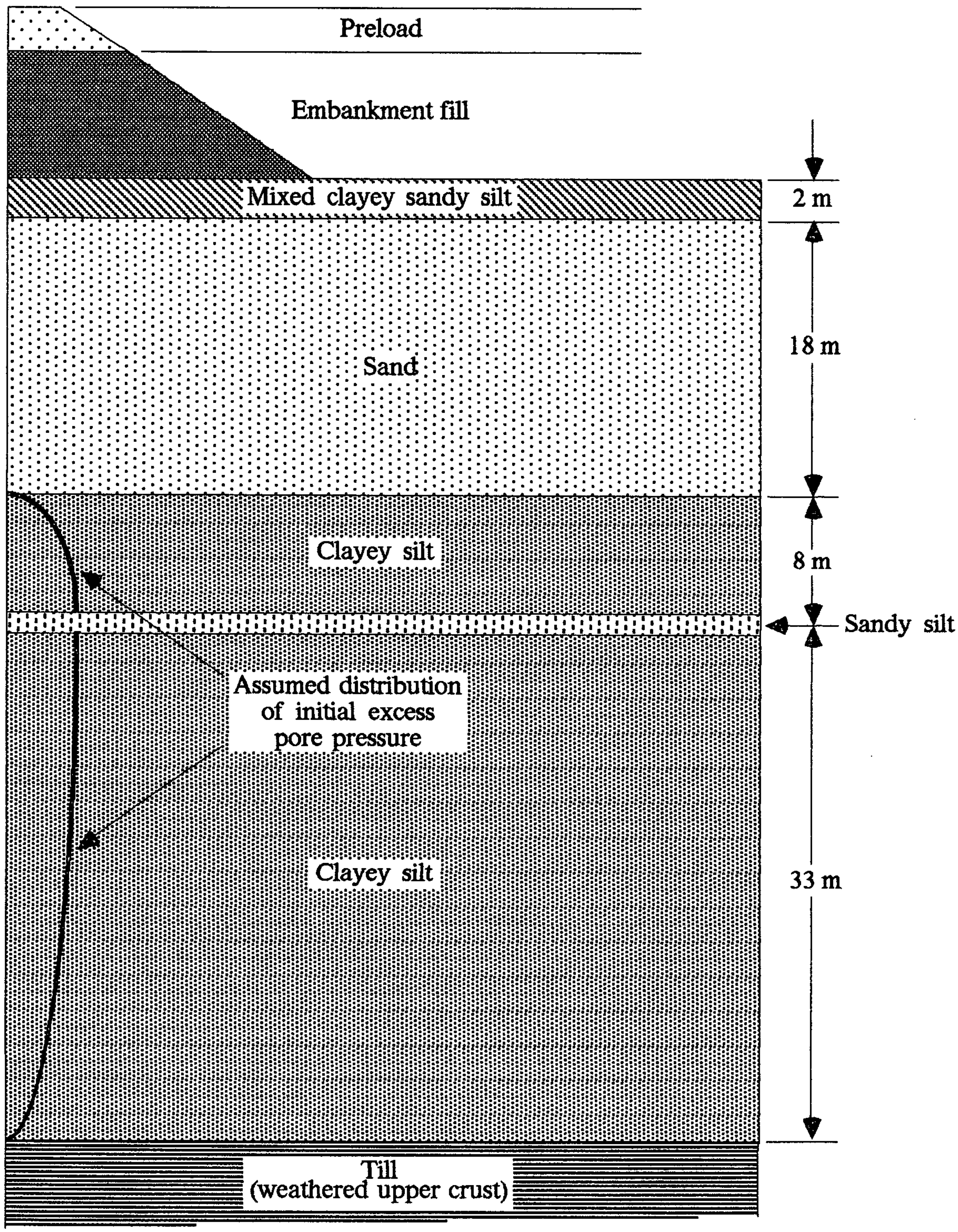

Fig. 6.5 Profile Assumed for Settlement Rate Analysis

assumed to have double drainage, the upper stratum draining to the overlying sand and to the sandy silt at 28 m, and the lower stratum draining to the sandy silt at a depth of 28 m and to the basal till at approximately 61 m. While dense glacial till would normally be assumed to act as an impermeable boundary, rapid dissipation of pore pressure was manifest in a CPTU dissipation test at a depth of 60.9 m, leading to the conclusion that drainage would take place at the interface of the clay silt and till. Local experience has shown that considerable weathering exists at the surface of the till, again supporting the idea of drainage at the base of the clay silt.

A drainage layer at a depth of 28 m was assumed based on the stratigraphy as defined by profiles of cone bearing with depth and on the coefficients of consolidation calculated from in-situ dissipation tests. Profiles of cone bearing 30 to 40 m apart at the embankment site gave evidence of considerable sandy silt layering surrounding the 30 m depth, therefore the areal extent of this more freely draining layer was judged sufficient for it to act as an effective drainage path. Furthermore, horizontal coefficients of consolidation interpreted from CPTU dissipation tests at this depth were approximately one order of magnitude greater than those in the remainder of the clay silt, again indicating preferential drainage.

A horizontal coefficient of consolidation of c_h = 0.004 cm^2/s was assumed for the two compressible clay silt strata. Fig. 5.15 shows only a narrow scatter band around this value, for dissipation and consolidation tests conducted throughout the deposit. The drainage layer at the 28 m depth was assumed to be of insufficient thickness to contribute to consolidation settlement, merely acting as a drainage interface.

Generally it is found that consolidation settlement in cohesionless soils occurs so rapidly it is virtually impossible to distinguish between settlement occurring as a result of consolidation and that occurring as a result of distortion. Dissipation tests conducted in the upper 20 m of sand revealed that any excess pore pressures generated during cone penetration dissipated within one minute. Given this information, it was assumed that consolidation settlement in the sand took place almost immediately with each new construction loading phase.

With the above system so defined, settlement at any time, t, was calculated using the following equations for the time factor, T, in each compressible stratum:

$$T_{upper} = \frac{c_h}{d^2} t = 0.066t, \text{ with t in months} \quad [6.14a]$$

$$T_{lower} = \frac{c_h}{d^2} t = 0.004t, \text{ with t in months} \quad [6.14b]$$

and a rearranged version of equation 6.11:

$$S_c(t) = U(t)S_c \quad [6.15]$$

Values of U(t) were interpolated from Case 2 (half sine curve) of the table relating U and T, which is given in Appendix A. A half-sine curve was assumed as the initial distribution of excess pore pressure, as it was expected that drainage would occur at a slightly slower rate at the 28 m depth than at either the boundaries between the clayey silt and upper sand or the clayey silt and basal till. Consequently pore pressures would remain higher at the 28 m boundary than at the ground surface or at the 61 m depth. Fig. 6.5 shows the assumed initial distribution of excess pore pressure.

Following surcharge removal from each embankment, the last value of settlement computed due to the surcharge load was maintained constant, continuing to act as a fixed contribution to the overall settlement throughout the remainder of the analysis. No rebound, or negative settlement, was assumed to occur. The determination of settlement during unloading and reloading requires assumptions as to how and when the foundation soil will respond. While the ground will likely continue to settle for some time after a portion of the surface load has been removed, this settlement may be counterbalanced by the potential rebound which may occur due to load removal.

6.1.6 Correction for Construction Period

As embankments, or other structures, in their final form, are not placed immediately, but require time for construction, time-settlement curves must be corrected to allow for the construction period. Terzaghi (1943) proposed an empirical correction method whereby it is assumed the net foundation load is applied at a uniform rate during the construction period, t_c, and that the degree of consolidation at the end of this time is the same as if the load had been acting for half that time, $t_c/2$. In other words, settlement during the construction period is the same as that which would be calculated assuming instantaneous loading at half the construction time, with the load reduced proportionally to account for the fact that the total load is not acting during this time.

For the example case of the McConachie Way Overpass embankments, 8.3 m of compacted fill and 2.1 m of uncompacted surcharge were placed in five months, that is, t_c = 5 months. The fill was not placed uniformly during this period, however, with approximately 2 m of fill being placed in three months, and the remaining 8.4 m being placed in two months. In order to match the construction sequence more closely when predicting settlement rate, the load due to an embankment 1 m high (one half the load due to placement of 2 m of fill) was assumed to act at 1.5 months (one half the time for placement of 2 m of fill), following which the load due to an additional embankment height of 3.15 m (one half of 6.3 m) was assumed to act at 3.5 months, and the surcharge load due to 1.05 m of uncompacted fill (one half of 2.1 m) assumed to act at 4.5 months.

In this manner, at the end of the construction period of five months, surface settlements due to consolidation in the clayey silt were found to be 6 cm and 4 cm for the normal loading approximation and elastic embankment method, respectively. Consolidation settlement in the sand, 12 cm and 9.3 cm, was assumed to have been completed by the end of the construction period, and the contribution of this component of settlement was added in linear increments from construction start to finish.

Construction of the south approach embankment for the Arthur Laing Bridge proceeded uniformly to completion within two months. At the end of the construction period, 2.5 cm and 2.6 cm of settlement were computed to have occurred, by the normal loading approximation and elastic embankment method, respectively, due to consolidation of the clayey silt, and the contribution of consolidation settlement from the 20 m of sand, 14.4 cm and 12.5 cm, was added in linear increments over the two months.

6.1.7 Secondary Compression

Observations both in the laboratory and in the field indicate that settlements continue under conditions of constant effective stress, that is, even after excess pore pressures have dissipated, or the process of primary consolidation is complete. This settlement, known as secondary compression, is believed to continue at a very slow rate for an indefinite period of time.

It is often assumed that secondary compression takes place after primary consolidation is complete. This is based on the observation that curves of settlement versus logarithm of time show a distinct inflection point at the time when primary consolidation is essentially complete, for laboratory consolidation tests run under a load increment ratio of unity. Secondary compression has been related to water content, consolidation pressure, clay mineralogy, temperature, and other effects (Mesri, 1973), but is recognized to be a function of time. The coefficient of secondary compression, C_α, is usually calculated from laboratory measurements, using the equation

$$\Delta e = -C_\alpha \log\left(\frac{t_2}{t_1}\right) \qquad [6.16]$$

where Δe is the change in void ratio as measured in a laboratory consolidation test between the times t_1 and t_2.

While much work has been done in qualitatively considering the concept, very little can be said about parameters which quantitatively describe the magnitude of secondary compression. Mesri and Castro (1987) suggest that, for a given soil, the ratio of C_α to C_c, the slope of the virgin compression portion of a laboratory consolidation curve, remains essentially constant, and that for a majority of inorganic, soft clays the ratio

$$\frac{C_\alpha}{C_c} = 0.04 \pm 0.01 \qquad [6.17]$$

Use of this relationship to determine C_α, however, requires an estimate of the laboratory-determined parameter, C_c.

Obviously, application of this concept to the full-scale field case requires many assumptions. Secondary compression is often ignored in practice. For the embankment site, the calculated time for completion of primary consolidation is approximately 35 years. Although it is generally assumed that secondary consolidation will occur after this time, it is likely that some secondary compression has occurred at the embankment site. In the present analysis, however, the component of settlement due to secondary compression has not been included.

6.2 Modified Approach

Where the thickness of a compressible stratum is large relative to the loaded area, the three-dimensional nature of the problem influences the magnitude and rate of settlement. Semi-empirical approaches are used in order to modify settlement magnitude to account for these effects.

When there is an axis of symmetry in a field loading case, as in the centreline of the subject embankments, Skempton and Bjerrum (1957) give an expression whereby consolidation settlement beneath the centreline, incorporating 3-D effects, can be expressed in terms of the settlement predicted from a 1-D test:

$$S_{3\text{-}D} = \lambda S_{1\text{-}D} \qquad [6.19]$$

where the correction factor, λ, is a function of stress history, and

$$\lambda = A + \beta(1\text{-}A) \qquad [6.20]$$

where

$$\beta = \frac{\int_0^d \Delta\sigma_3 dz}{\int_0^d \Delta\sigma_1 dz} \qquad [6.21]$$

and A is the Skempton pore pressure parameter expressing the proportion of the principal stress difference which is responsible for the increase in pore water pressure.

For normally consolidated soils, the factor λ approaches unity, therefore no correction was required in the present analysis. For overconsolidated soils, however, an adjustment should be made. Skempton and Bjerrum (1957) provide a chart for determining λ based on overconsolidation ratio and the foundation size relative to the thickness of the compressible stratum.

It should be noted that some account has been taken for foundation size with respect to the thickness of the substrata by the correction factors C_1 and C_2 used in the 1-D analysis for calculating distortion settlement.

6.3 Complex Approach

The advent of the personal computer has spawned increased interest in the use of numerical methods and finite element methods (FEM) to compute foundation settlements. While the prospect of handling non-linear constitutive relationships and complicated boundary conditions in a settlement analysis is certainly appealing, the material parameters required as input are not generally obtainable with the degree of accuracy required to justify a sophisticated analysis. Often, the approximations required to fit the real problem to that for which a FEM solution is available are inconsistent with the precision of the solution procedure (Perloff, 1975). Therefore, approximate analysis of settlements, or the one-dimensional, simplified, approach often remains appropriate and is still the most common method used in geotechnical practice.

Burland (1987), in reviewing the most commonly-used methods of settlement prediction for clay soils, demonstrated that traditional settlement calculations are usually adequate for practical purposes, provided the appropriate in-situ soil properties have been obtained. The settlement magnitudes predicted by conventional 1-D analysis, the Skempton and Bjerrum method, the stress path method, and the finite element method were evaluated as ratios to the exact theoretical values in the cases of a homogeneous, isotropic, elastic material, a homogeneous, anisotropic, elastic material, and an anisotropic material with increasing stiffness with depth. In most cases, the simple 1-D method gave the best predictions of total settlement, raising the questions of whether the sophistication of FEM analysis is necessary, and whether greater accuracy is, in fact, achieved.

The findings of Burland (1987) emphasize the importance of assuring a high quality of geotechnical data, obtaining as accurately as possible values such as m_V (=1/M), E and G, whereafter a simple 1-D settlement analysis should prove sufficient for most practical applications. A finite element settlement analysis was not conducted as part of the present research.

6.4 Comparison of Predictions with Observed Settlement

Fig. 6.6 and Fig. 6.7 present the combined results of the first and second steps of the one-dimensional settlement analyses, showing the time rate of settlement predicted using in-situ test results with the observed settlements recorded by Transport Canada for the McConachie Way Overpass embankments and the south approach embankment of the Arthur Laing Bridge, respectively.

6.4.1 McConachie Way Overpass Embankments

Both rate and magnitude of settlements were predicted with a high degree of accuracy by the elastic embankment method, when compared to the observed settlement, until the time of abutment loading in 1975. Following construction of the abutments, settlements predicted by in-situ test methods was greater than those observed. The rate of settlement, however,

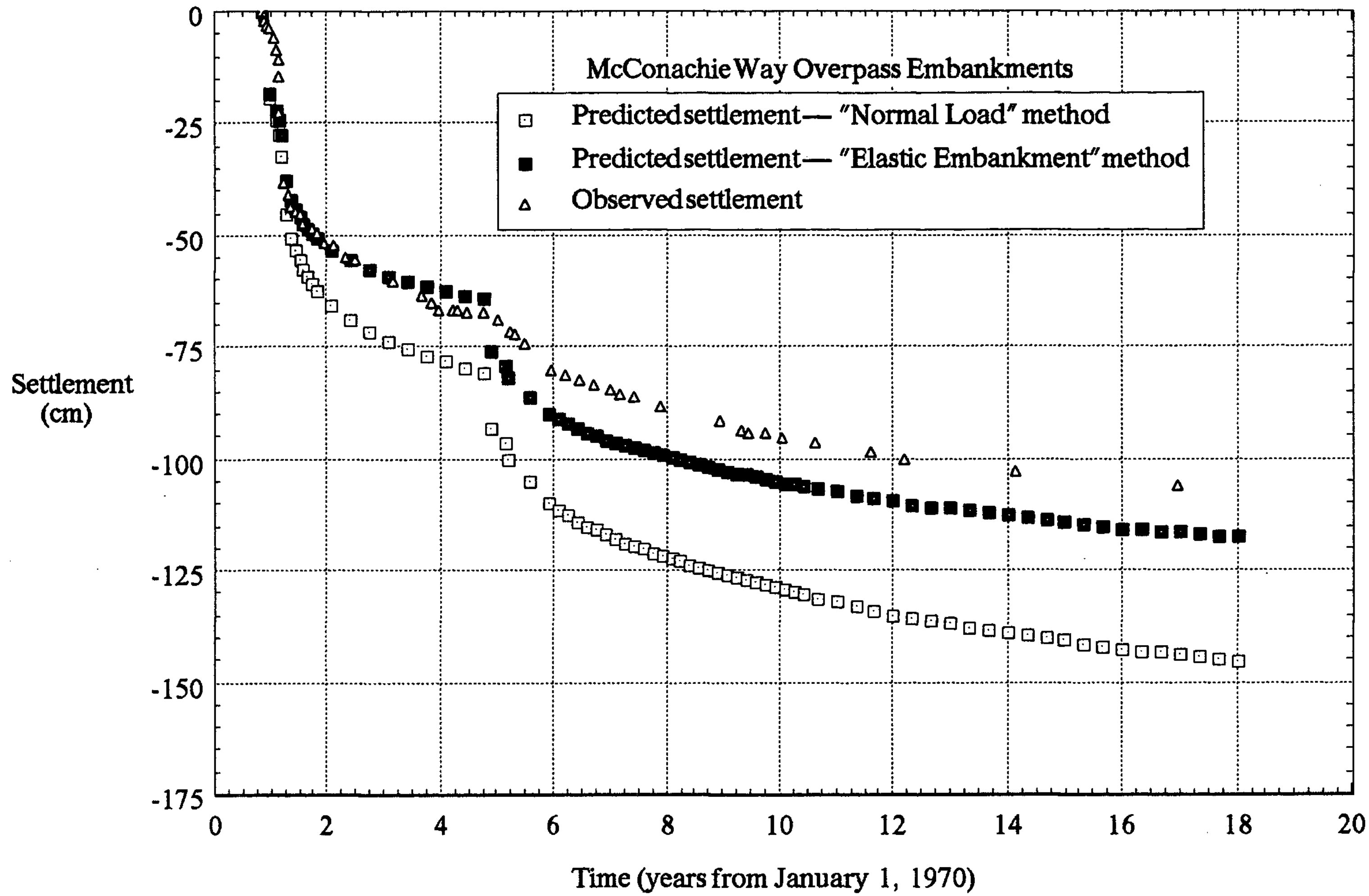

Fig. 6.6 Predicted and Observed Settlements — McConachie Way Overpass Embankments

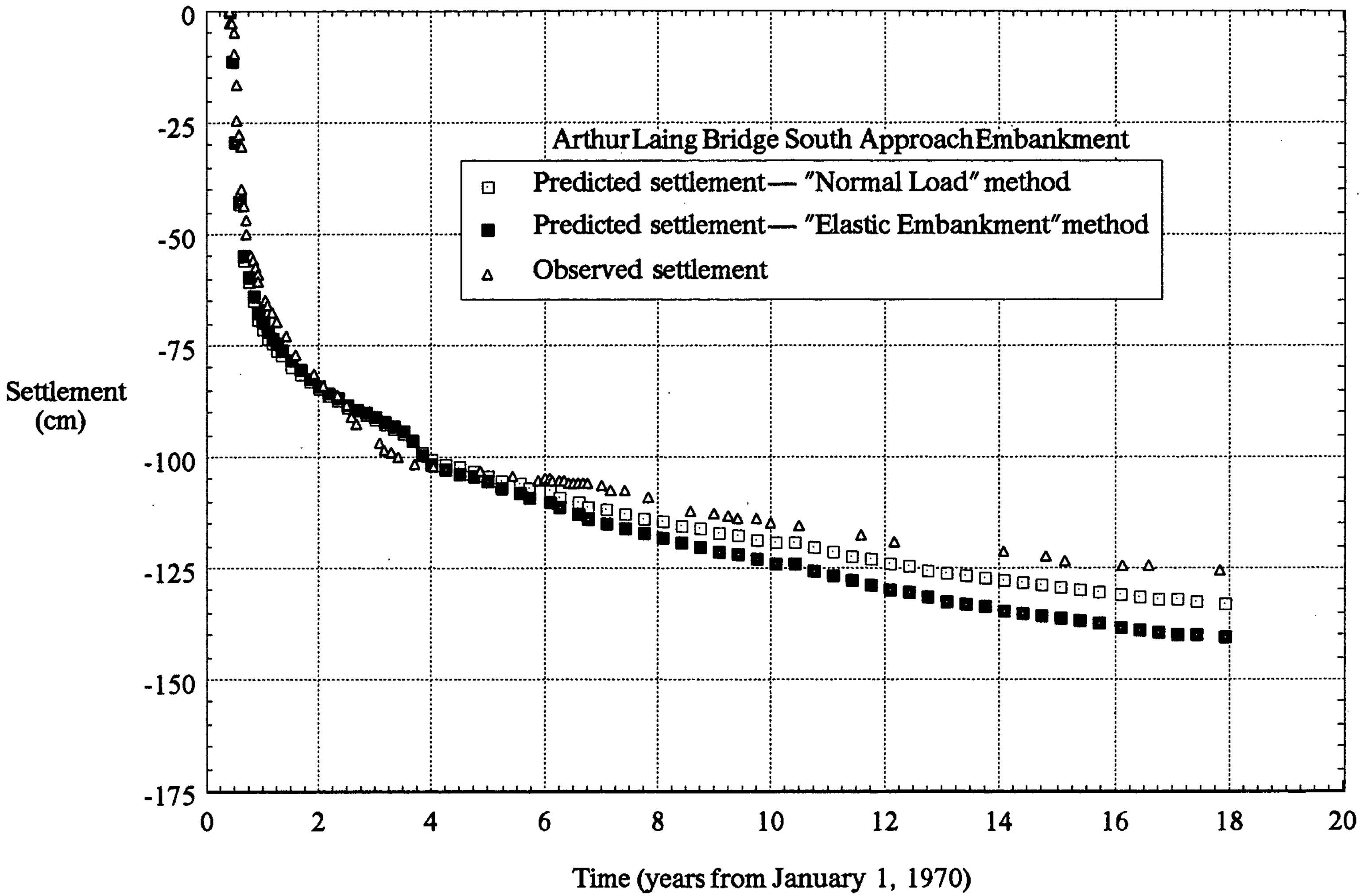

Fig. 6.7 Predicted and Observed Settlements — Arthur Laing Bridge South Approach Embankment

continued to closely model the actual rate, as all settlement curves on Fig. 6.6 are essentially parallel.

The normal loading approximation, overpredicts observed settlement from the outset of construction, however this result is not unexpected, as Boussinesq solutions, while widely used, are generally found to be conservative.

At the time of the most recent Transport Canada survey (December, 1986), total settlement had reached 106 cm. Using in-situ test parameters, the settlement predicted by the elastic embankment method was 116 cm, an overprediction of 10 cm (9%), and the settlement predicted by the normal loading approximation was 143 cm, an overprediction of 37 cm (35%). This represents a significant improvement over the original predictions given by Bertok (1987), based on laboratory data, where the predicted settlement due to abutment construction alone was 20 cm compared to the 33 cm observed, a difference of 13 cm (40%).

6.4.2 Arthur Laing Bridge South Approach Embankment

Rate and magnitude of settlements as predicted from in-situ test methods match observed settlements with remarkable precision. Fig 6.7 indicates that throughout the construction, preloading, and abutment construction phases, predicted settlements are very similar to the observed settlements. Following abutment construction, settlement is slightly overpredicted by in-situ test methods. The predicted rate of settlement, however, continued to closely model the actual rate through to 1987.

Differing from the McConachie Way Overpass embankments, the settlements predicted by the normal loading approximation matched the observed settlements more closely than that predicted by the elastic embankment method, although the difference is small. This may result from the assumption inherent in the Boussinesq analysis, that the loaded area is an infinite strip. The size and shape of the south approach embankment is closer to the assumed infinite strip than the embankments for the McConachie Way Overpass.

At the time of the most recent Transport Canada survey (November, 1987), total settlement had reached 126 cm. Using in-situ test parameters, the settlement predicted by the elastic embankment method was 143 cm, an overprediction of 17 cm (13%), and the settlement predicted by the normal loading approximation was 135 cm, an overprediction of 9 cm (7%). Again, this represents some improvement over the original predictions, where the predicted settlement due to abutment construction alone was 23 cm compared to the 20 cm observed, a difference of 3 cm (15%).

In general, the elastic embankment method proposed by Perloff *et al.* (1967) provided better predictions of settlement. This case record is not sufficient to state which is the better approach, however, since both the elastic embankment and the normal loading approximation methods yielded reasonable results.

7. DISCUSSION

The present analysis cannot be considered as a Class A estimate, since actual settlement data have been published, neither can it be considered as a Class C estimate, as presently-available data were not back analysed in an effort to refine estimated parameters. Back analysis of parameters from field monitoring, in fact, was not attempted, due to lack of monitoring data in this published case history.

It is unfortunate that the lack of monitoring data, such as pore pressure and surface and deep settlement measurements due to embankment loads, prohibited the evaluation of interpreted geotechnical parameters. The present study would have been improved if detailed monitoring data were available. The good prediction of settlements using in-situ test data may have been due to counterbalancing errors.

Nevertheless, the results of this research, in its present form, have a twofold significance. Firstly, it has been shown that, for this embankment case history, settlement magnitudes can be predicted with reasonable confidence based on parameters interpreted from in-situ tests. Also, it has been shown that the detailed stratigraphic information gathered using in-situ tests provides a solid basis for accurate prediction of the rate of settlement by increased precision in the identification of potential drainage layers within the soil profile. Secondly, it has been demonstrated, for this embankment case history, that a simple, one-dimensional analysis can adequately predict settlements.

For the south approach embankment of the Arthur Laing Bridge, predicted performance paralleled the observed performance with a degree of accuracy not often found in the prediction of settlement for large structures founded on compressible soils. For the McConachie Way Overpass embankment, performance predicted by in-situ test methods proved to be an improvement over that predicted by conventional methods, however, the predictions did not parallel observations as closely as in the case of the Arthur Laing Bridge south approach embankment. The original findings outlined in Bertok (1987) also were indicative of poorer performance predictions for the McConachie Way Overpass embankments.

The less precise performance prediction for the McConachie Way Overpass embankments may stem from several causes. However, a most obvious problem unique to these embankments is evident in Table 6.1 where a breakdown of the surface load imposed by each component of construction shows that the surcharge was insufficient to account for the final load imposed by the abutments. This problem may derive from two sources: one, that the preload itself was of inadequate thickness, or two, that placement of the footing was such that a larger portion of the abutment load than anticipated was placed on the original ground surface.

Bertok (1987) states that abutments of the McConachie Way Overpass were founded on spread footings located in the compacted sand fill approximately 1 m above the original ground surface. A review of the original design drawings (Phillips, Barratt, Hillier, Jones and Partners, 1974) confirmed that the underside of the spread footing was to rest 0.99 m (3.25 ft.) above original grade. Being placed at this elevation, full use was not made of the load-spreading capacity of the compacted embankment sand fill, and indeed, large loads would be applied to the original ground surface. Therefore, although the ground had been consolidating under the embankment and surcharge loads, once the final phase of construction began, the loads induced by the abutments soon exceeded the maximum past pressure, and virgin compression conditions once more came into effect.

Aside from the above complications due to this load-unload-reload sequence, considerable uncertainty exists in the distribution of excess pore pressure at this stage of construction. The excess pore pressures induced by the embankments and surcharge had not reached equilibrium before the abutment load was applied, imposing another, unknown, distribution of excess pore water pressure. As a result, prediction of settlement following abutment construction becomes a task laden with added uncertainty, and the results obtained appear to be far above what might be expected, even for the McConachie Way Overpass embankments.

In an effort to further refine the prediction of performance, perhaps the most influential parameter is the deformation characteristic, or modulus. The portion of settlement due to distortion, approximately 30% of the total, is directly dependent upon Young's modulus, E, whereas the consolidation settlement, in a one-dimensional analysis, is directly dependent upon the constrained modulus, M.

For the original analysis performed in 1968, the values of Young's modulus assumed in order to compute initial elastic settlements were:

$$E = \begin{cases} 48 \text{ MPa in cohesionless silty sand} \\ 1000S_u \text{ in cohesive soils} \end{cases} \qquad [7.1]$$

For this study, based on the in-situ screw plate test,

$$E = \begin{cases} 105 \text{ MPa in cohesionless silty sand} \\ (200 \text{ to } 300)S_u \text{ in cohesive soils} \end{cases} \qquad [7.2]$$

Comparing these values of modulus, however, does not automatically account for the differences in settlements predicted in 1968 and by the present analysis. While more settlement in cohesionless soils would have been predicted in the original analysis, due to a modulus roughly half as large as that interpreted from the screw plate test, it is not clear whether or not this would be counterbalanced by the fact that a larger modulus may have been predicted for the cohesive deposit, based on the correlations with undrained strength. The constant of proportionality between E and S_u is much larger in the case of the original analysis, however, S_u determined by the 1968 laboratory testing program was consistently lower than that interpreted from in-situ testing, as indicated on Fig. 5.6.

The empirical nature of the interpretation of constrained modulus makes its value highly questionable. An increase or decrease in M of 25% would result in a decrease or increase, respectively, in consolidation settlement of approximately 20%. Fortified by local experience, however, and given the consistency in correlations found in the present research and reported in the literature, a high degree of confidence may be expressed in the values used for this analysis. While some inadequacy may be suggested in the adjustment of M to account for changes in stress history, based on the performance of the south approach embankment of the Arthur Laing Bridge, it appears that this methodology produces reasonable results.

Changes in the assumed vertical stress increase, $\Delta\sigma_Z$, have approximately the same effect on the predicted settlement as changes in M, that is, a 25% increase in $\Delta\sigma_Z$ results in a 20% increase in computed settlement. In the original analysis, as reported in Bertok (1987), the Osterberg method, an elastic theory method utilizing influence factors and superposition, was used to compute stress increase. Of the methods used in the present analysis, both appear to be conservative, but distinctly adequate. The importance of the two-dimensional nature (shape) of the loaded area is evidenced here, as deviation from the assumed condition of an infinite strip appears to result in increasing conservatism in the estimation of vertical stress increase.

The value of Poisson's ratio, μ, affects the calculated distortion settlement, but only as a second order term, and it is less influential on the final result than the previously-discussed parameters. Use of μ= 0.5 in the present analysis assumes compressible soil deforms at constant volume. Researchers (Bozozuk and Leonards, 1972) have suggested values of μ = 0.3 to 0.35 may be more appropriate due to the inherent anisotropy of many cohesive soils, however, in-situ tests do not provide the means for determining the appropriate in-situ value.

No indication has been given of the original prediction of settlement rate. Bertok (1987) stated only that reliable prediction of the rate of settlement to be expected at this site was very difficult, adding that the reliability of predictions was tenuous due to sampling and testing problems in the soft, cohesive soil, and to lack of understanding of drainage effects from only one deep test hole.

By contrast, the simplicity and versatility of in-situ tests such as the CPTU and DMT are clear advantages. These in-situ tests provided excellent stratigraphic detail and definition of potential drainage seams, enabling rational decisions to be made on site geometry and drainage. As a result, when combined with pore pressure dissipation test information, rate of settlement was predicted with precision.

In relating soil properties determined in the laboratory with those determined from field measurements, Olson (1985) comments that the ultimate check on the usefulness of laboratory data is a comparison between predictions and field measurements. The same may be said for soil properties determined from in-situ tests. The ultimate check, in the case of the present performance prediction, provided a favourable endorsement for using in-situ tests to predict both rate and magnitude of settlement.

Recognizing this, it would appear that in-situ testing promises to be a preferential method of conducting geotechnical investigations. Still, the fact remains that there is some resistance to relying on in-situ testing. Despite the cost effectiveness of the CPTU and DMT, a substantial investment of both capital and technical expertise is required by the consultant, contractor, or agency committed to the successful use of in-situ testing.

Although laboratory testing of field samples will likely continue to be the basis for numerous geotechnical investigations and analyses for some time, in-situ testing offers the ability to enhance the quality of such investigations and will increasingly be recognized as a viable alternative or addition.

8. CONCLUSIONS AND RECOMMENDATIONS

In-situ testing is not without its drawbacks, and many areas remain where the complex soil behaviour during penetration is not well understood, however, given the limitations of alternative techniques, it becomes evident that practical problems can be handled with confidence when parameters have been interpreted from in-situ test results based on local correlations, experience, and sound judgment.

Based on the present research, the in-situ testing program undertaken provided adequate information concerning the settlement properties of the sensitive clay silt stratum which figured prominently in predicting embankment performance. Hence, the following conclusions can be made.

The soil profile beneath the areas covered by the south approach embankment of the Arthur Laing Bridge and McConachie Way Overpass embankments is reasonably uniform. The subsoil conditions consist of approximately 20 m of predominantly sand, underlain by an approximately normally consolidated clay silt to a depth of approximately 61 m at the north end of the site, and to a greater depth to the south. Underlying the clay silt is the Pleistocene till. More free draining sandy silt layers occur at a depth of about 30 m and were clearly identified in several tests. Thus these layers may be assumed to exist in sufficient areal extent to act as effective drainage layers for excess pore pressures generated from surface loads.

The undrained shear strength in the clay silt appears to increase linearly with depth from 50 kPa at a depth of 20 m to 90 kPa at 60 m. The undrained Young's modulus, E_u, of

$$E_u = \begin{cases} (200 \text{ to } 300)S_u \text{ by SPLT} \\ 100S_u \text{ by CPTU dissipation test correlations} \end{cases} \tag{8.1}$$

appears to provide a useful correlation, since S_u is often more readily and consistently obtained by a variety of methods than E_u. The range of rigidity index obtained by the two test methods,

E/S_u = 100 to 300, shows good agreement in view of the overall differences in the cone penetration and screw plate tests.

The correlation found between constrained modulus, M, and cone bearing, q_c, of

$$M = 2.4\, q_c \tag{8.2}$$

is in general agreement with previously published correlations given in the literature. The Special Method of Schmertmann (1986) provides a rational method by which to modify M when design stress conditions are other than those which existed at the time of in-situ testing.

Piezocone dissipation tests yielded a detailed record from which to assess the consolidation characteristics of the clay silt. Such dissipation tests are sensitive to changes in the behaviour type of soil in the vicinity of the porous element, and thereby provide a means of identifying potential drainage paths. Dissipation tests conducted with the flat dilatometer did not show the same sensitivity to potential drainage paths.

The spherical solution of Torstensson (1977) with E/S_u = 100 appeared to provide the best model for predicting consolidation characteristics of the Sea Island clay silt, and a horizontal coefficient of consolidation, c_h = 0.004 cm^2/s, was effective in predicting the rate of consolidation settlement. Based on the results of the present analysis, it appears that horizontal drainage dominates, and that the consolidation was controlled by c_h. It was not found necessary to adjust the value of c_h(piezocone) to c_h(NC) from dissipation tests conducted for a length of time sufficient to determine t_{50}.

The piezocone penetration test (CPTU) was capable of providing all the required information pertinent to a settlement analysis, especially when correlations are enhanced by local experience.

The flat dilatometer test (DMT) was found to be adequate as a stand-alone test for determining the parameters required to predict settlement. Dissipation tests with the dilatometer show promise in determining consoidation characteristics, however, longer times to reach t_{50} are required, as compared to the CPTU. The effective radius, R = 2.057 cm, used in this analysis to determine c_h from the dilatometer, provided good results, but requires local experience in a variety of soils before its general use may be recommended.

The appeal of the screw plate test lies in the correct orientation of the test for predicting vertical settlement. Site conditions, however, such as the dense sand encountered at the embankment site, may render the test difficult and cumbersome to conduct and may influence the interpreted parameters. Additionally, the screw plate test alone did not furnish all the required information for a settlement analysis. Researchers have reported success in determining consolidation characteristics from the SPLT, however, these tests have been in stiff clays. At Sea Island, in the soft, sensitive, compressible soils at depth, it was not possible to simulate small, constant stress increments and thereby ascertain displacement response.

The normal load approximation, or Boussinesq method, appears to provide a conservative prediction of the distribution of vertical stress increase with depth. When the embankment shape more closely resembles an infinite strip, the Boussinesq method more accurately predicts stress increase. However, the elastic embankment method outlined by Perloff (1967) appeared to give a more realistic stress distribution for the present analysis.

It would be instructive if settlement monitoring of the subject embankments could be continued into the year 2000. This would provide some assessment of the effects of secondary compression. At the present time, there is uncertainty as to when secondary compression begins and how to quantitatively account for it in practice. The process is not well understood, and it is not known if parameters interpreted from in-situ tests inherently include some measure of the secondary compression which may be on-going from the time of initial soil deposition.

The analytical techniques existing in the geotechnical community today appear to be adequate for conducting a one-dimensional settlement analysis. Complex finite element methods or numerical analyses generally are not required for settlement calculations, and do not necessarily provide results superior to the 1-D analysis. More important than the type of analysis performed is the accurate determination of soil parameters, in particular deformation and consolidation characteristics. The greatest effort should be expended in determining these characteristics as accurately as possible.

From this analysis, in-situ testing emerges as a viable alternative to the traditional approach of obtaining geotechnical parameters required in the prediction of settlement. While interpretation of in-situ test data is, by and large, empirical in nature, the large amount and diversity of the data obtained enables the engineer to obtain a better sense of site conditions and variability, leading to a generally more reliable geotechnical solution.

9. BIBLIOGRAPHY

Baldi, G., Bellotti, R., Ghionna, V., Jamiolkowski, M. and Pasqualini, E. (1981). "Cone Resistance of a Dry Medium Sand", *Proceedings, 10th International Conference on Soil Mechanics and Foundation Engineering,* Stockholm, Vol. 2.

Baligh, M. M. and Levadoux, J.-N. (1986). "Consolidation after Undrained Piezocone Penetration. II: Interpretation", *Journal of Geotechnical Engineering,* Vol. 112, No. 7, pp. 727 - 745.

Bertok, J. (1987). "Settlement of embankments and structures at Vancouver International Airport", *Canadian Geotechnical Journal,* Vol. 24, pp. 72 - 80.

Berzins, W. E. (1983). "Determination of Drained and Undrained Soil Parameters Using the Screw Plate Test", M. A. Sc. Thesis, The University of British Columbia.

Blunden, R. H. (1973). "The Urban Geology of Richmond, British Columbia", Adventures in Earth Sciences Series No. 15, Department of Geological Sciences, The University of British Columbia.

Boussinesq, M. J. (1885). *Application Des Potentiels, à L'Etude de l'Equilibre et du Mouvement Des Solides Elastiques.* Paris: Gauthier-Villars.

Bozozuk, M., and Leonards, G. A. (1972). "The Gloucester Test-Fill", *Proceedings, ASCE Specialty Conference, Performance of Earth and Earth-Supported Structures,* Purdue University, Lafayette, Vol. 1, Part 1, pp. 299 - 317.

Burland, J. B. (1987). "Analysis of Settlement on Clays", Short Course on Recent Developments in Foundation Analysis and Design, Imperial College, April, 1988.

Campanella, R. G. and Robertson, P. K. (1988). "Current Status of the Piezocone Test", *Proceedings of the First International Symposium on Penetration Testing, ISOPT-1,* Orlando.

Campanella, R. G., Robertson, P. K. and Gillespie, D. (1985). "A Seismic Cone Penetrometer for Offshore Applications", Soil Mechanics Series No. 93, The University of British Columbia.

Campanella, R. G. and Robertson, P. K. (1981). "Applied Cone Research", Soil Mechanics Series No. 46, The University of British Columbia.

Douglas, B. J. and Olsen, R. S. (1981). "Soil Classification Using Electric Cone Penetrometer", *Symposium on Cone Penetration Testing and Experience, Geotechnical Engineering Division, ASCE,* St. Louis, pp. 209 - 227.

Fadum, R. E. (1948). "Influence values for estimating stresses in elastic foundations", *Proceedings of the Second International Conference on Soil Mechanics and Foundation Engineering* Vol. 2.

Foster, C. R. and Ahlvin, R. G. (1954). "Stresses and deflections induced by a uniform circular load", *Proceedings, Highway Research Board,* Vol. 34, p. 467.

Gillespie, D. G. (1981). "The Piezometer Cone Penetration Test", M. A. Sc. Thesis, The University of British Columbia.

Harr, M. E. (1966). *Foundations of Theoretical Soil Mechanics.* New York: McGraw-Hill.

Jamiolkowski, M., Ladd, C. C., Germaine, J. T. and Lancellotta, R. (1985). "New developments in field and laboratory testing of soils", *Proceedings of the 11th International Conference on Soil Mechanics and Foundation Engineering,* San Francisco, pp. 57 - 153.

Janbu, N. (1967). "Settlement calculations based on the tangent modulus concept", University of Trondheim, Norwegian Institute of Technology, Bulletin No. 2.

Kay, J. N. and Avalle, D. L. (1982). "Application of Screw Plate to Stiff Clays", *Journal of the Geotechnical Engineering Division, ASCE,* Vol. 108(GT1), pp. 145 - 154.

Kummeneje, O. (1956). "Foundation of an Oil Tank in Drammen", Norwegian Geotechnical Institute Publication No. 12.

Levadoux, J.-N. and Baligh, M. M. (1986). "Consolidation after Undrained Piezocone Penetration. I: Prediction", *Journal of Geotechnical Engineering,* Vol. 112, No. 7, pp. 707 - 726.

Lunne, T. and Kleven, A. (1981). "Role of CPT in North Sea Foundation Engineering", *Symposium on Cone Penetration Testing and Experience, Geotechnical Engineering Division, ASCE,* pp. 49 - 75.

Marchetti, S. (1980). "In Situ Tests by Flat Dilatometer", *Journal of the Geotechnical Engineering Division, ASCE,* Vol. 106(GT3), pp. 299 - 321.

Marchetti, S. and Crapps, D. K. (1981). "Flat Dilatometer Manual", GPE Inc., Gainesville, Florida.

Mesri, G. (1973). "Coefficient of Secondary Compression", *Journal of the Soil Mechanics and Foundations Division, ASCE,* Vol. 99(SM1), pp. 123 - 137.

Mesri, G. and Castro, A. (1987). "C_α/C_c concept and K_o during secondary compression", *Journal of Geotechnical Engineering,* Vol. 113, No. 3, pp. 230 - 247.

Mitchell, J. K. and Gardner, W. S. (1975). "In-Situ Measurement of Volume Change Characteristics", State-of-the-Art Report, *Proceedings of the Conference on In-situ Measurement of Soil Properties, Specialty Conference of the Geotechnical Division, ASCE,* North Carolina State University, Raleigh, Vol. II.

Mitchell, J. K., Guzikowski, F. and Villet, W. C. B. (1978). "The Measurement of Soil Properties In-situ", Report prepared for the U. S. Department of Energy, Contract W-7405-ENG-48, Lawrence Berkeley Laboratory, University of California, Berkeley.

Olson, R. E. (1985). "State of the Art: Consolidation Testing", *Consolidation of Soils: Testing and Evaluation, ASTM Special Technical Publication 892,* R. N. Yong and F. C. Townsend, Eds., pp. 58 - 69.

Perloff, W. H. (1975). "Pressure Distribution and Settlement", *Foundation Engineering Handbook,* H. F. Winterkorn and H.-Y. Fang, Eds., New York: Van Nostrand Reinhold.

Perloff, W. H., Baladi, G. Y. and Harr, M. E. (1967). "Stress distribution within and under long elastic embankments", *Highway Research Record*, No. 181.

Phillips, Barratt, Hillier, Jones and Partners, (1974). Grant McConachie Way No. 1 Overpass, Drawings No. 7043-210D, 211D.

Robertson, P. K. (1988). "Penetration Testing in the U. K." Birmingham, England, July 6 - 8, 1988.

Robertson, P. K., Campanella, R. G., Gillespie, D. and By, T. (1988). "Excess Pore Pressures and the DMT", *Proceedings of the First International Symposium on Penetration Testing, ISOPT-1*, Orlando.

Robertson, P. K. and Campanella, R. G. (1986). "Guidelines for Use, Interpretation and Application of the CPT and CPTU", Soil Mechanics Series No. 105, Department of Civil Engineering, The University of British Columbia.

Robertson, P. K. (1985). "In-Situ Testing and Its Application to Foundation Engineering". 1985 Canadian Geotechnical Colloquium, *Canadian Geotechnical Journal*, Vol. 23.

Schleicher, F. (1926). "Zur Theorie Des Baugrundes", *Der Bauingenieur*, No. 48, 49.

Schmertmann & Crapps, Inc. (1988). "Guidelines for Geotechnical Design Using the Marchetti DMT", *Pennsylvania Department of Transportation*, Project 84-24 Manual, Vol. III.

Schmertmann, J. H. (1986). "Dilatometer to compute foundation settlement", *Proceedings of In Situ '86, Specialty Conference of the Geotechnical Engineering Division, ASCE*, Blacksburg, Virginia., pp. 303 - 321.

Schmertmann, J. H. (1983). "Revised Procedure for Calculating K_o and OCR from DMT's with I_D>1.2 and which Incorporate the Penetration Force Measurement to Permit Calculating the Plane Strain Friction Angle", *DMT Workshop*, Gainesville, Florida.

Schmertmann, J. H. (1970). "Static Cone to Compte Static Settlement Over Sand", *Journal of the Soil Mechanics and Foundations Division, ASCE*, Vol. 96(SM3), pp. 1011-1043.

Scott, R. F. (1963). *Principles of Soil Mechanics*, Reading, Mass.: Addison-Wesley Publishing Co., Inc.

Selvadurai, A. P. S. and Gopal, K. R. (1986). "Consolidation Analysis of the Screw Plate Test", *Proceedings, 39th Canadian Geotechnical Conference, In Situ Testing and Field Behaviour*, Ottawa, pp. 167 - 178.

Selvadurai, A. P. S. and Nicholas, T. J. (1979). "A Theoretical Assessment of the Screw Plate Test", *Proceedings, 3rd International Conference on Numerical Methods in Geomechanics*, Aachen, Germany, Vol. 3.

Selvadurai, A. P. S., Bauer, G. E. and Nicholas, T. J. (1980). "Screw plate testing of a soft clay", *Canadian Geotechnical Journal*, Vol. 17, No. 4, pp. 465 - 472.

Skempton, A. W. and Bjerrum, L. (1957). "A contribution to the settlement analysis of foundations on clay", *Géotechnique*, Vol. 7, No. 3.

Terzaghi, K. (1943). *Theoretical Soil Mechanics*, New York: John Wiley and Sons.

Thurber, R. C. and Associates Ltd. (1968). "Foundation Soils Investigation, Proposed Hudson Street Bridge Main Piers", Report No. 1 to Phillips, Barratt, Hillier, Jones and Partners.

Torstensson, B.-A. (1977). "The Pore Pressure Probe", *Nordiske Geotekniske Møte*, Oslo, Paper No. 34.1-34.15.

APPENDIX A - Tables Relating Degree of Consolidation and Dimensionless Time Factor

Table A.1 Values of the Dimensionless Time Factor, T

Method	Degree of Consolidation (%)*				
	20	40	50	60	80
Baligh and Levadoux (1986)	0.69	3.0	5.6	10	39
Torstensson Spherical (1977):					
E/Cu = 500	0.11	0.46	0.81	1.26	3.28
400	0.10	0.40	0.68	1.12	2.85
300	0.085	0.35	0.61	0.98	2.36
200	0.066	0.28	0.47	0.77	1.91
100	0.057	0.20	0.32	0.50	1.16
Torstensson Cylindrical (1977):					
E/Cu = 500	0.34	2.14	4.29	8.33	23.60
400	0.30	1.75	3.57	6.79	21.00
300	0.24	1.38	2.81	5.37	16.29
200	0.18	1.06	2.32	3.82	10.13
100	0.14	0.83	1.37	2.49	5.03

* Degree of consolidation, in percent = (1 - U)100%

Table A.2 Average Degree of Consolidation for Various Values of Dimensionless Time Factor, T

Distribution of initial excess pore water pressure:

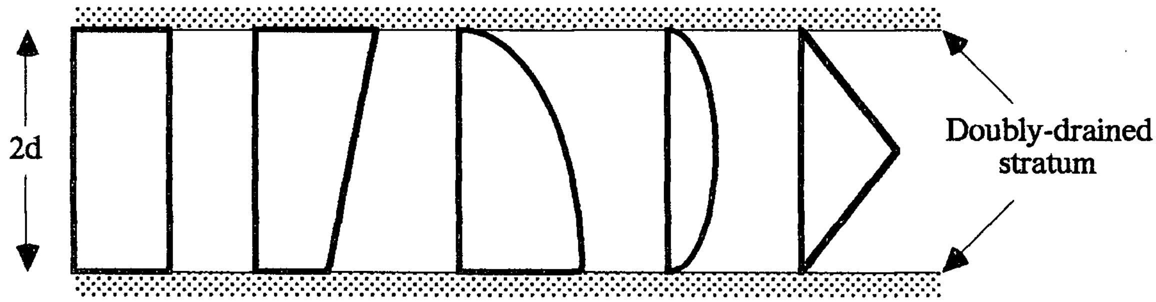

Constant | Linear variation | Half sine curve | Sine curve | Triangular

Case 1 | Case 2 | Case 3 | Case 4

T	U (%)			
	Case 1	Case 2	Case 3	Case 4
0.004	7.14	6.49	0.98	0.80
0.008	10.09	8.62	1.95	1.60
0.012	12.36	10.49	2.92	2.40
0.020	15.96	13.67	4.81	4.00
0.028	18.88	16.38	6.67	5.60
0.036	21.40	18.76	8.50	7.20
0.048	24.72	21.96	11.17	9.60
0.060	27.64	24.81	13.76	11.99
0.072	30.28	27.43	16.28	14.36
0.083	32.51	29.67	18.52	16.51
0.100	35.68	32.88	21.87	19.77
0.125	39.89	36.54	26.54	24.42
0.150	43.70	41.12	30.93	28.86
0.175	47.18	44.73	35.07	33.06
0.200	50.41	48.09	38.95	37.04
0.250	56.22	54.17	46.03	44.32
0.300	61.32	59.5	52.30	50.78
0.350	65.82	64.21	57.83	56.49
0.400	69.79	68.36	62.73	61.54
0.500	76.40	76.28	70.88	69.95
0.600	81.56	80.69	77.25	76.52
0.700	85.59	84.91	82.22	81.65
0.800	88.74	88.21	86.11	85.66
0.900	91.20	90.79	89.15	88.80
1.000	93.13	92.80	91.52	91.25
1.500	98.00	97.90	97.53	97.45
2.000	99.42	99.39	99.28	99.26

APPENDIX B - Field Test Data

UBC IN SITU TESTING

Site Location: Laing Bridge S. CPT Date : 08/12/87 10:58 Page No: 1 / 2

On Site Loc: McConachie O/P Cone Used: UBC#8 Std/BFS PP Comments: CPTU-1

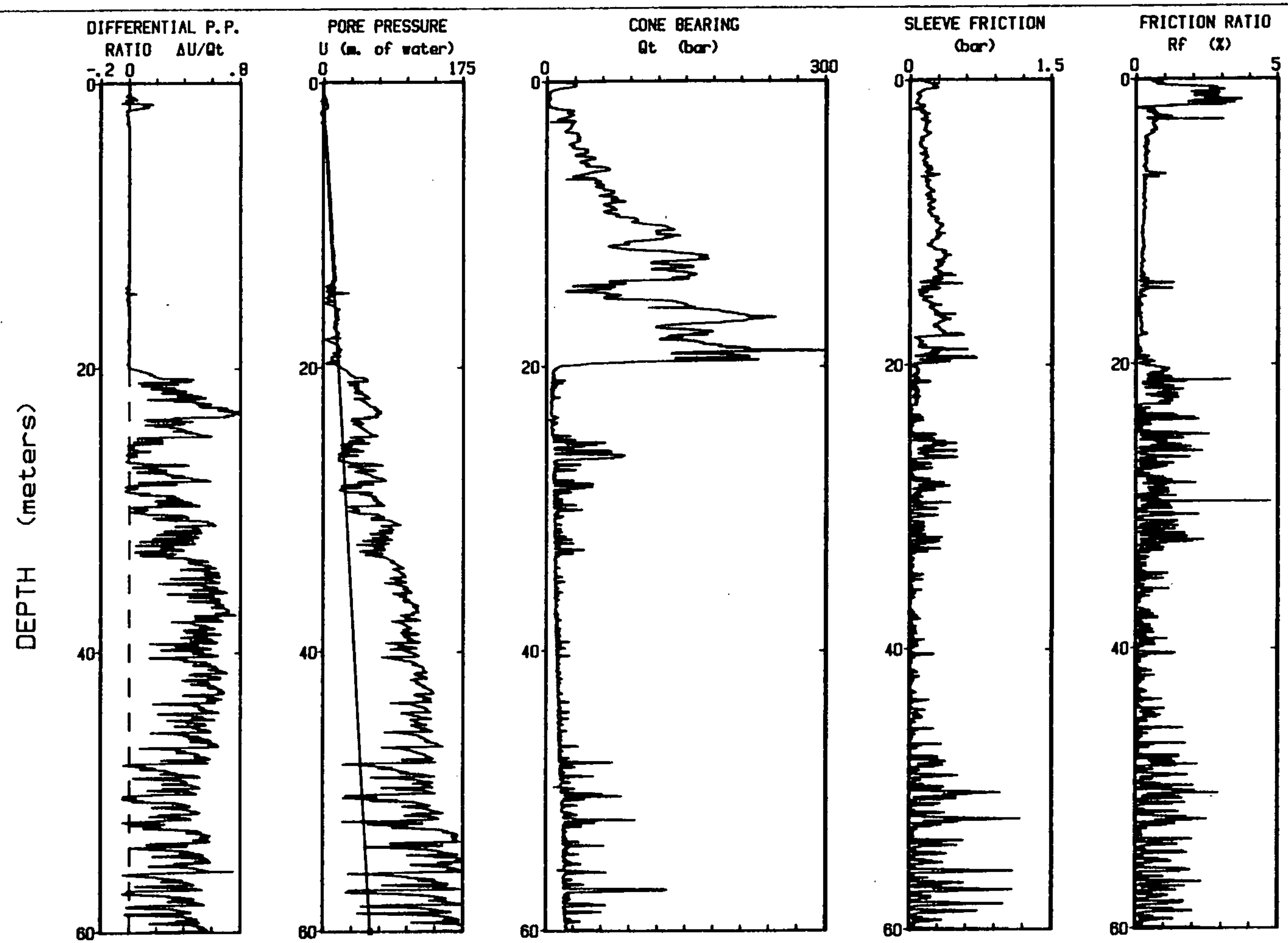

UBC IN SITU TESTING

Site Location: Laing Bridge S. CPT Date : 09/11/87 12:02 Page No: 1 / 2

On Site Loc: McConachie O/P Cone Used: Hog SuperCone Comments: CPTU-5

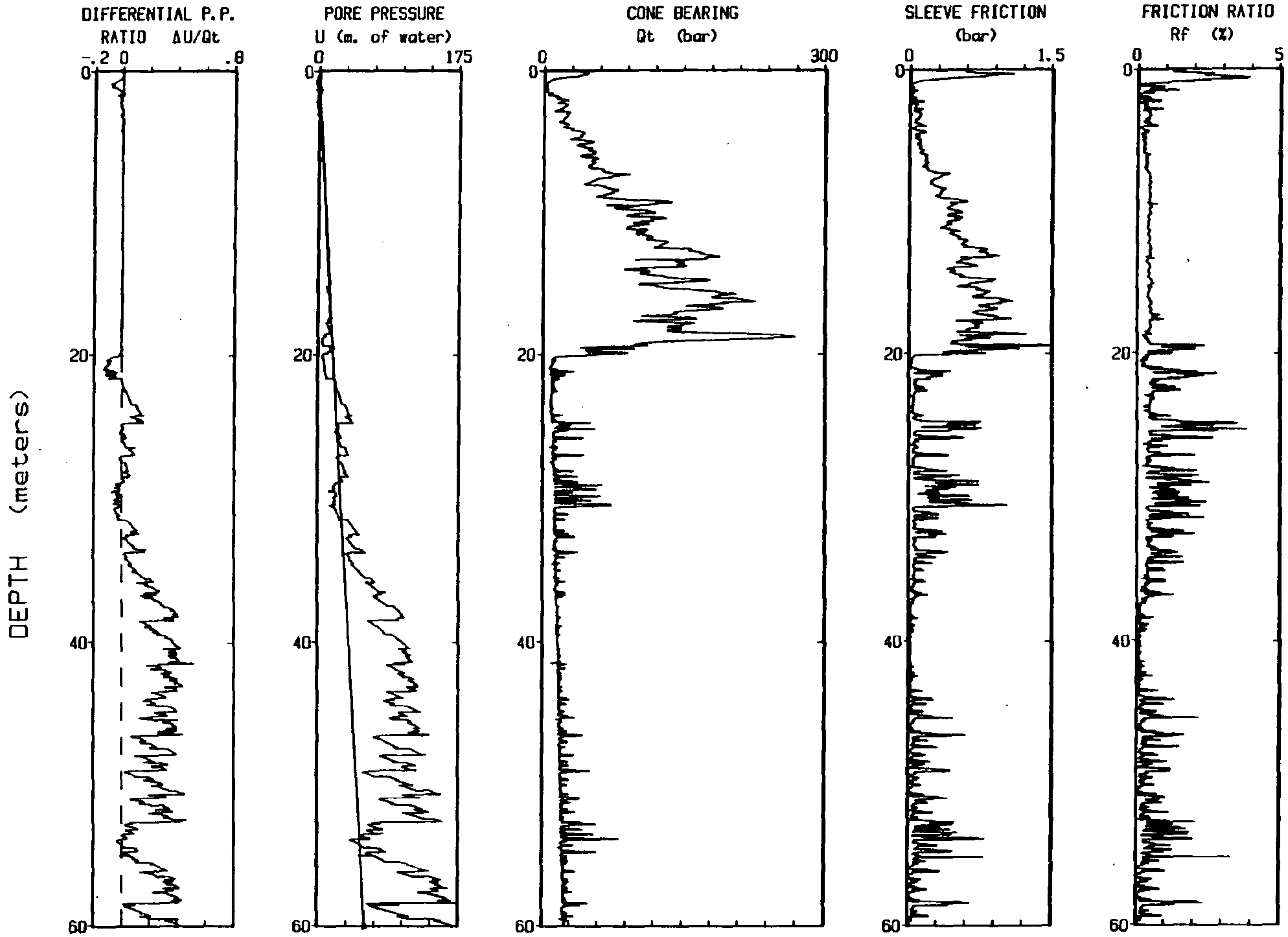

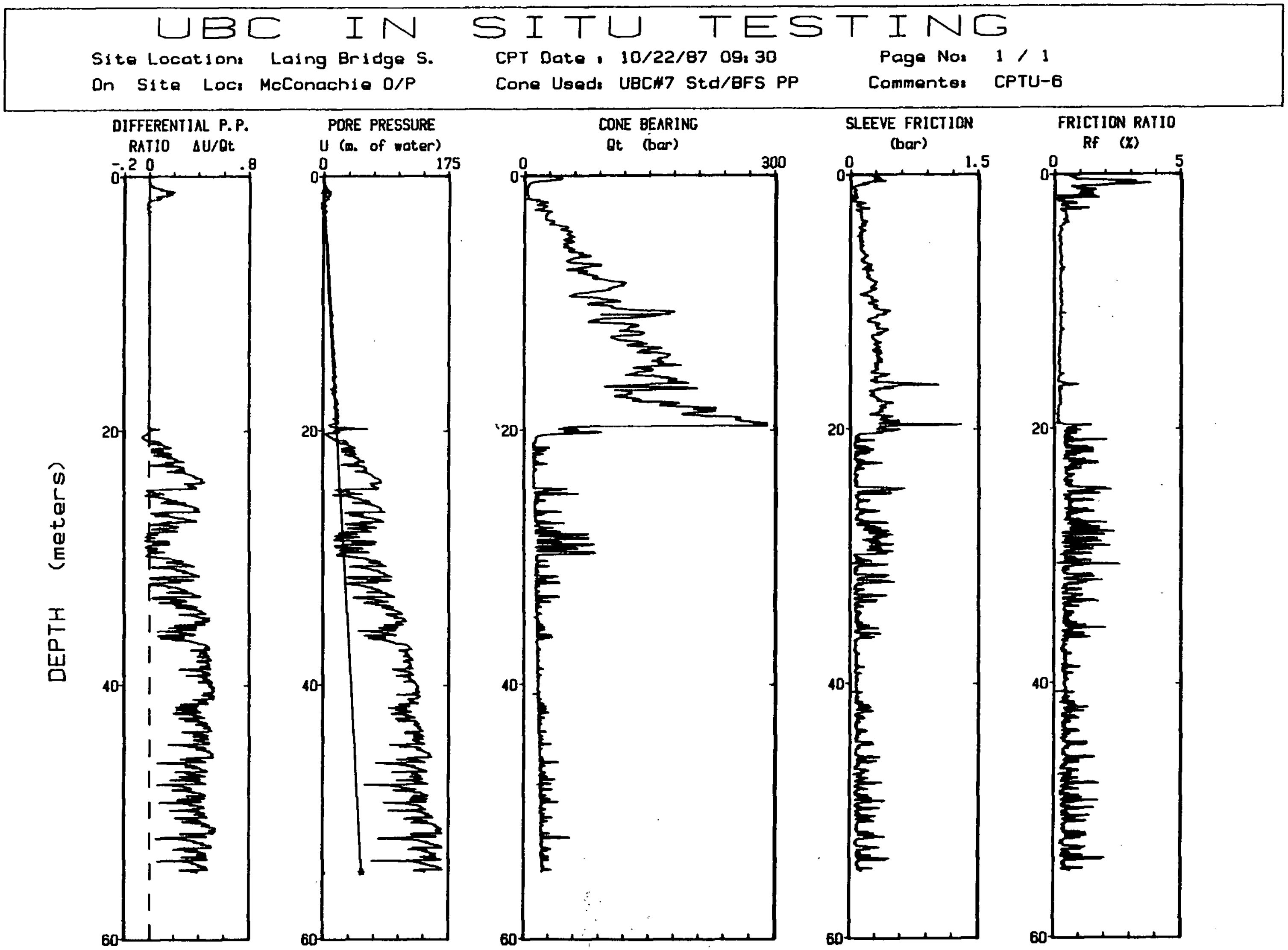
UBC IN SITU TESTING
Site Location: Laing Bridge S.
On Site Loc: McConachie O/P
CPT Date : 10/22/87 09:30
Cone Used: UBC#7 Std/BFS PP
Page No: 1 / 1
Comments: CPTU-6
DIFFERENTIAL P.P.
RATIO ΔU/Qt
PORE PRESSURE
U (m. of water)
CONE BEARING
Qt (bar)
SLEEVE FRICTION
(bar)
FRICTION RATIO
Rf (%)
DEPTH (meters)

Z (M)	THRUST (KG)	A (BAR)	B (BAR)	C (BAR)	U0 (BAR)	ED (BAR)	ID	KD	GAMMA (T/M3)	SV (BAR)	PC (BAR)	OCR	KO	CU (BAR)	PHI (DEG)	M (BAR)	SOIL TYPE
#####	######	#####	#####	#####	######	#####	#####	######	######	######	#####	#####	#####	#####	#####	######	###########
.60	1421.	1.20	3.90	.00	.000	63.	1.25	14.62	1.700	.099	1.14	11.50	1.20		46.0	179.2	SANDY SILT
.80	954.	.92	2.50	.00	.000	22.	.52	9.37	1.600	.130	1.45	11.13	1.77	.197		53.2	SILTY CLAY
1.00	331.	.61	1.90	.00	.000	11.	.35	5.79	1.500	.160	.84	5.25	1.29	.133		21.9	MUD
1.20	186.	.69	2.00	.00	.000	12.	.35	5.25	1.600	.191	.86	4.51	1.20	.141		22.1	CLAY
1.40	164.	.80	1.75	.00	.015	-1.	-.03		P01 =	1.13	P0 =	1.13	P1 =	1.10			QUESTIONABLE
1.60	130.	1.00	1.80	.00	.034	-6.	-.14		P01 =	1.34	P0 =	1.33	P1 =	1.15			QUESTIONABLE
1.80	8.	.61	2.00	.00	.054	15.	.50	3.74	1.600	.231	.61	2.66	.94	.111		22.3	SILTY CLAY
2.00	430.	.61	3.52	.00	.074	70.	2.63	3.14	1.700	.245	.49	1.98	.57		34.4	103.1	SILTY SAND
2.20	564.	.95	4.50	.00	.093	94.	2.55	4.09	1.700	.259	.72	2.78	.66		35.5	158.9	SILTY SAND
2.40	542.	1.28	1.70	.00	.113	-19.	-.37		P01 =	1.64	P0 =	1.61	P1 =	1.05			QUESTIONABLE
2.60	576.	1.19	1.25	.00	.132	-32.	-.66		P01 =	1.57	P0 =	1.52	P1 =	.60			QUESTIONABLE
2.80	598.	1.00	4.70	.00	.152	99.	2.74	3.44	1.800	.303	.66	2.17	.59		35.4	154.1	SILTY SAND
3.00	664.	1.35	6.40	.00	.172	148.	3.28	4.10	1.800	.319	.91	2.85	.67		35.4	255.7	SILTY SAND
3.20	642.	1.60	6.20	.00	.191	132.	2.44	4.66	1.800	.334	1.23	3.69	.77		34.2	238.6	SILTY SAND
3.40	587.	1.47	5.70	.00	.211	118.	2.39	4.08	1.800	.350	1.08	3.10	.72		33.6	199.5	SILTY SAND
3.60	698.	1.80	8.09	.00	.231	193.	3.41	4.47	1.800	.366	1.26	3.44	.75		34.5	348.3	SAND
3.80	854.	1.85	8.25	.07	.250	197.	3.43	4.35	1.800	.381	1.17	3.07	.69		36.1	250.9	SAND
4.00		2.02	12.58	.00	.270	349.	6.28	.00	1.900	######						295.7	SAND
4.20		2.01	12.81	.00	.289	358.	6.61	.00	1.900	######						304.1	SAND
4.40		2.25	12.20	.00	.309	327.	5.17	.00	1.900	######						277.8	SAND
4.60		2.35	13.13	.00	.329	357.	5.53	.00	1.900	######						303.5	SAND
4.80	0.	2.20	11.50	.00	.348	303.	4.95	.00	1.900	######						257.7	SAND
5.00		2.70	13.00	.00	.368	340.	4.46	.00	1.900	######						288.6	SAND
5.20		2.80	12.80	.00	.388	329.	4.13	.00	1.900	######						279.3	SAND
)		2.10	12.80	.00	.407	354.	6.64	.00	1.900	######						301.0	SAND
..60		1.48	13.85	.00	.427	415.	14.70	.00	1.800	######						352.7	SAND
5.80	1299.	2.40	16.60	.30	.447	482.	8.56	.00	1.900	######						409.4	SAND
6.00	1344.	4.80	17.60	.00	.466	431.	3.05	.00	2.000	######						366.1	SILTY SAND
6.20	1322.	2.80	15.80	.00	.486	438.	6.18	.00	1.900	######						372.3	SAND
0	1065.	3.60	13.10	.00	.505	310.	2.98	.00	1.900	######						263.9	SILTY SAND
o.60	1043.	2.30	12.80	.00	.525	347.	6.14	.00	1.900	######						294.8	SAND
6.80	1589.	3.10	18.50	.11	.545	525.	7.00	.00	1.900	######						446.6	SAND
7.00	1644.	4.02	4.39	.00	.564	-21.	-.16		P01 =	4.38	P0 =	4.35	P1 =	3.74			QUESTIONABLE
7.20		3.48	16.84	.00	.584	451.	4.99	.00	1.900	######						383.4	SAND
7.40	1410.	.65	13.70	.00	.604	419.	32.06	.00	1.800	######						356.0	SAND
									P01 =	.38	P0 =	.98	P1 =	13.05			
7.60	1322.	1.80	8.40	.00	.623	205.	4.81	.00	1.800	######						174.0	SAND
7.80	1455.	4.07	16.90	.25	.643	432.	3.93	.00	1.900	######						367.0	SAND
8.00	1622.	1.60	2.35	.00	.662	-8.	-.18		P01 =	1.94	P0 =	1.93	P1 =	1.70			QUESTIONABLE
8.20	1766.	2.90	15.00	.00	.682	405.	5.86	.00	1.900	######						344.4	SAND
8.40	1644.	4.00	18.50	.00	.702	493.	4.81	.00	1.900	######						418.7	SAND
8.60	1789.	4.70	22.30	.00	.721	606.	5.02	.00	2.000	######						514.7	SAND
8.80	1900.	3.50	17.80	.26	.741	485.	5.77	.00	1.900	######						412.5	SAND
9.00	1455.	4.10	18.00	.00	.761	471.	4.49	.00	1.900	######						400.1	SAND
9.20	1822.	2.80	20.80	.00	.780	620.	11.92	.00	1.900	######						527.1	SAND
9.40	2401.	3.70	24.60	.00	.800	726.	9.36	.00	1.900	######						616.9	SAND
9.60	2791.	4.60	30.50	.00	.819	908.	9.13	.00	2.000	######						771.8	SAND
9.80	2858.	5.10	28.20	.30	.839	806.	6.66	.00	2.000	######						685.1	SAND
10.00	2858.	5.00	29.20	.00	.859	846.	7.37	.00	2.000	######						719.1	SAND
10.20	2624.	3.80	24.60	.00	.878	722.	9.21	.00	1.900	######						613.8	SAND
10.40	2958.	3.70	28.20	.00	.898	857.	12.63	.00	1.900	######						728.4	SAND
10.60	3147.	7.80	30.50	.00	.918	791.	3.72	.00	2.000	######						672.7	SAND
10.80	2858.	7.90	26.80	.40	.937	653.	2.94	.00	2.000	######						555.0	SILTY SAND
11.00	2757.	5.50	25.80	.00	.957	704.	5.19	.00	2.000	######						598.3	SAND
'' 20	2512.	4.60	19.50	.08	.976	507.	4.49	.00	1.900	######						431.1	SAND
40	1889.	3.90	19.50	.00	.996	523.	6.13	.00	1.900	######						452.8	SAND
11.60	2346.	7.20	27.10	.00	1.016	689.	3.57	.00	2.000	######						585.9	SAND
11.80	2356.	6.60	25.50	.45	1.035	653.	3.76	.00	2.000	######						555.0	SAND
12.00	2179.	5.60	21.50	.00	1.055	544.	3.79	.00	2.000	######						462.1	SAND
12.20	2056.	4.20	19.20	.00	1.075	511.	5.34	.00	1.900	######						434.2	SAND
12.40	2702.	5.10	27.40	.00	1.094	777.	6.85	.00	2.000	######						660.3	SAND
12.60	2746.	6.10	26.90	.00	1.114	722.	4.81	.00	2.000	######						613.8	SAND
12.80	2546.	6.70	23.90	.49	1.133	591.	3.35	.00	2.000	######						502.3	SAND
13.00	1912.	4.00	16.80	.00	1.153	431.	4.80	.00	1.900	######						366.1	SAND
13.20	2601.	5.70	27.60	.00	1.173	762.	5.76	.00	2.000	######						647.9	SAND
13.40	2624.	4.60	21.40	.00	1.192	576.	5.64	.00	1.900	######						489.9	SAND
13.60	3292.	6.00	31.10	.00	1.212	879.	6.47	.00	2.000	######						747.0	SAND
13.80	3459.	6.50	30.40	.60	1.232	835.	5.41	.00	2.000	######						709.8	SAND
14.00	3615.	8.00	33.50	.00	1.251	893.	4.40	.00	2.000	######						759.4	SAND
14.20	3581.	7.60	25.50	.00	1.271	616.	3.06	.00	2.000	######						524.0	SILTY SAND
14.40	2312.	4.20	20.20	.00	1.290	547.	6.34	.00	1.900	######						465.2	SAND
14.60	2468.	5.30	22.00	.00	1.310	573.	4.67	.00	2.000	######						486.8	SAND
14.80	2590.	6.40	25.60	.60	1.330	664.	4.26	.00	2.000	######						554.3	SAND
15.00	2290.	5.60	23.00	.00	1.349	598.	4.59	.00	2.000	######						508.5	SAND

16.60	4127.	8.10	32.80	.00	1.506	864.	4.34	.00	2.000	******					734.6	SAND
16.80	3949.	8.40	29.10	.80	1.526	718.	3.33	.00	2.000	******					610.7	SAND
17.00	3514.	7.30	32.50	.00	1.546	882.	5.22	.00	2.000	******					750.1	SAND
17.20	3626.	6.10	32.10	.00	1.565	912.	7.27	.00	2.000	******					774.9	SAND
40	4349.	9.10	39.70	.00	1.585	1079.	4.89	.00	2.000	******					917.3	SAND
.60	4572.	8.30	39.50	.00	1.605	1101.	5.75	.00	2.000	******					935.9	SAND
17.80	4733.	14.00	39.10	.60	1.624	879.	2.20	.01	2.150	******					747.0	SILTY SAND
18.00	3893.	8.50	29.40	.00	1.644	726.	3.38	.00	2.000	******					616.9	SAND
18.20	5051.	13.20	40.00	.00	1.663	941.	2.56	.01	2.150	******					799.6	SILTY SAND
18.40	4928.	10.60	40.00	.00	1.683	1035.	3.81	.00	2.150	******					880.2	SAND
18.60	4516.	15.10	40.00	.00	1.703	872.	2.00	.01	2.150	******					740.8	SILTY SAND
18.80	4461.	8.80	38.40	1.30	1.722	1043.	5.03	.00	2.000	******					886.4	SAND
19.00	5574.	14.70	40.00	.00	1.742	886.	2.12	.01	2.150	******					753.2	SILTY SAND
19.20	5574.	11.10	40.00	.00	1.762	1017.	3.54	.01	2.150	******					864.7	SAND
19.40	5296.	8.40	10.40	.00	1.781	37.	.16	.00	1.800	******	.11	.00	-.54	.163	31.6	CLAY
19.60	4182.	14.40	39.60	.00	1.801	882.	2.17	.01	2.150	******					750.1	SILTY SAND
19.90	3715.	6.30	11.20	1.03	1.820	143.	.89	.00	1.800	******	.06	.00	-.55	.099	121.4	CLAYEY SILT
20.00	2802.	6.60	21.10	.00	1.840	493.	3.22	.00	2.000	******					418.7	SILTY SAND
20.20	2691.	5.40	14.20	.00	1.860	285.	2.36	.00	1.900	******					242.2	SILTY SAND
20.40	2023.	5.00	8.10	.00	1.879	77.	.67	.00	1.700	******	.04	.00	-.55	.066	65.7	CLAYEY SILT
20.60	1344.	5.90	7.30	.00	1.899	15.	.10	.00	1.700	******	.05	.00	-.55	.091	13.0	CLAY
20.80	720.	6.50	8.20	1.35	1.919	26.	.16	.00	1.700	******	.06	.00	-.55	.106	22.3	CLAY
21.00		6.50	7.60	.00	1.938	4.	.03	.00	1.500	******	.06	.00	-.55	.106	3.7	MUD

Z (M)	THRUST (KG)	A (BAR)	B (BAR)	C (BAR)	U0 (BAR)	ED (BAR)	ID	KD	GAMMA (T/M3)	SV (BAR)	PC (BAR)	OCR	KO	CU (BAR)	PHI (DEG)	M (BAR)	SOIL TYPE
#####	######	#####	#####	#####	######	#####	#####	######	######	######	#####	#####	#####	#####	#####	######	############
21.00		6.30	29.70	.00	1.938	812.	6.54	.34	1.500	10.500	7.35	.70	.45		28.8	690.3	SAND
[illegible] 70		9.80	18.90	4.30	1.958	291.	1.08	.74	1.950	10.518	2.23	.21	.12			247.4	SILT
.0		8.80	23.60	3.90	1.977	499.	2.22	.61	2.000	10.538	10.25	.97	.57		25.4	424.0	SILTY SAND
21.60		10.90	24.10	4.30	1.997	440.	1.47	.82	1.950	10.557	11.79	1.12	.60		25.0	374.4	SANDY SILT
21.80		10.80	16.70	3.90	2.017	175.	.57	.84	1.900	10.574	2.73	.26	.16	.786		148.3	SILTY CLAY
22.00		10.00	25.60	4.00	2.036	528.	2.01	.71	2.000	10.594	11.10	1.05	.59		25.1	448.8	SILTY SAND
22.20		9.80	20.50	4.50	2.056	349.	1.33	.72	1.950	10.613	11.15	1.05	.59		25.0	297.0	SANDY SILT
22.40		11.80	17.80	5.00	2.076	178.	.52	.92	1.900	10.630	3.18	.30	.20	.889		151.4	SILTY CLAY
22.60		13.70	21.60	4.50	2.095	247.	.61	1.09	1.950	10.649	4.12	.39	.26	1.096		210.3	CLAYEY SILT
22.80		12.00	23.50	4.70	2.115	379.	1.13	.91	1.950	10.668	3.12	.29	.19			321.8	SILT
23.00		10.20	23.50	4.60	2.134	444.	1.64	.73	1.950	10.686	11.32	1.06	.59		25.0	377.5	SANDY SILT
23.20		9.40	30.20	4.50	2.154	717.	3.14	.62	2.000	10.706	9.81	.92	.53		27.0	609.8	SILTY SAND
23.40		12.70	28.40	4.50	2.174	532.	1.51	.94	2.100	10.727	12.90	1.20	.61		25.0	451.8	SANDY SILT
23.60		14.80	20.80	5.20	2.193	178.	.40	1.18	1.900	10.745	4.73	.44	.29	1.224		151.4	SILTY CLAY
23.80		13.80	26.50	5.10	2.213	422.	1.07	1.05	2.100	10.767	3.96	.37	.25			359.9	SILT
24.00		12.50	23.30	5.20	2.233	353.	1.01	.94	1.950	10.785	3.31	.31	.20			300.1	SILT
24.20		12.90	29.60	4.80	2.252	568.	1.61	.94	2.100	10.807	13.00	1.20	.61		25.0	482.8	SANDY SILT
24.40		12.10	29.50	5.20	2.272	594.	1.83	.86	2.150	10.830	12.38	1.14	.60		25.1	504.5	SILTY SAND
24.60		12.00	37.70	5.40	2.291	896.	2.93	.81	2.150	10.852	11.09	1.02	.55		27.3	761.5	SILTY SAND
24.80		13.00	31.60	4.80	2.311	637.	1.81	.93	2.150	10.875	12.78	1.18	.60		25.5	541.7	SILTY SAND
25.00		14.00	36.70	5.00	2.331	787.	2.08	1.00	2.150	10.897	12.91	1.18	.59		26.3	668.6	SILTY SAND
25.20		14.00	28.50	4.90	2.350	488.	1.24	1.04	2.100	10.919	13.84	1.27	.63		25.0	414.7	SANDY SILT
25.40		12.00	25.00	4.90	2.370	433.	1.33	.86	1.950	10.938	12.50	1.14	.60		25.0	368.2	SANDY SILT
25.60		16.00	26.30	4.70	2.390	335.	.72	1.23	2.100	10.959	5.13	.47	.31	1.313		284.6	CLAYEY SILT
25.80		12.40	33.80	4.30	2.409	739.	2.29	.85	2.150	10.982	11.87	1.08	.57		26.4	628.4	SILTY SAND
26.00		13.20	30.00	4.80	2.429	572.	1.60	.94	2.100	11.003	13.19	1.20	.61		25.0	485.9	SANDY SILT
26.20		15.50	33.70	5.20	2.448	623.	1.43	1.14	2.100	11.025	14.79	1.34	.64		25.0	529.3	SANDY SILT
[illegible]		16.00	40.00	4.20	2.468	834.	1.89	1.15	2.150	11.047	14.29	1.29	.61		26.2	708.9	SILTY SAND
26.60		14.80	40.00	4.80	2.488	878.	2.21	1.03	2.150	11.070	13.20	1.19	.59		26.6	746.1	SILTY SAND
26.80		15.10	37.80	5.30	2.507	787.	1.91	1.07	2.150	11.093	13.75	1.24	.60		26.1	668.6	SILTY SAND
27.00		13.50	36.20	5.20	2.527	787.	2.22	.92	2.150	11.115	12.51	1.13	.58		26.4	668.6	SILTY SAND
27.20		12.40	40.00	6.00	2.547	965.	3.14	.80	2.150	11.138	11.16	1.00	.54		27.5	820.4	SILTY SAND
[illegible] 40		11.60	31.00	6.40	2.566	666.	2.27	.76	2.150	11.160	11.54	1.03	.57		26.1	566.4	SILTY SAND
[illegible]0		13.30	40.00	6.30	2.586	932.	2.75	.87	2.150	11.183	11.90	1.06	.56		27.2	792.5	SILTY SAND
27.80		16.20	40.00	5.00	2.605	827.	1.86	1.14	2.150	11.205	14.46	1.29	.61		26.2	702.7	SILTY SAND
28.00		12.30	40.00	6.00	2.625	969.	3.22	.77	2.150	11.228	11.07	.99	.54		27.5	823.5	SILTY SAND
28.20		20.00	40.00	6.40	2.645	688.	1.18	1.49	2.100	11.250	7.09	.63	.40			585.0	SILT
28.40		12.00	40.00	6.50	2.664	980.	3.39	.74	2.150	11.272	10.83	.96	.53		27.7	832.9	SAND
28.60		12.00	39.20	6.80	2.684	951.	3.28	.74	2.150	11.295	10.92	.97	.53		27.5	808.0	SILTY SAND
28.80		17.00	34.30	6.40	2.704	590.	1.23	1.22	2.100	11.316	15.91	1.41	.65		25.0	501.4	SANDY SILT
29.00		12.80	37.80	6.30	2.723	870.	2.72	.81	2.150	11.339	11.72	1.03	.55		27.0	739.9	SILTY SAND
29.20		18.50	32.70	6.50	2.743	477.	.89	1.36	2.100	11.360	6.21	.55	.35	1.541		405.4	CLAYEY SILT
29.40		11.20	40.00	4.80	2.763	1009.	3.94	.65	2.150	11.383	10.18	.89	.51		28.0	857.6	SAND
29.60		16.00	40.00	5.60	2.782	834.	1.94	1.09	2.150	11.406	14.25	1.25	.60		26.2	708.9	SILTY SAND
29.80		17.00	22.20	5.60	2.802	149.	.30	1.25	1.900	11.423	5.51	.48	.32	1.402		126.7	CLAY
30.00		14.20	40.00	6.00	2.821	900.	2.48	.92	2.150	11.446	12.65	1.10	.57		26.8	764.6	SILTY SAND
30.20		14.30	40.00	4.30	2.841	896.	2.45	.92	2.150	11.468	12.73	1.11	.57		26.8	761.5	SILTY SAND
30.40		14.00	36.60	6.00	2.861	783.	2.17	.90	2.150	11.491	12.88	1.12	.58		26.3	665.5	SILTY SAND
30.60		15.70	37.00	6.70	2.880	736.	1.75	1.05	2.100	11.513	14.42	1.25	.61		25.6	625.3	SANDY SILT
30.80		15.40	40.00	3.80	2.900	856.	2.12	1.01	2.150	11.535	13.68	1.19	.59		26.4	727.5	SILTY SAND
31.00		18.20	40.00	4.70	2.920	754.	1.49	1.26	2.100	11.557	16.61	1.44	.65		25.0	640.8	SANDY SILT
31.20		15.50	40.00	5.80	2.939	852.	2.10	1.01	2.150	11.579	13.77	1.19	.59		26.4	724.4	SILTY SAND
31.40		16.80	33.50	8.00	2.959	568.	1.22	1.15	2.100	11.601	15.72	1.36	.64		25.0	482.8	SANDY SILT
31.60		14.60	37.30	7.20	2.978	787.	2.09	.94	2.150	11.623	13.31	1.15	.59		26.2	668.6	SILTY SAND
31.80		19.00	40.00	7.10	2.998	725.	1.36	1.32	2.100	11.645	17.25	1.48	.66		25.0	616.0	SANDY SILT
32.00		13.60	39.50	6.70	3.018	903.	2.69	.83	2.150	11.668	12.19	1.04	.56		27.0	767.7	SILTY SAND
32.20		14.00	40.00	7.20	3.037	907.	2.60	.86	2.150	11.690	12.47	1.07	.56		26.9	770.8	SILTY SAND
32.40		14.00	39.60	7.10	3.057	892.	2.56	.86	2.150	11.713	12.51	1.07	.56		26.9	758.4	SILTY SAND
[illegible]		14.00	40.00	7.60	3.077	907.	2.61	.85	2.150	11.735	12.46	1.06	.56		26.9	770.8	SILTY SAND
3[illegible].80		15.00	38.20	7.20	3.096	805.	2.08	.95	2.150	11.758	13.54	1.15	.59		26.2	684.1	SILTY SAND
33.00		17.70	40.00	7.60	3.116	772.	1.61	1.18	2.100	11.780	15.91	1.35	.63		25.4	656.2	SANDY SILT
33.20		13.90	40.00	6.40	3.135	911.	2.67	.83	2.150	11.802	12.38	1.05	.56		27.0	773.9	SILTY SAND
33.40		13.50	38.00	7.00	3.155	852.	2.58	.80	2.150	11.825	12.27	1.04	.56		26.8	724.4	SILTY SAND
33.60		13.30	40.00	5.70	3.175	932.	2.93	.77	2.150	11.847	11.88	1.00	.54		27.2	792.5	SILTY SAND
33.80		13.20	40.00	6.60	3.194	936.	2.98	.76	2.150	11.870	11.80	.99	.54		27.2	795.6	SILTY SAND
34.00		12.90	37.50	7.50	3.214	856.	2.79	.74	2.150	11.892	11.83	1.00	.55		26.9	727.5	SILTY SAND
34.20		11.80	32.50	7.40	3.234	714.	2.60	.66	2.150	11.915	11.52	.97	.55		26.4	606.7	SILTY SAND
34.40		13.00	40.00	7.10	3.253	943.	3.10	.74	2.150	11.938	11.64	.97	.54		27.3	801.8	SILTY SAND
34.60		13.10	40.00	6.50	3.273	940.	3.05	.74	2.150	11.960	11.72	.98	.54		27.2	798.7	SILTY SAND
34.80		14.80	40.00	7.60	3.292	878.	2.38	.89	2.150	11.983	13.13	1.10	.57		26.6	746.1	SILTY SAND
35.00		13.60	40.00	6.20	3.312	921.	2.84	.78	2.150	12.005	12.13	1.01	.55		27.1	783.2	SILTY SAND
35.20		18.00	40.00	8.00	3.332	761.	1.57	1.16	2.100	12.027	16.35	1.36	.64		25.0	647.0	SANDY SILT
35.40		16.60	39.10	7.50	3.351	779.	1.80	1.04	2.100	12.048	14.89	1.24	.61		25.8	662.4	SANDY SILT
35.60		16.00	40.00	8.30	3.371	834.	2.03	.98	2.150	12.071	14.18	1.17	.59		26.2	708.3	SILTY SAND

Z (M)	THRUST (KG)	A (BAR)	B (BAR)	C (BAR)	U0 (BAR)	ED (BAR)	ID	KD	GAMMA (T/M3)	SV (BAR)	PC (BAR)	OCR	K0	CU (BAR)	PHI (DEG)	M (BAR)	SOIL TYPE
*****	******	*****	*****	*****	******	*****	*****	******	******	******	*****	*****	*****	*****	*****	******	***********
15.00	2900.	8.60	28.00	.40	1.374	681.	3.05	4.71	2.000	1.367	4.98	3.64	.76		37.3	1257.3	SILTY SAND
16.00	4450.	13.80	42.50	.60	1.472	1020.	2.65	7.52	2.150	1.473	11.34	7.70	1.07		38.4	2290.8	SILTY SAND
17.00	4600.	14.40	42.00	.30	1.570	980.	2.43	7.34	2.150	1.586	11.79	7.43	1.06		38.3	2174.6	SILTY SAND
18.00	4650.	13.60	40.50	1.40	1.668	954.	2.55	6.34	2.150	1.698	9.72	5.73	.93		38.6	1995.5	SILTY SAND
19.00	4075.	7.80	25.00	2.00	1.766	601.	3.23	2.97	2.000	1.804	2.86	1.59	.50		39.7	868.6	SILTY SAND
20.00	2850.	7.00	10.00	3.00	1.865	83.	.47	2.73	1.800	1.892	3.08	1.63	.73	.615		97.6	SILTY CLAY
20.20	1300.	5.00	11.60	1.40	1.884	215.	2.08	1.56	1.900	1.910	2.42	1.27	.53		31.5	182.4	SILTY SAND
20.40	1560.	8.30	18.40	1.60	1.904	342.	1.62	3.15	1.950	1.929	5.32	2.76	.74		30.7	476.7	SANDY SILT
20.60	1640.	6.40	8.60	1.90	1.923	54.	.34	2.34	1.800	1.944	2.49	1.28	.63	.521		54.9	CLAY
20.80	1160.	7.20	8.80	3.60	1.943	32.	.17	2.74	1.700	1.958	3.20	1.63	.73	.638		38.0	CLAY
21.00	640.	5.90	7.30	3.80	1.963	25.	.18	2.06	1.700	1.972	2.06	1.04	.56	.449		22.1	CLAY
21.20	480.	6.30	7.30	4.30	1.982	11.	.07	2.25	1.500	1.982	2.38	1.20	.61	.504		10.2	MUD
21.40	350.	5.40	6.90	2.80	2.002	29.	.24	1.76	1.700	1.995	1.63	.82	.48	.374		24.5	CLAY
21.60	750.	6.20	11.90	1.80	2.022	182.	1.28	2.03	1.800	2.011	4.27	2.12	.74		25.1	170.2	SANDY SILT
21.80	700.	6.00	7.70	2.70	2.041	36.	.26	2.00	1.700	2.025	2.03	1.00	.55	.447		30.8	CLAY
22.00	700.	4.90	6.60	2.60	2.061	36.	.35	1.44	1.700	2.038	1.22	.60	.38	.298		30.7	SILTY CLAY
22.20	430.	4.60	6.10	2.80	2.080	29.	.32	1.28	1.700	2.052	1.02	.50	.33	.259		24.5	CLAY
22.40	425.	5.10	6.90	2.70	2.100	40.	.37	1.50	1.700	2.066	1.32	.64	.40	.317		33.8	SILTY CLAY
22.60	360.	6.50	7.80	3.90	2.120	21.	.14	2.16	1.700	2.080	2.35	1.13	.59	.505		20.0	CLAY
22.80	790.	5.80	9.20	2.10	2.139	98.	.77	1.75	1.800	2.095	1.71	.82	.48	.391		83.3	CLAYEY SILT
23.00	670.	6.30	7.40	4.10	2.159	14.	.10	2.03	1.700	2.109	2.15	1.02	.55	.471		12.3	OFF CHART
23.20	490.	6.50	7.80	4.20	2.179	21.	.14	2.09	1.700	2.123	2.28	1.07	.57	.494		19.3	CLAY
23.40	360.	6.70	7.90	4.90	2.198	18.	.11	2.17	1.700	2.137	2.42	1.13	.59	.519		16.6	CLAY
23.60	300.	7.20	8.50	5.40	2.218	21.	.12	2.37	1.700	2.150	2.81	1.31	.64	.586		22.0	CLAY
23.80	300.	7.20	8.30	5.40	2.237	14.	.08	2.35	1.700	2.164	2.79	1.29	.64	.583		14.5	OFF CHART
24.00	320.	7.20	8.20	5.50	2.257	11.	.06	2.33	1.700	2.178	2.77	1.27	.63	.580		10.6	MUD
24.20	380.	7.20	8.30	5.30	2.277	14.	.08	2.31	1.700	2.192	2.74	1.25	.62	.576		14.2	OFF CHART
24.40	370.	6.90	7.80	5.10	2.296	7.	.04	2.16	1.500	2.201	2.47	1.12	.59	.532		6.4	MUD
24.60	340.	7.20	8.50	5.00	2.316	21.	.12	2.26	1.700	2.215	2.68	1.21	.61	.568		21.0	CLAY
24.80	590.	6.50	10.60	2.20	2.336	124.	.86	1.86	1.800	2.231	1.99	.89	.51	.448		105.0	CLAYEY SILT
25.00	650.	7.20	8.30	5.00	2.355	14.	.08	2.22	1.700	2.245	2.64	1.17	.60	.562		13.6	OFF CHART
25.20	400.	6.70	9.00	3.10	2.375	58.	.39	1.94	1.800	2.260	2.16	.96	.53	.480		49.2	SILTY CLAY
25.40	990.	8.30	15.00	2.20	2.395	218.	1.09	2.53	1.950	2.279	3.28	1.44	.68			247.4	SILT
25.60	920.	8.30	12.40	2.70	2.414	124.	.61	2.56	1.800	2.295	3.37	1.47	.68	.686		136.2	CLAYEY SILT
25.80	1700.	9.30	13.50	2.60	2.434	127.	.54	2.96	1.800	2.310	4.26	1.84	.78	.830		159.3	SILTY CLAY
26.00	1260.	7.50	8.60	5.00	2.453	14.	.08	2.23	1.700	2.324	2.75	1.18	.60	.585		13.7	OFF CHART
26.20	700.	7.30	8.80	5.00	2.473	29.	.17	2.11	1.700	2.338	2.55	1.09	.57	.551		26.1	CLAY
26.40	550.	7.50	9.00	5.20	2.493	29.	.16	2.18	1.700	2.352	2.68	1.14	.59	.575		27.0	CLAY
26.60	790.	7.30	11.00	2.90	2.512	109.	.66	2.02	1.800	2.367	2.41	1.02	.55	.528		94.5	CLAYEY SILT
26.80	960.	8.10	12.80	2.80	2.532	145.	.76	2.32	1.800	2.383	3.00	1.26	.63	.630		147.7	CLAYEY SILT
27.20	420.	8.50	10.00	5.00	2.571	29.	.14	2.50	1.700	2.412	3.42	1.42	.67	.703		31.1	CLAY
27.60	500.	8.30	10.00	6.00	2.610	36.	.18	2.37	1.800	2.442	3.18	1.30	.64	.665		37.0	CLAY
27.80	730.	9.50	11.50	6.00	2.630	47.	.19	2.83	1.800	2.458	4.22	1.72	.75	.834		56.7	CLAY
28.20	520.	8.90	10.20	6.30	2.669	21.	.10	2.55	1.700	2.487	3.64	1.46	.68	.743		23.7	OFF CHART

Calculation of Young's Modulus* from Screw Plate Test
Sea Island Embankment Site

Plate Diameter = 18 cm
Gamma Sand = 17.5 kPa/m
Gamma Water = 9.81 kPa/m
Water table at -1.25 m

Depth (m)	Po' (kPa)	ΔP (kg) Measured	Rods	Total	ΔP (kPa)	Δ (cm)	E (MPa)	Pult (kPa)
3	35.33	1400	52.78	1452.78	570	0.10	123	†
4	43.02	1600	63	1663	652	0.11	128	†
5	50.71	750	73	823	323	0.10	70	†
6	58.40	2500	83	2583	1013	0.20	109	†
7	66.09	4250	92	4342	1704	0.40	92	†
8	73.78	3760	102	3862	1516	0.20	164	†
9	81.47	4240	112	4352	1708	0.30	123	†
10	89.16	4350	122	4472	1755	0.40	95	†
11	96.85	4250	132	4382	1720	0.30	124	†
12	104.54	4500	142	4642	1822	0.40	98	†
13	112.23	5400	152	5552	2179	0.40	118	†
14	119.92	5010	162	5172	2029	0.40	110	†
15	127.61	4550	172	4722	1853	0.40	100	†
16	135.30	3350	182	3532	1386	0.30	100	†
17	142.99	4900	192	5092	1998	0.50	86	†
18	150.68	4900	201	5101	2002	0.50	86	†
19	158.37	4150	211	4361	1711	0.40	92	†
20	166.06	1700	221	1921	754	0.20	25	933
21	173.75	2800	231	3031	1189	0.30	26	1295
22	181.44	2300	241	2541	997	0.20	33	1357
22.5	185.29	1940	246	2186	858	0.20	28	1301
23	189.13	2320	251	2571	1009	0.22	30	1224
23.5	192.98	2760	256	3016	1183	0.26	30	1120
24	196.82	2400	261	2661	1044	0.24	29	1233
24.5	200.67	2030	266	2296	901	0.29	21	1359

* An equivalent Young's Modulus is calculated for the sand layer; an undrained Young's Modulus is calculated for the clayey silt.
† An ultimate plate load, Pult, was not reached in the sand layer.

Po' = effective vertical overburden pressure
ΔP = measured screw plate load
[from slope (ΔP/Δ) of field SPLT load-deflection curve]
Δ = measured screw plate deflection
[from slope (ΔP/Δ) of field SPLT load-deflection curve]
E = Young's Modulus (Es in sand; Eu in clayey silt)